KAO, DIANA, Ph.D. Steps in the Journey to Advance the Study of Nature's Chemistry. (2019)
Directed by Dr. Nicholas H. Oberlies. 135 pp.

"A journey of a thousand miles begins with a single step" is a saying from the philosopher of Laozi, the founder of Taosim, and Taoism believes in living in harmony with the universe or nature itself. This seems particularly appropriate to describe the journey of this body of work, which itself is not beginning nor the end of the journey for research in natural products' chemistry, which is to find new treatments by studying the nature herself. However, over the course of the past three decades, rational drug design and combinatorial chemistry have become major methods to develop pharmacologically significant drugs. Whereas, in the last 30 years, 64% of the approved small-molecule drugs originated from natural products, which studies nature's building blocks.

Classically, plants are the first image that comes to mind when one thinks of natural products when in fact, there is a wide diversity of sources such as microorganisms remain relatively unexplored. One such microorganism is fungi. Literature estimates there to be about 5 million fungal species and only 100,000 species having been identified-even fewer measured for their potential bioactivity. The way we think of natural products is changing, and so the way we work with natural products also needs to change. Presented here are the characterization of new and known compounds from a filamentous fungus (Aim 1), methods to augment the isolation techniques for a compound of interest from a fungal endophyte (*Pencillium restrictum*) for laboratory scale (Aim 2), and applying droplet probe, a unique *in situ* technique, to study natural products (Aim 3).

Aim 1 was achieved through examining a filamentous fungus with very prominent cytotoxicity, which our group is interested in for anticancer activity. Macrocyclic trichothecenes, which are known to be complex and very cytotoxic, were isolated. However, many of these compounds were first identified in the early 1960s so absolute configuration was not available, but modern techniques were applied to solve and complete the literature for this class of compounds.

Aim 2 was achieved two-fold through a media study to determine the best growing conditions for *P. restrictum* and then further optimizing the extraction, partitioning, and purification techniques compared to those previously published in literature. These techniques are important for compounds from fungi that have important biological activity because a large quantity of compound is necessary in order to conduct larger studies to get these potential drugs from the benchtop to the bedside.

Aim 3 was achieved through the examination of a herbarium specimen of *Garcinia mangostana* with droplet probe. Although not a fungus, this plant produces prenylated xanthones, which are also known for their cytotoxic activities. This technique has been applied to fungi many times in our lab, and this is the first time a sample as delicate as a herbarium specimen has been examined. This method paves the way for the use of this technique for precious, older natural products that would have previously been permanently damaging during the analysis process.

STEPS IN THE JOURNEY TO ADVANCE THE STUDY OF NATURE'S CHEMISTRY

by

Diana Kao

A Dissertation Submitted to
the Faculty of The Graduate School at
The University of North Carolina at Greensboro
in Partial Fulfillment
of the Requirements for the Degree
Doctor of Philosophy

Greensboro
2019

Approved by

Nicholas H. Oberlies
Committee Chair

APPROVAL PAGE

This dissertation, written by DIANA KAO, has been approved by the following committee of the Faculty of The Graduate School at The University of North Carolina at Greensboro.

Committee Chair Nicholas H. Oberlies

Committee Members Nadja B. Cech

Daniel A. Todd

Pamela R. Hall

October 10, 2019
Date of Acceptance by Committee

October 10, 2019
Date of Final Oral Examination

ACKNOWLEDGMENTS

To my family, which set expectations that I would not have otherwise strove for if not for their presence. My mother and my brother have set before me models of strength, independence, dignity, and success in the face of impediments. They turned their challenges into opportunities, and because of them, I am always chasing to become better. The steps of my journey have not always been easy, but those steps have been made easier because my family take care to let me know I do not have to walk this path alone and at any time I can call on them for aid. It is with great honor to say that 'my family' exceeds those two I have mentioned despite not being able to name them all here, but several have supported me to which I am grateful towards.

To Dr. Nicholas Oberlies, who opened his lab to me, I thought I was just going to get a Masters degree but you let me into your lab and believed in me enough to let me stay to achieve more than what I had initially planned. Thank you to my committee members: Drs. Nadja Cech, Daniel Todd and Pamela Hall, whom were able to give advice and support so that might I might overcome the challenges ahead of me in my projects. Thank you to Tyler Graf, Drs. Huzefa Raja and Amninder Kaur, whom taught me everything I know about Natural Products from scratch; thank you. Thank you to Dr. Grzybowski, whom let me do undergraduate research in his lab and to Dr. Funk, whom gave me the appreciation and foundation for structure elucidation. And to my friends, all of whom I won't name because there are too many, but I don't know how I could have

gotten by without them being there for me at the end of each day, week, month, and longer.

This research was supported by the National Center of Complimentary and Integrated Health, NIH via grant F31 AT009264 and the National Cancer Institute, NIH, via grant P01 CA125066.

TABLE OF CONTENTS

Page

LIST OF TABLES

Page

LIST OF FIGURES

Page

CHAPTER I

NEW TRICKS FOR OLD DOGS: TWO NEW MACROCYLIC TRICHOTHECENE EPIMERS AND ABSOLUTE CONFIGURATION OF 16-HYDROXYVERRUCARIN B

This is intended to be submitted to Magnetic Resonance Chemistry and is presented in that style. Flores-Bocanegra, L., Raja, H. A., Darveaux, B. A., Pearce, C. J., Oberlies, N. H.

Introduction

Macrocyclic trichothecenes are a class of metabolites, reported from both fungi and a few plant species, which are characterized by a cyclic sesquiterpene core that features an epoxide, resulting in unique configurations between the fused ring systems.[1, 2] A review in 2016 surveyed over 80 trichothecene analogues reported in the literature,[3] starting with the seminal work on a mixture of verrucarins A and B reported in 1946.[4, 5] There was an initial wave of interest in these compounds, likely due to potent cytotoxicity against a number of cell lines in the 1980s.[6, 7] However, more recently, research on these as potential anticancer leads has stalled due to concerns regarding general toxicity.[2] Indeed, a few methods have been reported for dereplication of trichothecenes, likely with the goal of eliminating their investigation.[8, 9] Despite the potential biological drawbacks, chemically the trichothecenes also have a complex and interesting structural core.[1, 10]

Some have posited that these compounds should be evaluated in more detail, since much of the toxicological data are reported on only a few prominent members of this structural class.[3] Certainly, scientists continue to be intrigued by this class of compounds, since new analogues are reported fairly regularly, together with studies on cytotoxic and insecticidal activities.[11, 12] For example, a 2017 review[13] supports the continued study of this class of compounds due to their immunomodulatory effects, which could be better understood with further mechanistic studies, particularly with respect to the growing interest in cancer immunotherapy.[14, 15]

There are over 150 trichothecene analogues that could be studied for structure activity relationships and/or other biological activities (**Figure A20**). However, some members of this class of compounds were first isolated, characterized, and reported in the 1970s and early 1980s (**Figures A20** and **A21**). As such, the NMR data are often reported with broad ranges in chemical shift values and lack the precision expected by modern standards. In addition, the absolute configuration of some stereogenic centers were not reported, and those data could be critically important with respect to the structure-activity relationships of these compounds, especially when discriminating between favorable vs. detrimental attributes. In this paper, we present two new macrocyclic trichothecenes and five known compounds, including reporting for the first time the absolute configuration of the epoxide across the C-2′ and C-3′ positions. These data are illustrative of an approach that can be used to study trichothecenes, and probably other well-known secondary metabolites, to better define their characterization data.

Results and Discussion

In the course of ongoing studies to pursue the Mycosynthetix library of fungal cultures for anticancer drug leads,[16] a culture identified as *Stachybotriaceae* sp., *Hypocreales, Ascomycota* (strain MSX72235) was prioritized for investigation. Using natural products chemistry protocols, two new and five known macrocyclic trichothecenes were isolated: 3′-epi-16-hydroxyverrucarin A (**1**), 16-hydroxyverrucarin B (**2**),[17] 3′-epiverrucarin X (**3**), verrucarin Z (**4**),[18] epiroridin acid (**5**),[19] 16-hydroxyroridin A (**6**),[20] and verrucarin X (**7**)[21] (**Figure 1**). For compounds **4** through **7**, the mass spectrometry and NMR spectroscopy data were comparable to literature values.

Compound **1** was isolated as a white solid, and its molecular formula was determined to be $C_{27}H_{34}O_{10}$ by HRESIMS, indicating 11 degrees of unsaturation. ^{13}C NMR data showed the presence of 27 carbons, inclusive of three carbonyl, six vinylic, eight oxygenated, and ten aliphatic carbons. ^{1}H and HSQC NMR experiments revealed the presence of five vinylic protons, congruent with three double bonds, and two aliphatic methyl groups. The ^{1}H NMR data also highlighted eight methylene and one methine protons, along with twelve protons on carbons adjacent to an oxygen. There were two hydroxy groups to account for the remainder of the protons in the molecular formula. The DEPT edited HSQC experiment noted 14 diastereotopic protons, which resembled the structure of verrucarins and indicated a macrocyclic trichothecene core,[3] along with two homotopic protons corresponding to the hydroxy methylene at position C-9. HMBC and COSY correlations were used to confirm a macrocyclic trichothecene core (**Table 1**), and in doing so, **1** was preliminarily identified as an isomer of 16-hydroxyverrucarin A.

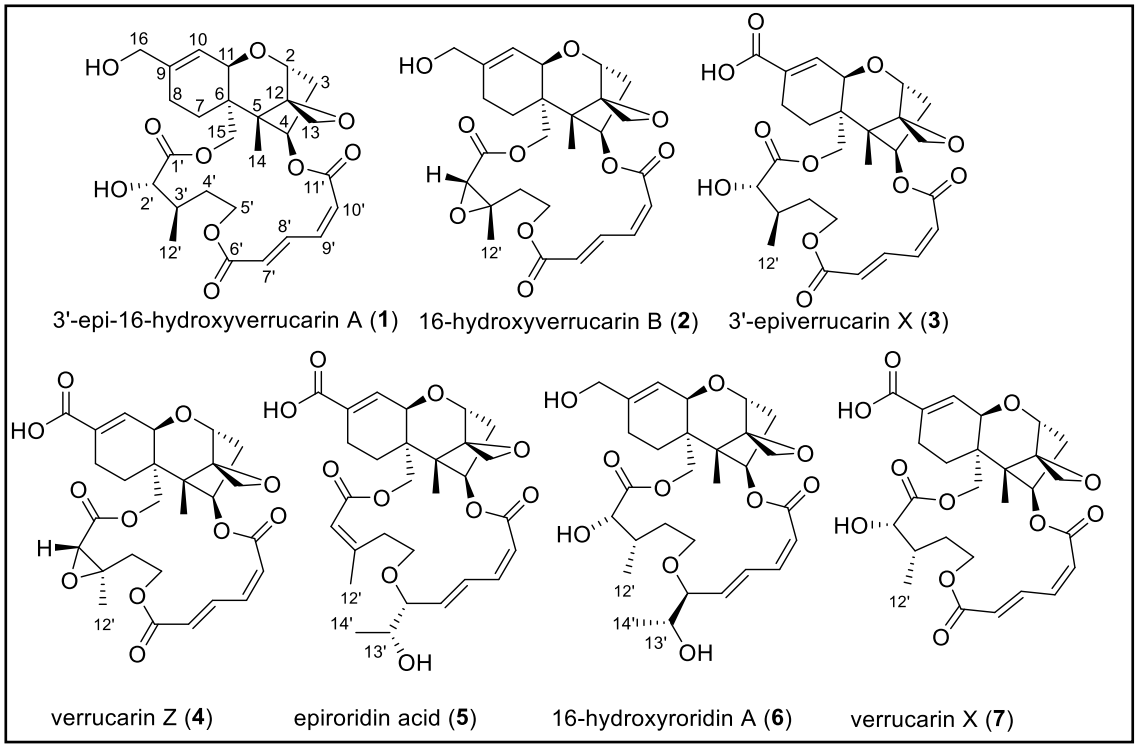

Figure 1. Structures of the Isolated Macrocyclic Trichothecenes (1-7).

Table 1. NMR Data (400 MHz ^{1}H, 100 MHz ^{13}C, $CDCl_3$) for 3′-epi-16-hydroxyverrucarin A (1).

Position	δ_C, type	δ_H (*J* in Hz)	NOESY	HMBC
2	79.1, CH	3.86, d (5.1)	13a	5, 12, 13, 14
3α	34.9, CH_2	2.48, dd (15.5, 8.2)	11	2, 5, 12
3β		2.26, dt (15.5, 4.7)		2, 4
4	75.5, CH	5.81, dd (8.2, 4.1)	11, 15	2, 5, 6, 12, 11′
5	49.6, C			
6	44.7, C			
7α	19.7, CH_2	1.76, tt (11.7, 2.7)		6, 7, 8, 9, 16
7β		1.91, m	2’	6, 7, 8, 9, 10, 15, 16
8α	23.0, CH_2	1.92, m	3’	7, 9, 10
8β		2.06, m		6, 7, 9, 10, 15
9	143.9, C			
10	117.5, CH	5.71, d (5.2)		6, 8, 16
11	66.4, CH	3.62, d (5.3)	3α, 4	2, 7, 9, 10, 15
12	65.2, C			
13a	47.9, CH_2	3.1, d (3.8)	2	2, 5, 12
13b		2.8, d (4.1)	14	2, 5, 12
14	7.4, CH_3	0.85, s	13b, 8′	4, 5, 6, 12
15a	63.3, CH_2	4.71, d (12.2)	4	5, 6, 7, 11
15b		4.22, d (12.1)	4	5, 6, 7, 1′
16	65.9, CH_2	4.07, m		9, 10
1′	174.8, C			
2′	74.3, CH	4.13, d (5.7)	7β	1′, 4′, 12′
3′	33.3, CH	2.34, dtd (11.4, 4.3, 2.1)	8α, 8′	4′, 12′
4′a	32.3, CH_2	1.9, m	2’	2′, 3′, 5′, 12′
4′b		1.76, tt (11.7, 2.7)		12′
5′a	61.2, CH_2	4.49, ddd (11.4, 5.4, 2.5)		3′, 6′
5′b		3.96, td (11.8, 3.3)	12	4′, 6′
6′	165.5, C			
7′	127.6, CH	6.04, d (15.7)		6′, 8′
8′	138.8, CH	8.03, dd (15.8, 11.7)	14, 3′	6′, 7′, 9′, 10′
9′	139.2, CH	6.67, t (11.4)		7′, 8′, 11'
10′	125.8, CH	6.14, d (11.0)		8′, 11′
11′	166.2, C			
12′	10.1, CH_3	0.87, d (6.9)	5′b	2′, 4'

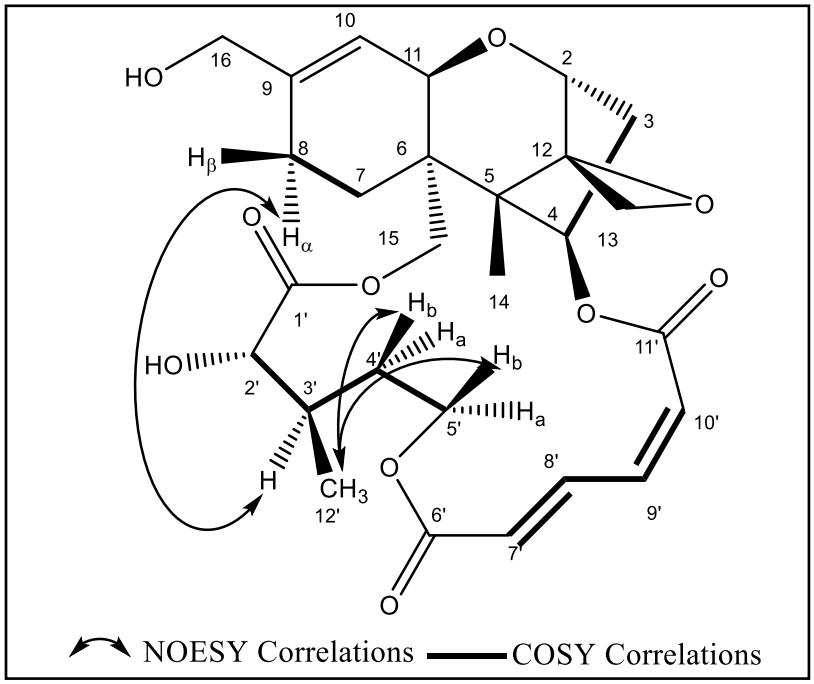

Figure 2. Key COSY and NOSEY Correlations for Compound 1.

While the ^{1}H and ^{13}C NMR signals of **1** were very similar to literature values of 16-hydroxyverrucarin A,[21] the *J*-value at position H-2′ was 5.7 Hz (**Table 1**), which was nearly double that reported in literature.[21] COSY correlations confirmed similar connectivity through the spin systems of H-2′ to H-3′ to H_2-4′ to H_2-5′ and of H-3′ to H_3-12′. Most NOESY correlations matched those reported previously, also supporting a trichothecene core (**Table 1, Figure 2**).[21] However, there was a key difference in the data associated with position C-3′. Specifically, there was a NOESY correlation between H-3′ and H-8α, suggesting inversion of that stereogenic center relative to the literature. Moreover, there were additional correlations in the NOESY spectrum between H_3-12′ and H-4′b and H-5′b, further supporting epimerization at C-3′. Using Mosher's esters methodology,[22] the absolute configuration at C-2′ was confirmed to be identical to 16-

hydroxyverucarrin A (**Figure 3**). Thus, the absolute configuration of **1** was determined based on the sum of the Mosher's data for position C-2′ and the relative configuration assigned via the NOESY spectrum, confirming the new trichothecene as 3′-epi-16-hydroxyverrucarin A (**1**).

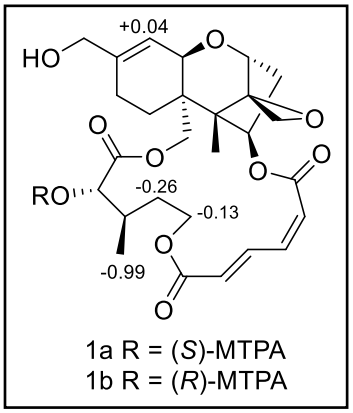

Figure 3. Determination of the Absolute Configuration of Compound 1 Using Mosher's Esters: $\Delta\delta_H$ Values [$\Delta\delta_H$ (in ppm) = $\delta_S - \delta_R$].

For compound **2**, the spectroscopy and spectrometry data were in agreement with the literature for 16-hydroxyverrucarin B.[7] However, the absolute configuration of the epoxide across positions C-2′ and C-3′ was not elucidated previously. Given the structural similarities of compounds **1** and **2**, and since the absolute configuration of **1** was fully elucidated, the absolute configuration of **2** was assigned via analysis of ECD (**Figure 4**) and NOESY data. Key NOESY correlations between H-2′ and H-15β, between H_3-14 and H_3-12′, and between H_3-14 and H-11 were used to establish the relative configuration of the epoxide from C-2′ and C-3′ (**Figure 5**) as well as the relative configuration of the trichothecene. Coupling those data with the nearly identical ECD spectra between **1** and **2** (**Figure 4**), the major trichothecene core was retained, and the

absolute configuration for **2** was discerned from the NOESY data. This marks the first time the absolute configuration of **2** has been established, illustrating the power of using modern techniques to fully interrogate the structure of a compound first reported in the 1980s.[7]

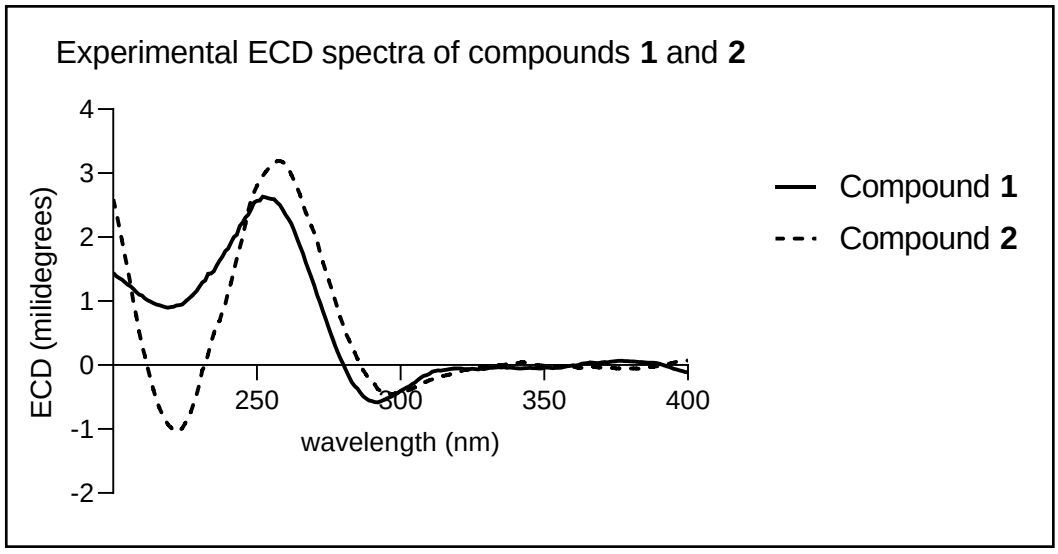

Figure 4. **Comparison of the ECD Data Between Compounds 1 and 2; Both Were Recorded in MeOH at 0.05 mg/mL.**

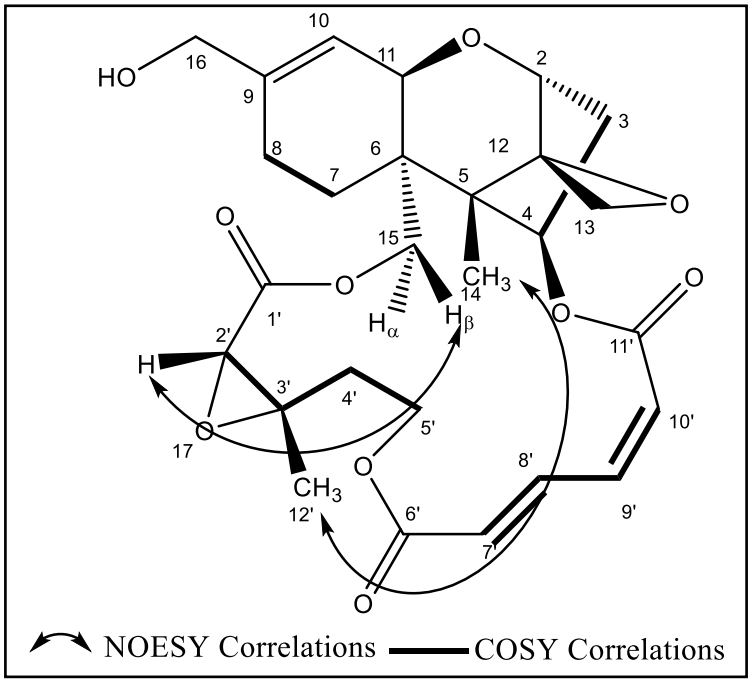

Figure 5. Key COSY and NOSEY Correlations for Compound 2.

Compound **3** presents yet another example where a superficial examination of the literature could yield an incorrect structure. The molecular formula ($C_{27}H_{32}O_{11}$) and NMR data initially suggested that the compound was verrucarin X.[21] However, further analysis of a subsequent fraction that yielded compound **7**, which had the identical molecular formula and a very similar NMR spectrum, but a different chromatographic profile, caused us to reconsider this presumption. Compound **3**, compound **7**, and the literature for verrucarin X[21] demonstrate overlapping chemical shifts at H-2′ with H-15β and H-3′, which yields a multiplet that prevents interpretation of the relevant *J*-values that might differentiate them (**Table 2**). Thus, compounds **3** and **7** were subjected to Mosher's esters analysis (**Figures 6 and A19**). The assignment of *S* at C-2′ was consistent between compounds **1**, **3**, and **7**. NOESY data was then utilized to confirm the configuration of C-

3′ in **3** via correlations between H_3-12′ and 5′b and between H-3′ and H-7α (**Figure 7**). In total, this demonstrated that compound **3** was 3′-epiverrucarin X, and the absolute configuration of compound **7** matched that of verrucarin X.

Of the remaining compounds, **4** was elucidated in 2015 via NOESY to determine relatively configuration and confirm the *trans* substitution across the epoxide by calculating the coupling constants that are better measured by modern NMR instruments.[18] Compound **5** was elucidated in 2016 after identifying two related but known compounds, which enabled them to base their stereochemical assignments by comparing the new and known compounds' observed coupling constants and chemical shifts, which is more accurate and reliable with modern instrumentation.[19] Finally, due to the potential renewed interest in macrocyclic trichothecenes, and because of the limited NMR technology available in 1987, the NMR data of 16-hydroxyroridn A (**6**) has also been included in the supporting information (**Figures A18-22**).

Table 2. NMR Data (700 MHz ^{1}H, 175 MHz ^{13}C, DMSO-*d*$_6$) for 3′-epiverrucarin X (3).

Position	δ_C, type	δ_H (mult., *J*)	NOESY	HMBC
2	78.1, CH	3.75, d (5.0)	13a	
3α	34.5, CH_2	2.43, d (8.1)	11	2, 5, 11
3β		1.98, dt (15.7, 4.8)		
4	75.7, CH	5.79, dd (8.1, 3.8)	11, 15	
5	48.9, C			
6	43.6, C			
7α	19.3, CH_2	1.60, t (12.8)	3′	7
7β		1.70, t (15.7)	2′, 4′b	
8α	22.1, CH_2	1.80, m		
8β		2.28, d (8.1)		
9	137, C			
10	131.0, CH	6.43, brs		16
11	65.1, CH	3.87, d (3.4)	3α, 4	5, 9, 10
12	65.2, C			
13a	46.9, CH	3.00, d (4.0)	2	12
13b		2.75, d (4.1)	14	12
14	7.0, CH_3	0.71, s	13b	4, 5, 6, 11
15a	61.6, CH_2	4.23, d (12.3)	4, 3′	5, 6, 11, 1′
15b		4.05, d (12.7)		5, 6, 7
16	168, C			
1′	173.5, C			
2′	72.7, CH	4.02, d (1.9)	7β, 4′b	1′, 3′, 4′, 12′
3′	32.3, CH	2.15, m	7α, 15a	
4′a	31.9, CH_2	1.76, t (15.7)		
4′b		1.59, t (12.8)	7β, 2′	
5′a	61.1, CH_2	4.29, m		
5′b		3.89, t (4.8)	12	
6′	164.9, C			
7′	127.3, CH	6.18, d (15.6)		6′, 9′
8′	138.5, CH	7.79, dd (15.6, 11.6)		6′, 10′
9′	138.1, CH	6.82, d (11.4)		7′, 11′
10′	126.3, CH	6.28, d (11.1)		8′, 11′
11′	165.6, C			
12′	10.5, CH_3	0.73, d (6.8)	5′b	2′, 3′, 4′

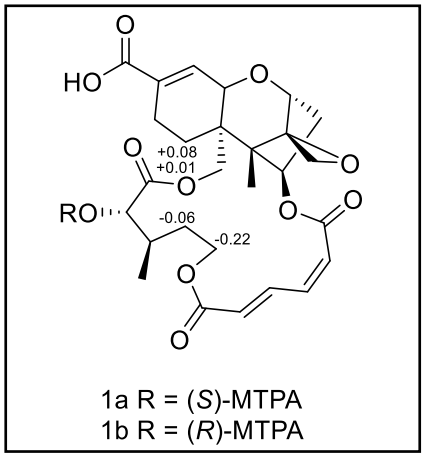

Figure 6. Determination of the Absolute Configuration of Compound 3 Using Mosher's Esters: $\Delta\delta_H$ Values [$\Delta\delta_H$ (in ppm) = $\delta_S - \delta_R$].

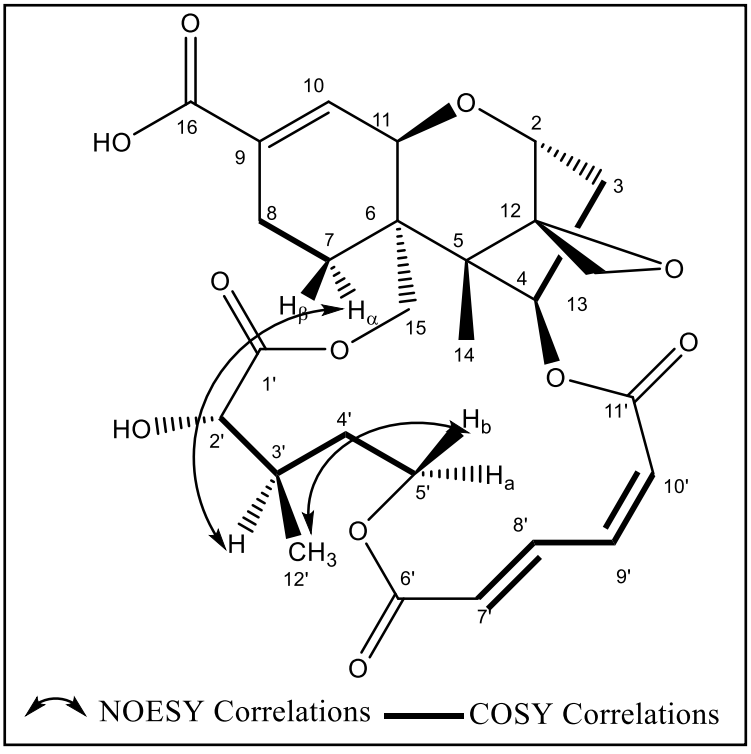

Figure 7. Key COSY and NOSEY Correlations for Compound 3.

Conclusions

The direct results from this project were the isolation and characterization of two new macrocyclic trichothecenes, as well as, refining the characterization data of a series of five other related, but known, analogues. A key component of this was to not presume the structure of the compounds, simply due to a molecular formula match in a database. Rather, we used Mosher's esters, ECD, and a suite of NMR spectroscopy data to both define the structures of the new compounds, as well as, refine the characterization data of the known compounds. A similar approach may be prudent when a well known class of secondary metabolites is re-evaluated for new biological activity, particularly with all the tools coming online as part of the genomics revolution.

Experimental

General experimental procedures

ECD data were collected in MeOH using an Olis DSM 17 CD spectrophotometer (Olis, Bogard, GA, USA). HRESIMS data were collected via a Thermo QExactive Plus MS (Thermo Fisher Scientific, San Jose, CA, USA) in positive and negative ionization modes coupled to a Waters Acquity ultraperformance liquid chromatography system (Waters Corp., Milford, MA, USA; 1.7 μm; 50 × 2.1mm column). A CombiFlash Rf system using a 12 g RediSep Rf Si-gel Gold column (both from Teledyne-Isco, Lincoln, NE, USA) was employed for normal-phase flash column chromatography. High-performance liquid chromatography (HPLC) separations were performed utilizing Varian ProStar HPLC systems equipped with ProStar 210 pumps and a ProStar 335 photodiode

array detector, using Galaxie Chromatography Workstation software (version 1.9.3.2, Varian Inc.). A Gemini–NX C_{18} preparative (Phenomenex, Torrance, CA, USA; 5 µm; 250 × 21.2 mm) column was used for HPLC. The solvents were obtained from Fisher Scientific.

Identification of fungal strain

Fungal strain MSX72235 was isolated in May 1993 from leaf litter. On difco potato dextrose agar and malt extract agar, strain MSX72235 grew only as yellowish - white sterile mycelium, and thus, morphological identification was not available for identification. For molecular identification, the ITSrDNA region of the fungal strain was sequenced with primers ITS1F and ITS4[23, 24] using methods noted in a recent review.[25] GenBank BLAST search with the ITS region of MSX72235 using the RefSeq database (https://www.ncbi.nlm.nih.gov/refseq/targetedloci/) showed high coverage and percent identity (≥97%) with genera such as *Xepicula, Myrothecium,* and *Paramyrothecium.*[26] These taxa are mitosporic, asexual fungi with affinities to the family *Stachybotriaceae, Hypocreales, Ascomycota.*[26] According to Lombard et al.[26] members of *Stachybotriaceae* have been reported as saprobes from plants, which agrees with the habitat from which MSX72235 was isolated. Since we only sequenced the ITS region in this study, strain MSX72235 can be identified as a *Stachybotriaceae* sp. Additional studies are warranted with sequence data from *RPB2, TEF1, CaM,* and LSU regions to more accurately identify strain MSX72235 in the order *Hypocreales* to genus and/or

species level.[26] The sequence data were deposited in GenBank using Accession numbers: MN328732, MN328733.

Fermentation, extraction and isolation

The fungal fermentation procedures have been outlined previously.[27] Briefly, strain MSX72235 was grown on malt extract agar Petri plates, and subsequently, cultures were inoculated in a medium containing 2% soy peptone, 2% dextrose, and 1% yeast extract (YESD media). Following incubation (7-10 days) at room temperature with agitation, the cultures were used to inoculate a small-scale solid-state fermentation, 50 mL of a rice medium, prepared using rice to which was added a vitamin solution and twice the volume of rice with H_2O in a 250 mL Erlenmeyer flask. This culture was incubated at 22˚C until it showed sufficient growth before initial chemical extraction and analysis. For the scale-up culture used for isolation of trichothecenes, strain MSX72235 was grown in a 2.8 L Fernbach flask containing 150 g of rice and 300 mL of H_2O and was inoculated using a seed culture grown in YESD medium as outlined above. This culture was also incubated at 22˚C before chemical extraction and analysis.

To the large-scale culture of strain MSX72235 grown on solid rice media was added 500 mL of 1:1 MeOH-$CHCl_3$. The culture was chopped with a spatula and shaken overnight (~16 hours) at ~100 rpm at room temperature. The sample underwent vacuum filtration, and the remaining residue was washed with 100 mL of 1:1 MeOH-$CHCl_3$. To the filtrate, 500 mL $CHCl_3$ and 1000 mL H_2O were added; the mixture was stirred for 30 min and then transferred into a separatory funnel. The bottom layer was drawn off into a

round-bottom flask, which was evaporated to dryness. The dried organic extract was re-constituted in 200 mL of 1:1 MeOH-CH_3CN and 200 mL of hexanes. The biphasic solution was shaken vigorously and then transferred to a separatory funnel. The MeOH-CH_3CN layer was evaporated to dryness under vacuum.

The organic extract (750 mg) was adsorbed to Celite 545 (Acros Organics, Geel, Belgium) with a minimal amount of solvent. The dried sample was purified using normal-phase silica gel flash column chromatography (RediSep RF Gold Si-gel column; 12g) using a gradient starting at 100% hexanes to $CHCl_3$ to 100% MeOH over a flow rate of 30 mL/min and 61 column volumes. Utilizing UV and ELSD data, the eluent was pooled into 5 fractions. Fractions 3 and 4 were purified further via preparative RP-HPLC. The elution gradient of fraction 3 was 35 to 40% CH_3CN-H_2O with 0.1% formic aid over 30 min with a flow rate of 21.20 mL/min. The following compounds were isolated: 3′-epi-16-hydroxyverrucarin A (**1**; 7.08 mg; t_R 9.5 min), 16-hydroxyverrucarin B (**2**; 0.85 mg; t_R 13.5 min), 3′-epiverrucarin X (**3**; 3.31 mg; t_R 14.0 min), verrucarin Z (**4**; 1.78 mg; t_R 18.5 min), epiroridin acid (**5**; 2.08 mg; t_R 22.0 min). The elution gradient of fraction 4 was 30 to 40% CH_3CN-H_2O with 0.1% formic acid over 20 min with a flow rate of 21.20 mL/min. The following compounds were isolated: 16-hydroxyroridin A (**6**; 1.45mg; t_R 13.0 min) and verrucarin X (**7**; 3.27 mg; t_R 17.5 min). The known compounds were identified by comparing ^{1}H NMR, ^{13}C NMR, and mass spectrometry data with the literature.[17-21]

3′-epi-16-hydroxyverrucarin A (**1**): White powder. $[\alpha]_D^{23}$ +1.52 (0.1, $CHCl_3$) UV ($CHCl_3$) CD (0.05 mg/ml, MeOH) λmax (Δε) 253 (+2.6), 291 (-1.6) nm, ^{1}H NMR

($CDCl_3$, 400 MHz) and ^{13}C NMR ($CDCl_3$, 100 MHz) data, see Table 1. HRESIMS obsd. 519.2233 m/z $[M+H]^+$ (calcd. for $C_{27}H_{35}O_{10}$, 519.2230).

16-hydroxyverrucarin B (**2**): White powder. CD (0.05 mg/ml, MeOH) λmax (Δε) 230 (-1), 251 (+4), 286 (-0.5) nm, ^1H NMR ($CDCl_3$, 700 MHz) and ^{13}C NMR ($CDCl_3$, 175 MHz) data. HRESIMS obsd. 517.2076 m/z $[M+H]^+$ (calcd. for $C_{27}H_{33}O_{10}$, 517.2073). The NMR data were consistent with those reported in literature.[17]

3′-epiverrucarin X (**3**): White powder. $[\alpha]_D^{25}$+0.66 (0.1, DMSO) UV (DMSO) ^1H NMR ($(CD_3)_2SO$, 700 MHz) and ^{13}C NMR ($(CD_3)_2SO$, 175 MHz) data, see Table 2. HRESIMS obsd. 533.2026 m/z $[M+H]^+$ (calcd. for $C_{27}H_{33}O_{11}$, 533.2023).

verrucarin Z (**4**): White powder. HRESIMS obsd. 531.1869 m/z $[M+H]^+$ (calcd. for $C_{27}H_{31}O_{11}$, 531.1866). The NMR data were consistent with those reported in literature.[18]

epiroridin acid (**5**): White powder. HRESIMS obsd. 545.2392 m/z $[M+H]^+$ (calcd. for $C_{29}H_{37}O_{10}$, 545.2386). The NMR data were consistent with those reported in literature.[19]

16-hydroxyroridin A (**6**): White powder. ^1H NMR ($CDCl_3$, 700 Mhz) and ^{13}C NMR ($CDCl_3$, 175 MHz) data. HRESIMS obsd. 549.2702 m/z $[M+H]^+$ (calcd. for $C_{29}H_{41}O_{10}$, 549.2700). The NMR data were consistent with those reported in literature.[20]

verrucarin X (**7**): White powder. HRESIMS obsd. 533.2026 m/z $[M+H]^+$ (calcd. for $C_{27}H_{33}O_{11}$, 533.2023). The NMR data were consistent with those reported in literature.[21]

Acknowledgements

Diana Kao was supported by the National Center for Complementary and Integrated Health, NIH *via* grant F31 AT009264. Support also came from the National Cancer Institute, NIH *via* grant P01 CA125066. The mass spectrometry data were acquired in the Triad Mass Spectrometry Facility. We thank Ms. A. Scott from UNCG for assistance with the graphical abstract.

CHAPTER II

LESSONS LEARNED VIA SCALED-UP PRODUCTION OF ω-HYDROXYEMODIN FROM *PENICILLIUM RESTRICTUM* (STRAIN G85)

This is intended to be submitted to Planta Medica and is presented in that style. The contribution to this manuscript is approximately one third. Co-authors include Graf, T. N., Raja, H. A., Rivera-Chávez, J. Gallagher, J. M., Oberlies, N. H.

Introduction

Penicillium restrictum (strain G85) is a fungal endophyte that was isolated from surface sterilized stems of milk thistle (*Silybum marianum*).[28] From an organic extract of a solid phase rice culture of strain G85, a series of polyhydroxyanthraquinones were isolated.[29] Among these, ω-hydroxyemodin showed promising activity as a quorum sensing inhibiter against clinical isolates of methicillin-resistant *Staphylococcus aureus* (MRSA) both *in vitro*[29] and *in vivo*.[30] For example, in the murine model, we postulate that ω-hydroxyemodin inhibited the DNA-binding capacity of a virulence regulator, AgrA, resulting in decreases in disease severity, abscess and ulcer area, bacterial burden, and certain pro-inflammatory cytokines.[30]

The National Institute of Allergy and Infectious Diseases (NIAID) has called for strategic approaches to combat antibiotic resistant strains by disarming the bacteria of its toxins, but leaving it unharmed, so the body's immune system can clear the infection.[31] To work, antivirulence or quorum quenching molecules are thus necessary to fight

bacterial infections,[32] and ω-hydroxyemodin has shown some promise in this regard.[29, 30] With MRSA growing as a global health concern, it is important to carry out further pharmacology studies on quorum sensing inhibitors, otherwise, testing the feasibility of the strategy proposed by NIAID is not possible. As such, this required a substantial increase in production of ω-hydroxyemodin.

Supply of natural products is always an important issue when scientists are trying to demonstrate the biological efficacy of chemical entities for future studies, i.e. either preclinical or clinical undertakings.[33] While total synthesis would likely be pursued for future development, if initial preclinical work demonstrated promise, we performed fermentation studies for rapid turn around and laboratory scale control. Moreover, since strain G85 was isolated as an endophyte, and since those cultures are sometimes fickle when it comes to repeated growths in the laboratory, we thought it presented an interesting test case of scaling up a promising lead on the laboratory scale. Current synthetic approaches require emodin as a starting material for producing ω-hydroxyemodin,[34] and emodin has to either be first synthesized,[35, 36] obtained commercially, or isolated from a natural source, such as various plant (Rhubarb, Aloe) or fungal sources, including lichens.[29, 36] As synthesis of ω-hydroxyemodin from emodin can be inefficient, cost prohibitive, and time consuming, most companies supplying ω-hydroxyemodin as a pure compound are also known to isolate it from a natural source. Thus, newer and more effective methods are necessary for the isolation of ω-hydroxyemodin in large-scale (gram) quantities for future studies towards the goal of preclinical studies.

In our previous work using a *Penicillium* sp. we were able to isolate approximately 19 mg of pure ω-hydroxyemodin from one large-scale grain based fermentation (4 x 25 g rice flasks).[29] Interestingly, the very first isolation of ω-hydroxyemodin as a new compound (at that time it was termed citreorosein) was also reported from a fungal strain, *Penicillium cyclopium*,[37] which was more recently identified as *P. chrysogenum*.[38, 39] In this study, various growth conditions of strain G85 were screened using media studies, and the resulting cultures were analyzed using a droplet-liquid microjunction-surface sampling probe (droplet probe).[40-44] The droplet probe allows us to rapidly screen the cultures *in situ* by direct analysis of the surface of the fungus and carry out a targeted analysis of ω-hydroxyemodin. In addition, we modified and optimized our traditional extraction, separation, and isolation protocols[29, 45] to more efficiently obtain 850 mg of the purified ω-hydroxyemodin by solid-state fermentation for preclinical study. Our goal was to increase the supply of ω-hydroxyemodin by lowering both cost and time while also accomplishing it in an environmentally friendly manner.

The aim of this article is to express strategies that could be used for enhancing compound production in a laboratory setting, discussing both mycological growth conditions and analytical chemistry methodologies. As such, it is the intent not to only produce a report of what we did, but rather, utilize our results as an example of what happens during the scale up process. In short, this study provides a modern example of laboratory-based scale up of solid-state fermentation cultures in an academic setting, resulting in the isolation of a fungal natural product from a *Penicillium* sp.

Materials and Methods

Mycology: Media and fermentation

When strain G85 was first isolated and cultured on nutrient media such as potato dextrose agar (PDA; Difco Laboratories, Sparks, MD), malt extract agar (MEA; Difco Laboratories), and yeast extract, soy peptone, dextrose agar (2% soy peptone, 2% dextrose and 1% yeast extract; YESD; Difco Laboratories), it produced red guttates in both PDA and MEA media (**Figure 8a**).[29] The red guttates were indicative of the presence of the polyhydroxyanthraquinone compounds, including ω-hydroxyemodin, which was the compound of interest. However, when the fungus was grown out on the same three media used previously to make a seed culture for large-scale production, we noticed that the red guttates were absent in all three of the media conditions (**Figure 8b**). It has been noted previously in the literature that repeated sub-culturing of fungal strains leads to attenuation of target compounds due to domestication.[46, 47]

Therefore, for the large-scale isolation of ω-hydroxyemodin, the fungal strain G85 was grown on multiple media types and pH to determine the most optimal seed culture media for scale-up purposes. Both solid and liquid broths were utilized to grow strain G85. including media we used in our previous study.[29]

Figure 8. *Penicillium restrictum* (G85) at the Time of the Initial Study (2014). Note the red guttates (1A). *Penicillium restrictum* in 2016 using the same media conditions (1B). Potato dextrose agar (A) Malt Extract agar (B) Yeast extract soy peptone dextrose agar (C).

For solid (agar-based) media we used PDA, MEA, and Sabouraud dextrose agar (SDA; Difco Laboratories). The PDA and MEA media were grown under 3 different pH conditions: 5, 8 and 11, respectively. Further, MEA media was supplemented with L-cysteine and G85 was grown in both light and dark conditions at pH 5, and 8, respectively. Strain, G85 was grown on SDA media, which was supplemented with 20, 40, 60, and 80% peptone and allowed to grow in both light and dark conditions. Finally, we also grew strain G85 with SDA media made with tap water and 50, 75, and 100% deuterated water, both under light and dark conditions, respectively.

Liquid broths used for growing strain G85 include: potato dextrose broth (PDB; Difco Laboratories), malt extract broth (MEB; Difco Laboratories), and Czapek Dox broth (CDB; Honeywell Fluka, Morris Plains, NJ). Strain G85 was grown on PDB and MEB at pH, 5, 8, and 11, respectively. The CDB media was supplemented with NaF, and

CaF_2, respectively. Other media conditions employed were 1:1 PDB:MEA with and without CaF_2, and MEB supplemented with 50 mg of streptomycin sulfate, and penicillin G antibiotics (**Figure B1**).

Droplet-liquid microjunction-surface sampling probe (droplet probe)

Monitoring the biosynthesis of secondary metabolites in agar-based fungal cultures *in situ* was performed using the droplet probe coupled with a Waters Acquity ultraperformance liquid chromatography (UPLC) system (Waters Corporation, Milford, MA) to a Thermo QExactive Plus (Thermo Fisher Scientific, Waltham, MA) via procedures described previously by Sica et al[40, 42, 44] and reviewed recently. This mass spectrometry technique is a non-invasive and non-destructive method that allows for "mini extractions" as well as mapping of the location of secondary metabolites on the surface of a fungal culture.[40, 42, 44, 48] Droplet probe analysis showed that SDA media was the most suitable growth agar media for production of polyhydroxyanthraquinones including ω-hydroxyemodin (see Results).

All fungal cultures were grown by solid-state fermentation in screener scale conditions (10 grams) using either Botan Calrose rice, 1:1 Botan:Indian Rice, Cheerios, breakfast Oatmeal, or Kokuho Rose rice, respectively in 250 mL Erlenmeyer flasks. Two different seed cultures, YESD broth and Sabouraud dextrose broth (SDB), were utilized to inoculate each of the solid media (**Figure B2**). The screener scales were grown to determine the most suitable grain-based substrate for our scale-up. Solid state-fermentation was used for scaling-up production of ω-hydroxyemodin in the laboratory,

because it is less expensive than pure liquid broth medium and often yields higher amounts of the fungal extract.[49] Results of the small screener scale study suggest that both Botan and Kokuho varieties of rice were suitable grain-based substrates (see Results).

Large scale solid-state fermentations

To prepare large-scale solid-state fermentation cultures, 50 mL of SDB seed cultures were initiated by cutting a piece of agar with fungal mycelium from the leading edge of a 14-day old Petri dish agar culture of strain G85 grown on SDA. Following incubation (7 days) at 22 °C with agitation, the SDB seed culture was used to inoculate Botan rice. We started grain-based fermentation cultures in different sizes for scale-up, which encompassed small and large sterile mycobags, 250 mL Erlenmeyer flasks, and 2.8 L Fernbach flasks. For example, 10 g of Botan Calrose rice were prepared by adding 10 g of rice to a 250 mL flask with 20 mL of DI-H_2O, followed by autoclaving at 221 °C for 30 min. For larger fermentations, 100 g of Botan rice was autoclaved with 200 mL of distilled water and inoculated with 50 mL of SDB seed culture; 150 g of rice was autoclaved with 300 mL of distilled water and inoculated with 75 mL of seed culture; while 1000 g of rice was autoclaved with 2000 mL of distilled water and inoculated with 200 mL of SBD seed culture. All cultures were grown for approximately 3-5 weeks before they were extracted. During our study, we observed that cultures grown 4-5 weeks produced a higher yield of the target compound (**Figure B3**).

Chemistry: Extraction and isolation of the target compound

All solvents used for HPLC and automated flash chromatography were HPLC grade. Solvents used for extractions, partitions, and open column fractionation were of ACS grade or better. All solvents were obtained from Thermo Fisher Scientific or PHARMCO-AAPER (Brookfield, CT)

Extraction and filtration using chloroform and methanol

Solid phase rice cultures of 100-150 g (large scale) were extracted using 400 mL of 1:1 $CHCl_3$:MeOH. For solid phase rice cultures of 10 g (small scale), 60 mL of 1:1 $CHCl_3$:MeOH was used to extract. All extraction mixtures were shaken overnight, filtered on a Büchner funnel, and rinsed with a small amount of $CHCl_3$ and MeOH. Later samples had celite added (10-15 g celite per 10 g of rice culture) to hasten filtration.

Extraction and filtration using ethyl acetate

Several solid phase rice cultures totaling 500 g were extracted using 1.5 L of ethyl acetate (EtOAc). The extraction was allowed to stand overnight, 150 g of celite was added, and the sample was filtered on a Büchner funnel. The solids on the filter were resuspended in 1 L of MeOH and filtered again. The combined effluent was dried to a volume of 200 mL.

Extraction and filtration using acetone

Solid phase rice cultures of various sizes were mixed with celite (15 g celite per 10 g of rice culture), transferred to a large mixing bowl and acetone added until the mixture had the consistency of wet cement. Samples were allowed to sit for 15 minutes before being filtered using a Büchner funnel. The pellet in the funnel was transferred back into the mixing bowl and acetone added again to the same consistency as before. The sample was re-filtered using the Büchner funnel. This resuspension and filtration of the pellet was repeated two or three times until most of the orange color of the pellet was extracted out.

Extract cleanup using an open silica column

Acetone extracts were passed through a layer of silica (~400 mL of silica per 100 g of rice culture) on a glass-fritted vacuum filter funnel, and the silica was washed with acetone until little color eluted. The effluent was evaporated under a mild vacuum (~120 mbar) to recover much of the acetone for reuse.

Partitioning using chloroform and water

The 1:1 $CHCl_3$:MeOH extract was transferred to a separatory funnel and mixed with 600 mL of $CHCl_3$ and 2.5 L of H_2O. The combined mixture was partitioned and the $CHCl_3$ layer collected. The methanolic aqueous layer was repartitioned with 600 mL of $CHCl_3$ two or three more times. The combined $CHCl_3$ layers were dried completely, recovering the evaporated $CHCl_3$ for recycling.

Partitioning of aqueous layers using ethyl acetate and water

Residual methanolic aqueous layers from the $CHCl_3$ partitions were observed to contain substantial quantities of ω-hydroxyemodin. These methanolic aqueous layers were evaporated to remove the MeOH, and then partitioned between EtOAc and H_2O (250 mL of each layer per 40 g of rice culture). The aqueous layer was repartitioned with half the amount of fresh EtOAc two to three more times (until the organic phase lost color).

Partitioning of extracts using ethyl acetate and water

Extracts from any of the extraction techniques ($CHCl_3$:MeOH or acetone) were evaporated to remove all organic solvent (recovering much of the organic solvent for recycling) before partitioning between EtOAc and H_2O (100-200 mL of each layer per 100 g of rice culture). The aqueous layer was repartitioned with half the initial amount of fresh EtOAc two to three more times (until the organic phase lost color).

Partitioning using CH_3CN and methanol versus hexanes

All $CHCl_3$ and EtOAc partition products were evaporated completely (recovering the organic solvent for recycling) before partitioning between 1:1 CH_3CN:MeOH and hexanes. Partition volumes were 50-100 mL of each phase per 100 g of rice culture. The hexanes layer was partitioned against 40-80 mL of fresh 1:1 CH_3CN:MeOH twice more. The defatted CH_3CN:MeOH layers were combined and evaporated completely

(recovering the solvent for reuse). Hexanes layers from numerous partitions were combined and evaporated to recover the solvent for reuse.

Sample purity analysis by UPLC

Samples were analyzed using a Waters Acquity ultraperformance liquid chromatography (UPLC) system (Waters Corporation) running a gradient elution from 10% CH_3CN in H_2O (0.1% formic acid) to 100% CH_3CN over 4.5 minutes at a flow rate of 0.4 mL/min, a column temperature of 40 °C and observing at 288 nm. Using pure ω-hydroxyemodin isolated from this study, a calibration curve was created for the measurement of ω-hydroxyemodin content in various extracts and fractions.

Automated flash silica chromatography (linear gradient method)

Samples were separated on a Teledyne ISCO CombiFlash Rf 200 using RediSep RF Gold HP Silica columns (both from Teledyne ISCO, Lincoln, NE) and chromatography monitored by UV at 288 nm and with ELSD. Defatted extracts from 2 to 4 g were separated using an 80-g gold silica RediSep column running isocratic at 100% $CHCl_3$ for 3 column volumes, then a ramped gradient from 0 to 10 % MeOH in $CHCl_3$ over 11 column volumes, then to 100 % MeOH over 1 column volume and washing with 100 % MeOH for 2 column volumes. ω-Hydroxyemodin eluted at 6-8 % MeOH and for isolations of extracts with >8 % ω-hydroxyemodin content, crystals of ω-hydroxyemodin were observed in fractions containing ω-hydroxyemodin. For extracts with <8 % ω-hydroxyemodin content, no crystals were observed. After allowing the crystal containing

fractions to crystalize overnight, the fractions containing crystals were filtered and the crystals washed with $CHCl_3$.

Automated flash silica chromatography (step gradient method)

Samples were separated on the CombiFlash Rf 200 using RediSep Gold Silica columns (as above). Polyhydroxyanthraquinones from extracts with less than 8% ω-hydroxyemodin content were isolated using an 80-g gold silica RediSep column running isocratic at 100% $CHCl_3$ for 3 column volumes, isocratic at 15 % MeOH in $CHCl_3$ for 3 column volumes and washing at 100 % MeOH for 3 column volumes. Polyhydroxyanthraquinones eluted between 4.5 and 5.5 column volumes.

HPLC purifications

HPLC separations were carried out on a Varian ProStar HPLC system equipped with ProStar 210 pumps, a ProStar 701 fraction collector, a ProStar 335 diode array detector (DAD), and Galaxie Chromatography Workstation software (version 1.9.3.2, Varian Inc.). Separations were monitored by UV absorbance at 288 nm. Semi-preparative HPLC separations were carried out using a Phenomenex Luna 5 µm particle size Silica (2) column (10 x 250 mm) at a flow rate of 4.7 mL/min. Preparative HPLC separations were carried out using a Phenomenex Luna 5 µm particle size Silica (2) column (21.2 x 250 mm) at a flow rate of 21.2 mL/min. All semi-preparative and preparative separations were run utilizing a gradient from 0:100 to 90:10 of A:B, where A = 1:9 MeOH:$CHCl_3$ and B = $CHCl_3$.

Chloroform cleanup

Extracts were suspended in $CHCl_3$ (1-2 mL per gram of extract), vortexed and sonicated, then centrifuged to produce a pellet. The supernatant was removed leaving behind a sample enriched for polyhydroxyanthraquinones. This procedure would be repeated several times to highly reduce the non-polyhydroxyanthraquinones, at which point little benefit was derived from further rounds as a small quantity of polyhydroxyanthraquinones was lost during each round.

For semi-pure ω-hydroxyemodin, the sample was resuspended in $CHCl_3$ (1-2 mL per 800 mg of sample), vortexed and sonicated, then centrifuged to produce a pellet. This procedure was repeated several times while monitoring the purity of the pellet and supernatant by UPLC to determine completeness.

Final product analysis

NMR experiments were conducted in $CDCl_3$ on a JEOL ECA-500 NMR spectrometer operating at 500 MHz for ^{1}H and 125 MHz for ^{13}C (JEOL USA, Inc., Peabody, MA, USA). HRESIMS data was obtained using a Thermo QExactive Plus mass spectrometer (ThermoFisher Scientific) paired with an electrospray ionization source.

Results and Discussion

Mycology: Media and fermentation

Among the different media tested with strain G85 (**Figure B1**), SDA turned red after 14–21 days of growth (**Figure 9**). Repeated growth on the same media gave

identical results. Since ω-hydroxyemodin and other polyhydroxyanthraquinones have a strong orange color, which might be the cause of the plate coloration, we hypothesized that growing the culture in SDB for large-scale isolation would increase yield. Droplet probe analysis of this media showed an increased production of polyhydroxyanthraquinones including ω-hydroxyemodin and that the compounds had exuded into the culture media.

Mycology: Droplet-liquid microjunction-surface sampling probe

Using the droplet probe a compound map was constructed with the G85 strain grown on SDA media showing the presence of the major compounds produced, which include the target compound, ω-hydroxyemodin (**Figure 10**). The compounds were identified by comparison of their high-resolution mass, retention time, and tandem mass chromatogram to the pure compounds. This examination showed that the compounds were no longer on the surface of the mycelia including guttates but had been secreted into the surface of the media, thus the media developed a dark red color (**Figure 9** and **10**).

Mycology: Which seed culture is better for large-scale fermentation?

Penicillium restrictum (G85) was grown on commercial rice (variety: Botan Calrose) using SDB (left) and YESD (right) as seed culture (**Figure 11**). Results showed that the amount of ω-hydroxyemodin isolated per flask was higher when SDB was used as seed culture using Botan rice (**Figure B2**). The brightness of the yellow color was

correlated with higher production of ω-hydroxyemodin (**Figure B4**). Therefore, for all subsequent growths of strain G85 for large-scale production, we grew the fungus in SDB.

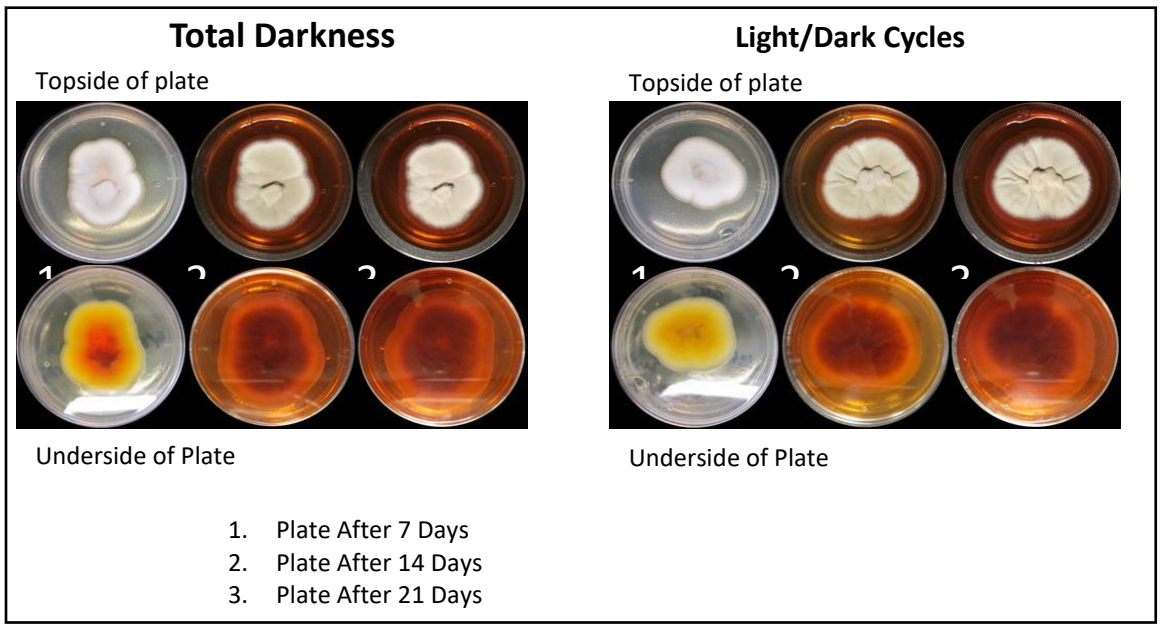

Figure 9. When Strain G85 was Grown on Sabouraud Dextrose Agar (Difco Laboratories, Sparks, Maryland), the Fungus Produced Red Color, which Diffused into the Media; this Correlated Well with the Production of Polyhydroxyanthraquinones Along with the Target Compound, ω-Hydroxyemodin.

Mycology: Large scale solid-state fermentations with Botan rice

To permit large scale purification of the target compound, the growth conditions of fungal strain G85 was scaled-up in 266 small 250 mL Erlenmeyer flasks (10 g of rice), 10 large 2L Fernbach flasks (100 g of rice), 6 small sized mycobags (150 g of rice), and one large sized mycobag (1000 g of rice), respectively, with approximately double the rice weight in water added and autoclaved.

Previous studies on large-scale production of fungal secondary metabolites have also successfully used solid-state fermentation.[41, 50] We did not use liquid fermentation for large-scale isolation because it was not feasible for our laboratory and we did not have access to large bioreactors routinely utilized for liquid fermentation.[41, 49]

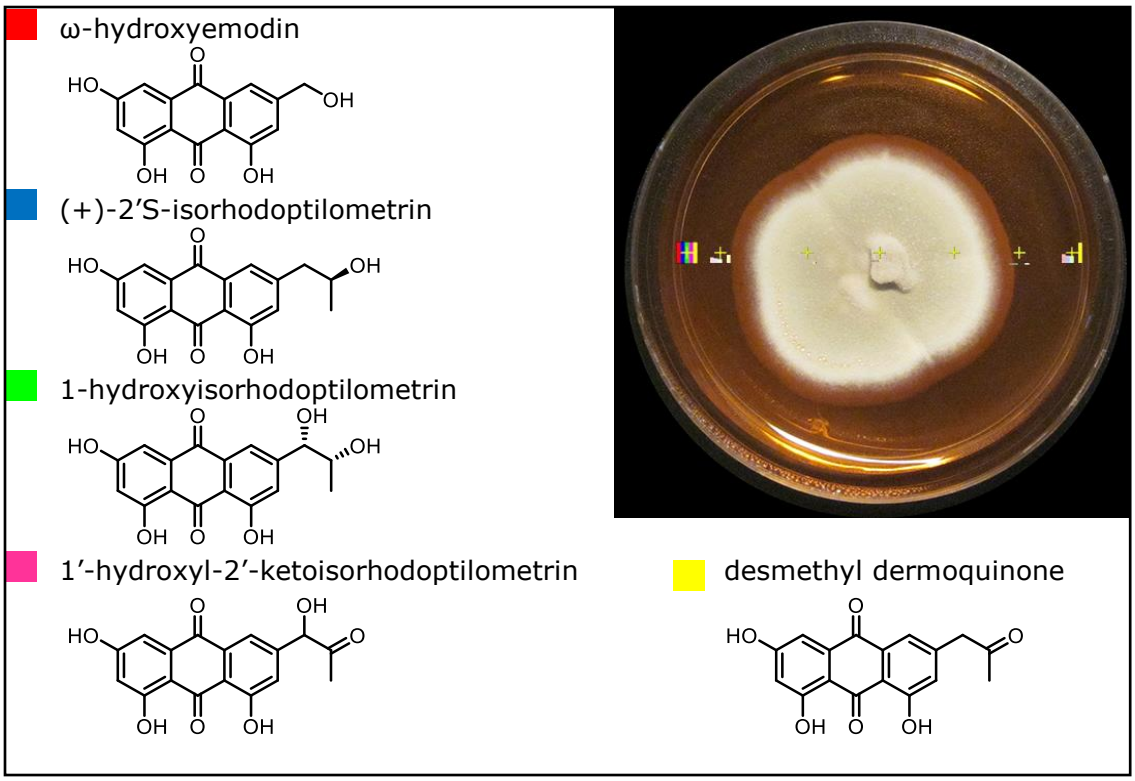

Figure 10. Surface Sampling of the *Penicillium restrictum* Strain G85 using Droplet-LMJ-SSP. A scanned image of *P. restrictum* on SDA. Bars refer to identified compound produced by strain G85. Red = ω-hydroxyemodin; Blue = (+)-2'*S*-isorhodoptilometrin; Green = 1-hydroxy-isorhodoptilometrin; Pink = 1'-hydroxy-2'-ketoisorhodoptilometrin; and Yellow = desmethyl dermoquinone. *Via* heat mapping experiments with the droplet probe, ω-hydroxyemodin and other polyhydroxyanthraquinones were shown to be present predominantly in the highly colored areas of the media.

Figure 11. *Penicillium restrictum* (G85) on Commercial Rice (Variety: Botan) Using Sabouraud Dextrose Media (Left), and YESD (Right) as Seed Culture. The amount of ω-hydroxyemodin isolated per flask was higher when Sabouraud Dextrose media was used as seed culture. The brightness of the yellow color was correlated with higher production of ω-hydroxyemodin.

Mycology: Which grain-based fermentation is better for large-scale production?

Among the five different grain-based media we tested for large-scale production, Botan rice showed the best yield (20 mg per 10g rice using in YESD as seed culture), and (30 mg per 10g rice using SDB as seed culture) followed by Kokuho rice (25 mg per 10g rice using SDB as seed culture) (**Figure B2**). For all subsequent large-scale growths, we used Botan rice and SDB for scale-up purposes (**Figure 12**).

The G85 fungal cultures were initially extracted using standard methods in our laboratory for extractions of fungal cultures.[29, 45] An extraction of 100g of solid phase rice culture led to slow filtration due to clogging by fungal spores, starches, and an immiscible particle suspension-all of which led to emulsions and blockage of the filter

paper. This is because often large amounts of solid material would be extracted along with the fungal metabolites, diluting potency, complicating purification of fungal metabolites.[50] To overcome these issues, Celite was added to absorb the water, which allowed greater surface area for filtration, which resulted in filtration up to ten times faster. Initial partitioning methods utilized 4:1:5 $CHCl_3$:MeOH:H_2O, but ω-hydroxyemodin was recognized to have a low solubility in $CHCl_3$, leaving as much as 50% of the available ω-hydroxyemodin in the aqueous phase during the this partitioning step (**Figure B5**). Due to this low solubility in $CHCl_3$, acetone was selected as the extraction solvent due to its miscibility with water when compared to $CHCl_3$ for extraction efficiency, capacity for rapid drying compared to methanolic water, and status as a green solvent.

Chemistry: Modifications to extraction protocols

Extractions with acetone were completed within 15 minutes of mixing the solvent (**Figure B2**) due to the ability of acetone to penetrate deeply into the rice media. Filtrations occurred quickly with the addition of celite. Any gold-orange color (indicative of the unextracted polyhydroxyanthraquinones) remaining in the residual pellet on the filter was re-extracted with acetone. The final pellet was gray, indicating complete recovery of available polyhydroxyanthraquinones from the fungal culture.

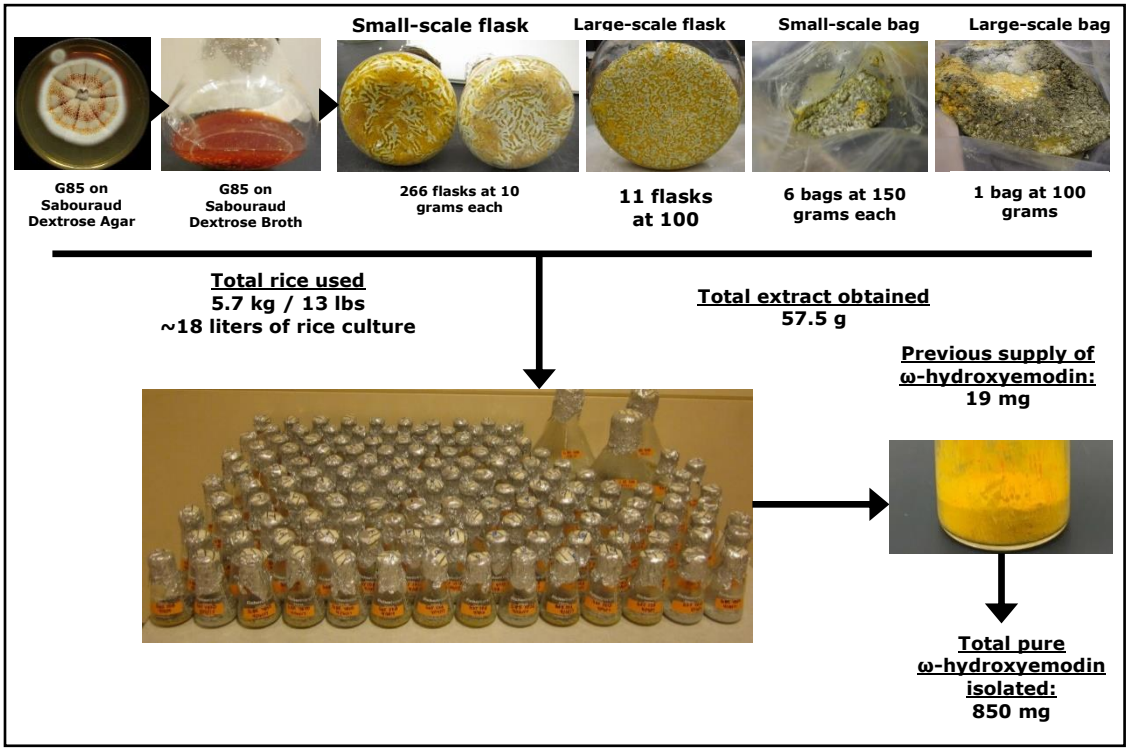

Figure 12. General Growth Schematic. Large-scale laboratory fermentation of strain G85 on rice using different modes of growth on commercial rice (variety: Botan).

Chemistry: Modification of partition method

Due to the more thorough extraction by acetone, including very polar sugars and peptides, which had also been scaled up in addition to the polyhydroxyanthraquinones.[51] The filtrate (90% acetone, 10% water) was passed through an open silica column via vacuum as an additional clean up step. Without this additional step, the following EtOAc partitioning step led to difficulties in partitioning and further purification. With this additional step, a layer of polar molecules remained bonded to the top of the silica (giving the silica a fondant consistency). The clarified acetone effluent was dried under vacuum until only the water from the rice remained. If the acetone is thoroughly removed, the

EtOAc partition separates very rapidly with no emulsions and can be run with very small volumes of solvent. The final defatting step, utilizing 1:1 CH_3CN:MeOH and hexanes, remain unchanged from previously reported methods except that the solvent volumes used are a quarter that of previous work (due to the sample being cleaner at this step). Overall, this method uses less solvent, is greener than the previous methods, and recycles virtually all the solvent used. The increased time taken at each step does not increase linearly with increasing sample size allowing much larger samples to be extracted with little more effort.

Chemistry: Modification of automated flash chromatography

The improvements to the growth conditions led to higher percentages of ω-hydroxyemodin. Extracts that contained 8% or greater ω-hydroxyemodin content produced fine crystalline precipitate during the initial round of automated flash chromatography in the tubes that corresponded to ω-hydroxyemodin. Those fractions were allowed to crystalize overnight to maximize their formation, then rinsed with $CHCl_3$. Initial analysis indicated the crystals were ω-hydroxyemodin, and the sample was determined to be >99% ω-hydroxyemodin after a further clean up with $CHCl_3$. The enhanced growth conditions allowed isolation of ω-hydroxyemodin at an earlier stage, which greatly accelerates the purification process.

To increase the quality of extracts, each extract is evaluated for ω-hydroxyemodin content via UPLC and those extracts that are less than 8% ω-hydroxyemodin are processed with an additional automated flash chromatography step. A rapid stepwise

gradient was utilized to concentrate the polyhydroxyanthraquinones by removing the non-polar and polar compounds. ω-Hydroxyemodin and the other polyhydroxyanthraquinones were previously observed to elute between 4 and 10% MeOH in $CHCl_3$. These combined fractions with greater than 8% ω-hydroxyemodin were passed through the previously discussed automated flash chromatography method to encourage precipitation of ω-hydroxyemodin.

Chemistry: Modifying high performance liquid chromatography

A portion of the ω-hydroxyemodin was isolated from the initial flash silica chromatography step, but this does not remove all the ω-hydroxyemodin present, especially in extracts with less than 8% ω-hydroxyemodin. Normal-phase HPLC methods were developed because previous studies using reverse-phase HPLC led to substantial loss on column due to insolubility of ω-hydroxyemodin in water. There were still some solubility issues in $CHCl_3$, but this was overcome using a make-up flow pump teed in directly after the column to infuse methanol at 5 mL/min during preparative separations. This prevented precipitation of ω-hydroxyemodin in the post-column flow lines and PDA detector that would otherwise lead to failed runs and afforded higher loading of the column for more efficient separations. Utilization of DMSO as an injection solvent allowed for higher injection volumes (100 mg/200 μL) as ω-hydroxyemodin is five times more soluble in DMSO than dioxane (the next best solvent used).

The isolates from HPLC appeared clean by UPLC but demonstrated up to 30% fatty contaminants by NMR. This was removed by re-suspension of the ω-

hydroxyemodin as a colloidal suspension in $CHCl_3$, pelleted by centrifugation, and the supernatant drawn off. After three rounds of clean up, the fatty contaminant was removed with only minor loss of ω-hydroxyemodin mass.

Summary

In this study, we were able to increase the production of ω-hydroxyemodin from 18 mg to 850 mg within a period of 3 months. We did so by utlizing a greener solvent for extraction (acetone rather than chloroform), and a greener solvent for the partition step (ethyl acetate rather than chloroform). We also designed a new method of extraction and purification which was superior to the methodology employed when ω-hydroxyemodin was originally isolated, taking advantage of the economies of scale. Most importantly, we were able to use a new mass spectrometry tool (droplet probe) to rapidly evaluate different solid media used routinely for fungal growth to determine the most appropriate nutrient media for seed culture, thus optimizing fermentation conditions for laboratory-scale production of the target compound, ω-hydroxyemodin. Many of the isolation methods mentioned herein could be used on an industrial scale with little modification. The benefits obtained from using the improved method are summarized in **Figure 13**.

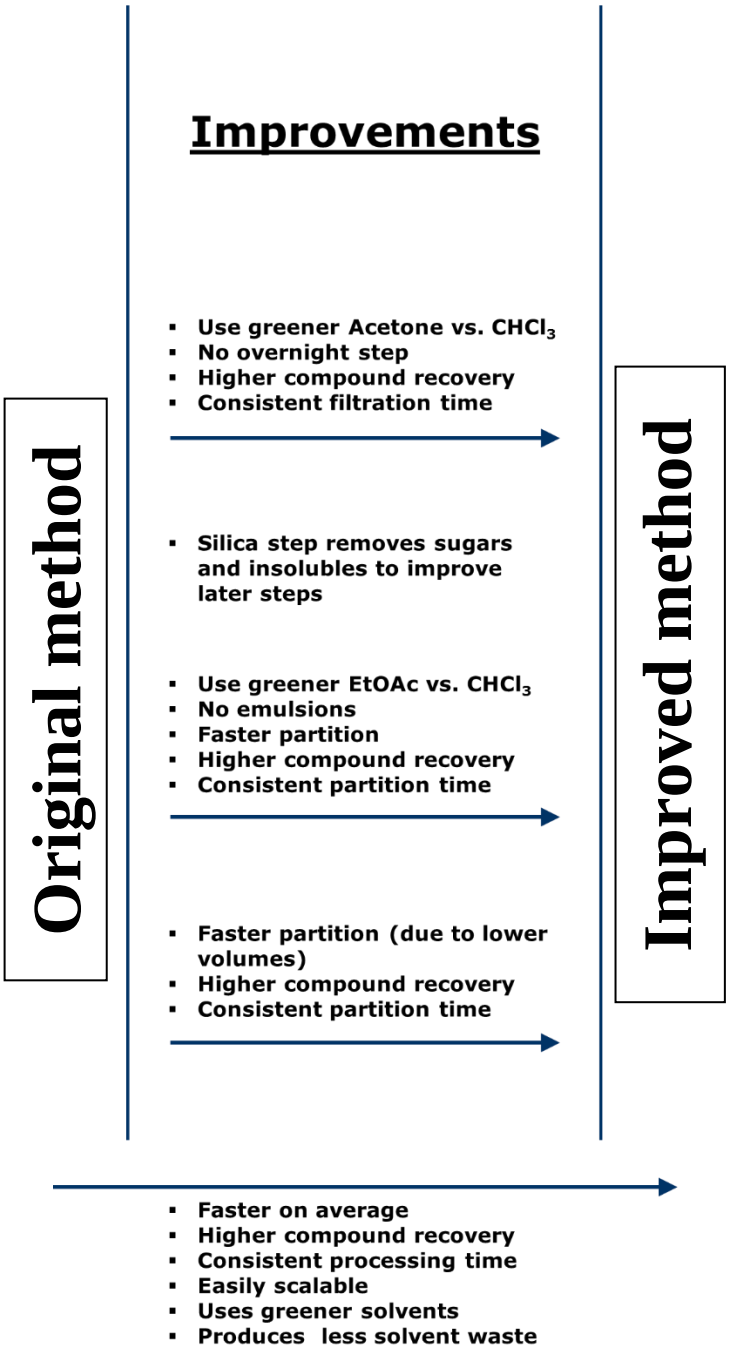

Figure 13. Summary of the Improved Methodologies for the Laboratory Scale-Up.

CHAPTER III

DROPLET PROBE: COUPLING CHROMATOGRAPHY TO THE *IN SITU* EVALUATION OF THE CHEMISTRY OF NATURE

This chapter has been modified from the review paper accepted for publication in *Natural Product Reports* and is presented in that style. Coauthors include Knowles, S. L., Amrine, S. A., Raja, H. A., Kertesz, V., and Oberlies, N. H.

Introduction

From the earliest points in history, people have capitalized on the chemistry of nature regardless of whether they knew the reason nature work such as the specific method of action. The investigation of the underlying mechanisms began roughly two centuries ago[52] but since then, these methods to determine the underlying structures were reductionistic and to now have remained relatively unchanged in natural products.[53] Typically, compounds were isolated and characterized from the extract of an entire organism without context in time or environment. While there could be subtexts to that approach, the general premise has been to determine the chemistry with very little in the way of tools to differentiate spatial and/or temporal changes in secondary metabolite profiles.[54] However, the past decade has seen exponential advances in our ability to observe, measure, and visualize the chemistry of nature *in situ*.[55, 56]

In many ways, this review on the droplet-liquid microjunction-surface sampling probe (droplet probe) originates in attempting to carry out similar *in situ* chemistry

experiments but on fungal cultures. However, the medium of these experiments has since been expanded upon beyond fungi. We believe that the process of studying the chemistry of nature *in situ* is here to stay, and most likely, it will only become more powerful, more accessible, and have more applications in the future. The ability to probe research questions that address the context of when and where in natural products will become important to ignore for understanding the chemistry of nature.

Optimized Production of Fungal Metabolites on the Lab Scale

It has long been known that media studies can be used to optimize the production of fungal metabolites, sometimes codified as an OSMAC (one strain, many cultures) approach.[57, 58] However, how one goes about that can be quite variable, and we have found that evaluating the chemistry of fungal cultures *in situ* via droplet probe enables scouting growth conditions rapidly, especially when spatial and temporal studies are taken into consideration.

ω-Hydroxyemodin (spatial considerations)

From the fungal strain *Pencillium restrictum*, a series of polyhydroxyanthraquinones were isolated. Among these, ω-hydroxyemodin showed promising activity as a quorum sensing inhibiter against clinical isolates of methicillin-resistant *Staphylococcus aureus* (MRSA) both *in vitro*[59] and *in vivo*.[30] Initially, this fungal strain, which was isolated as an endophyte of a medicinal herb,[60] produced blood red guttates, which contained a high concentration of ω-hydroxyemodin;[59] however,

upon successive transfers and cultivation on nutrient media in the lab, the fungus stopped producing the red guttates. The interactions that occur between plants and their fungal endosymbionts are unclear,[61] and reduction in secondary metabolite production upon subculturing of endophytes is a major challenge.[62] While it is easy to think of this as a result of 'domestication' of the fungus, the root causes are unknown. It is hypothesized that endophytic fungi stop biosynthesizing secondary metabolites due to lack of host stimuli.[47] Recent genome studies predict a linkage between attenuated secondary metabolite production and the silencing of biosynthetic gene clusters.[63-65] In search of a solution to enhance the production of ω-hydroxyemodin, a media study via droplet probe was performed to rapidly screen different media types, with the goal of identifying conditions that stimulated secondary metabolite biosynthesis.

A suite of media types were explored, and this included varying pH. Among these, *P. restrictrum* seemed to upregulate biosynthesis of the polyhydroxyanthraquinones on Sabouraud dextrose agar (SDA), where a colour change was noted from light yellow in young cultures to the diffusion of red into the agar after about 2 to 3 weeks of growth (**Figure 14**). Analysis with droplet probe showed enhanced production of the target compound, ω-hydroxyemodin, with SDA. Similar to studies with mevalocidin, very little compound was detected on the surface of the mycelium, as most of the ω-hydroxyemodin was exuded into the surrounding agar (**Figure 14**).

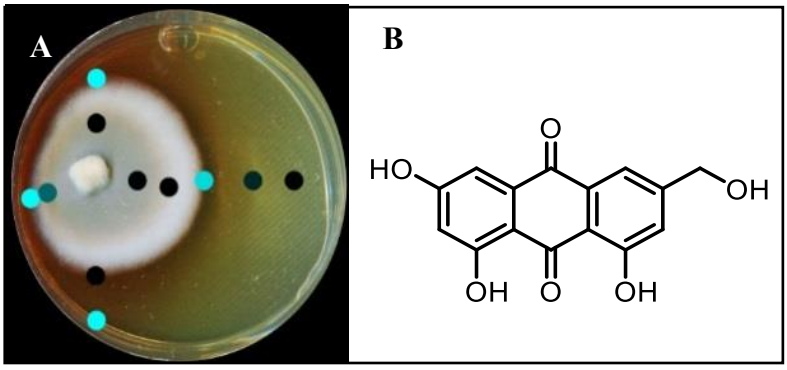

Figure 14. **(A) An Inoculum of *P. restrictum* was Placed to the Side of a Petri Dish of Sabouraud Dextrose Agar, Rather than the Traditional Center, so as to Visualize the Spread of the Compound as it is Exuded into the Media.** The dots show where the chemistry was analyzed *in situ*. The teal colour represents higher amounts of ω-hydroxyemodin, as detected via droplet probe analysis; black spots represent less or the absence of ω-hydroxyemodin. (B) structure of ω-hydroxyemodin.

Cyanobacteria

As part of a project to identify anticancer drug leads from a range of study materials, some of our collaborators work with cyanobacteria collected from fresh water habitats.[66] As noted previously, dereplication is a key component for natural products drug discovery studies, irrespective of the source material. For our colleagues, scaling up the production of cyanobacteria is resource and time intensive, requiring lighted chambers and as many as 4 to 6 months to go from strain isolation to an 8 L culture. Obviously, it is a great disappointment if, at the end of that process, the cyanobacterium then yields known or uninteresting chemistry.

In an attempt to improve this process, the droplet probe was used to examine the chemistry of cyanobacterial cultures *in situ*.[67] In a pilot study, about 25 different cyanobacterial cultures were grown on solid Z medium, a process that takes about 2 to 3 weeks. These were then examined by droplet probe, and one culture, identified as a

Calothrix sp. (strain UIC 10520), revealed two compounds of interest via *m/z* values of 515.3817 and 515.3975. Each of these signals was attributed to sodiated molecular ions, and the molecular formulae for the cyanobacterial metabolites were computed as $C_{29}H_{52}N_2O_4$ and $C_{29}H_{54}N_2O_4$, respectively. Since these formulae did not match any known secondary metabolites, this culture was targeted for scale up, whereupon two new compounds were isolated and elucidated using a suite of NMR and MS techniques.[67]

Given the aforementioned studies of fungi, it may not be surprising that *in situ* analysis of secondary metabolite profiles by droplet probe can also be applied to cyanobacteria. However, at the time, it was not clear if cyanobacterial cultures grown on solid phase media would recapitulate the same chemistry as what was observed in liquid cultures. Indeed, of the 25 strains that were examined, not all of them yielded valuable chemical information, for reasons that are unknown at this time. However, of the ones that did (representing about 70% of the strains), it was possible to either rule them out based on dereplication or prioritize them for scaled up isolation and structure elucidation. Given that this analysis can be completed within 2 to 3 weeks of plating a culture, vs months for scale up, the investment in carrying out such *in situ* analyses seems worthwhile. We hypothesize that natural product researchers will be able to efficiently seek out and prioritize unique compounds from many different kinds of natural resources using the droplet probe.

Plant Studies

Spatial mapping of acetogenins in Asimina triloba

Plants of the Annonaceae have been the subject of intense phytochemical studies for over 30 years due to the biological activity of their secondary metabolites, termed acetogenins.[68, 69] These plants typically biosynthesize a suite of structurally related acetogenins, and like peptides, they often fragment in predictable patterns, helping to establish the position of each hydroxy, the length of the hydrocarbon chains, and the position of THF rings (**Figure 15**).

One of our initial goals was to test the limits of the droplet probe to sample a range of botanical specimens. Much of the literature on acetogenins from *Asimina triloba* (paw paw) has been from the seeds ,[70, 71] twigs[72, 73] and leaves.[74] The flowers of this plant have not been explored, likely due to the difficulty in obtaining them, and acetogenins have not been reported from the flowers of any plant in the Annonaceae. This presented an interesting test case for the droplet probe, as the flowers were a plant organ that was not amenable to traditional natural products procedures, and thus, *in situ* chemistry could answer a question that had never been probed. Acetogenins were detected via *in situ* analysis of the seeds, fruit pulp, twigs, leaves, flower petals, and ovaries, and interestingly, the ovaries had the most extensive list of acetogenins,[75] suggesting that the plant may be sequestering the secondary metabolites there to protect its progeny. Two pragmatic details were also uncovered, which were to strip any waxy layer from plant tissue by rubbing with $CHCl_3$ prior to *in situ* analysis or implementing cryotome cross-sectioning to sample internal plant tissue.

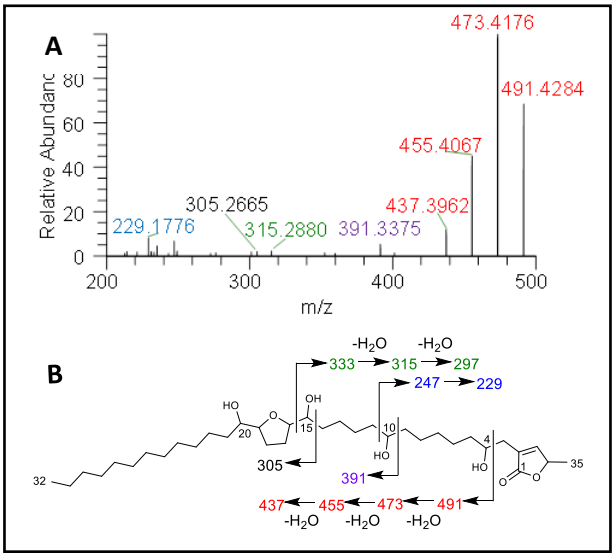

Figure 15. (A) *In situ* Analysis of Seeds of *Asimina triloba* Shows the Fragmentation Pattern of Annonacin. (B) Structure and key fragments for annonacin. Diagnostic signals are shown in the same colour in both panels. Adapted from Sica *et al*.[75]

An additional goal was to elucidate the structures of the acetogenins based on comparisons to the rich literature on these compounds.[68-70, 76] However, much of that was developed at a time when electron impact and fast atom bombardment mass spectrometry techniques were used. Unfortunately, under typical electrospray ionization techniques, which is how the eluent from the column is infused into the mass spectrometer using droplet probe (Fig. 1), acetogenins do not form prominent product ions, and this confounds the use of tandem mass spectrometry for structure elucidation. However, recent studies have shown that the infusion of lithium ions, post column, enhances the fragmentation of acetogenins.[77] Thus, Sica *et al*.[75] infused a 2 mM solution of LiF (dissolved in MeOH), and this greatly facilitated structure elucidation efforts based on tandem mass spectrometry fragmentation patterns (**Figure 15**), even when analysing samples *in situ*. Again, the ability to add detectors, or in this case, infuse

a counter ion post column, represents an advantage of the modular set up of droplet probe.

Mapping of phytochemicals on herbarium specimens

Herbarium voucher specimens are used most often for taxonomic purposes. However, those specimens also hold a record of the metabolic profile of a plant, at least at the time of sampling, and possibly at the time of collection. The setup of the droplet probe is quite versatile, making it straight forward to sample materials of various shapes and sizes. Thus, the droplet probe was tested for the analysis of phytochemicals on a herbarium voucher specimen.[78] Importantly, a major goal was to do so in a manner that does not mar or in any way destroy the integrity of the voucher, such that its appearance remained intact.

A voucher of *Garcinia mangostana* (mangosteen) was analysed for xanthones (**Figure 16**). Similar to acetogenins, there are many analogues and isomers of the xanthones, and thus, chromatographic separation was a key element to enhance detection and elucidation via *in situ* studies. There were two interesting modifications that grew out of this study. First, due to the fact that xanthones were poorly soluble in MeOH and CH_3CN, the droplet solution was modified to 1:1 DMSO:H_2O. In addition, due to the low concentration of the xanthones in the herbarium voucher, the droplet was replicated as many as a dozen times on a single spot, so as to concentrate the secondary metabolites. While it was easier to measure the concentration of some metabolites over others, based on their relative abundance, the droplet probe was able to discern the chemistry of the

herbarium voucher specimen in a manner that did not damage the appearance of the voucher. While the direct application to herbarium vouchers could be considered niche, we believe this study is proof of concept that the droplet probe could be used to analyse the chemistry of delicate documents and other artifacts.

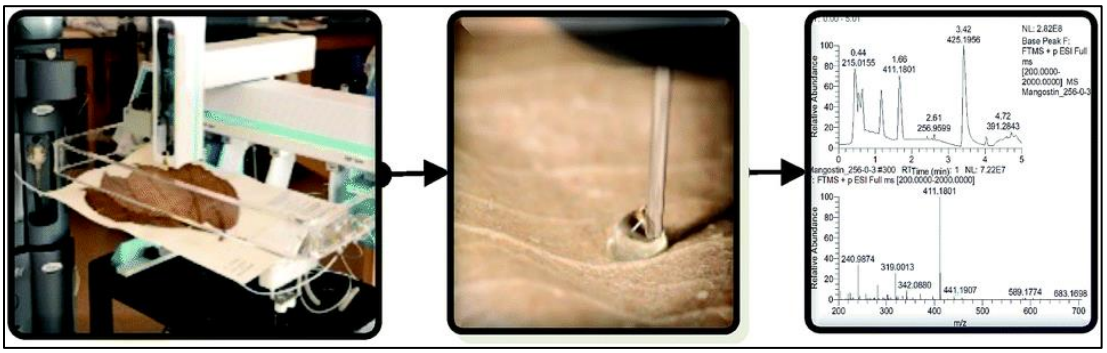

Figure 16. An Example of Sampling a Herbarium Voucher Specimen of *Garcinia mangostana* with Droplet Probe. The left shows the herbarium voucher being analysed by droplet probe, the middle shows how the droplet interacts with the surface of the voucher, and the right shows the chromatographic and spectrometric data that are acquired. Adapted from Kao *et al.*

Conclusion

In general, the advent of ambient ionization mass spectrometry techniques has made an enormous impact on natural products research, since organisms can be examined *in situ* with limited sample preparation.[79] When it comes to the droplet probe, and with the caveat that we may be biased based on our mycological research, fungi represent ideal candidates for *in situ* mass spectrometry mapping experiments. Compared to plants, microorganisms respond quickly to changes in environment (i.e. media)[80, 81] or by the introduction of other organisms (i.e. co-cultures),[57, 82] thus creating unique profiles of their biosynthesized secondary metabolites. Furthermore, as opposed to many bacteria,

fungi are morphologically diverse and often develop unique physical characteristics as the culture grows. The presence of stroma (finger–like projections),[83, 84] guttates or liquid exudates[59, 85-87] and mycelium color changes/gradients give rise to several questions about the spatial distribution of the metabolites associated with such features.

Once the droplet probe has sampled the surface of an organism, that extract can then be interfaced with a wide range of analytical tools that are common to natural products laboratories. Chromatographic separation is the most unique aspect, as that is how it differs from the range of ambient ionization techniques that are also used to study the chemistry of nature *in situ*. In turn, chromatographic resolution of the extract from *in situ* sampling via droplet probe serves to enhance the measurements from any detectors added post column, including UV/Vis and HRMS/tandem mass spectrometry.

We have found that it is a great tool for determining ways to enhance the production of secondary metabolites, to probe conditions for the biosynthesis of non-natural natural products, and to examine the generation of new chemical diversity via co-culturing. Opportunities to study the chemistry of a range of materials *in situ* abound, and only time will tell what other questions can be analysed using the droplet probe.

Acknowledgements

SLK and DK were supported by the National Center for Complementary and Integrative Health/National Institutes of Health (NIH), under award numbers T32 AT008938 and F31 AT009264, respectively. VK was supported by the U. S. Department of Energy, Office of Science, Basic Energy Sciences, Chemical Sciences, Geosciences,

and Biosciences Division. Research on bioactive fungal metabolites in NHO's lab is supported by the National Cancer Institute/NIH under grant P01 CA125066.

CHAPTER IV

LOOKING DEEP INTO THE CHEMISTRY OF METHICILLIN-RESISTANT *STAPHYLOCOCCUS AUREUS* TO OBSERVE ANTIVIRULENCE *IN SITU*

Introduction

Methicillin-resistant *Staphylococcus aureus* (MRSA) is a prevalent cause of skin infection in our society. Administration of antibiotics to eradicate this bacterial infection has led to drug resistance. This is a risk for all antibiotics, which leads us to seeking antivirulent strategies to overcome this. By targeting the quorum sensing pathway, we also target the pathway that controls toxin secretion and pathogenesis. If this pathway can be inhibited, the human body has a chance to naturally clear the infection.

Because no drugs on the market target virulence, we are studying ω-hydroxyemodin, which has shown great promise towards quorum sensing inhibition.[88] ω-Hydroxyemodin and 8 other polyhydroxyanthraquinones were identified to be biosynthesized by a fungal endophyte, which live symbiotically with plants. The funguns was identified as *Pencillium restrictum* and was isolated from *Silybum marianum* (milk thistle).[88] Of that suite of polyhydroxyanthraquinones identified from *P. restrictum*, ω-hydroxyemodin demonstrated the highest activity *in vitro* and was therefore pursued to be studied for *in vivo* efficacy.[89] The application was by subcutaneous injection, and

pathogenesis rather than infection was reduced.[89] We want to explore methods to detect the effects of this known interaction between this compound and MRSA.

To perform this study, we are utilizing the droplet probe, which is a surface sampling technique that can be coupled to liquid chromatography and mass spectrometry. This technique was first used in our lab to detect fungal metabolites on the surface of fungal samples, which have highly variable topography. We are interested in measuring the surface production of the autoinducing peptide (AIP), which is a signaling molecule in the accessory gene regulatory system that can trigger virulence. When a threshold or quorum of AIP has been reached, this system can signal pathogenesis. Although AIP-regulated toxins, rather than AIP, is responsible for the negative effects in microbial infection, the production of both these compounds is controlled by AgrA, a regulator in the quorum-sensing pathway.[90] ω-Hydroxyemodin has been reported to bind to AgrA and provide therapeutic effects through antivirulence.[88, 89] In this experiment we are interested in observing these effects *in situ* by monitoring AIP with droplet probe.

Results and Discussion

Initial studies were conducted as a co-culture experiment between *P. restrictum* and *S. aureus* because of the Oberlies lab previous experience with fungal co-culture experiments. This was the first instance in which a fungus and a bacterium were cultured together for the purpose of droplet probe analysis. The preliminary studies included the determination of the average droplet recovery based on the different surfaces that were being analyzed in this experiment. Alizarin Red S was used as an internal standard due

to its similarity to ω-hydroxyemodin and water solubility, which is key when using droplet probe. The droplet that forms when performing the surface extraction must include enough water to maintain the surface tension so the liquid with the dissolved metabolites can be drawn back up into the syringe. These studies on the different surfaces are shown in **Figure 17**.

Each droplet included the same concentration of Alizarin Red S. This amount was compared to direct injection of Alizarin Red S to determine how much of the droplet was recovered. Based on the results, there was approximately 40-60% recovery of the droplet from the surface of the plate. The fungal mycelium showed the greatest deviation in the return of the droplet. This is not abnormal because the mycelium can behave somewhat like a sponge, absorbing the droplet. However, different areas on the mycelium may reach capacity of the amount of liquid and thus have a higher return of the droplet itself. However, the droplet showed reasonable consistency when drawn from the media-agar surface. This is the first reported instance of determining average droplet recovery. This also lays the foundation for normalizing all the droplets to compare the production of specific metabolites.

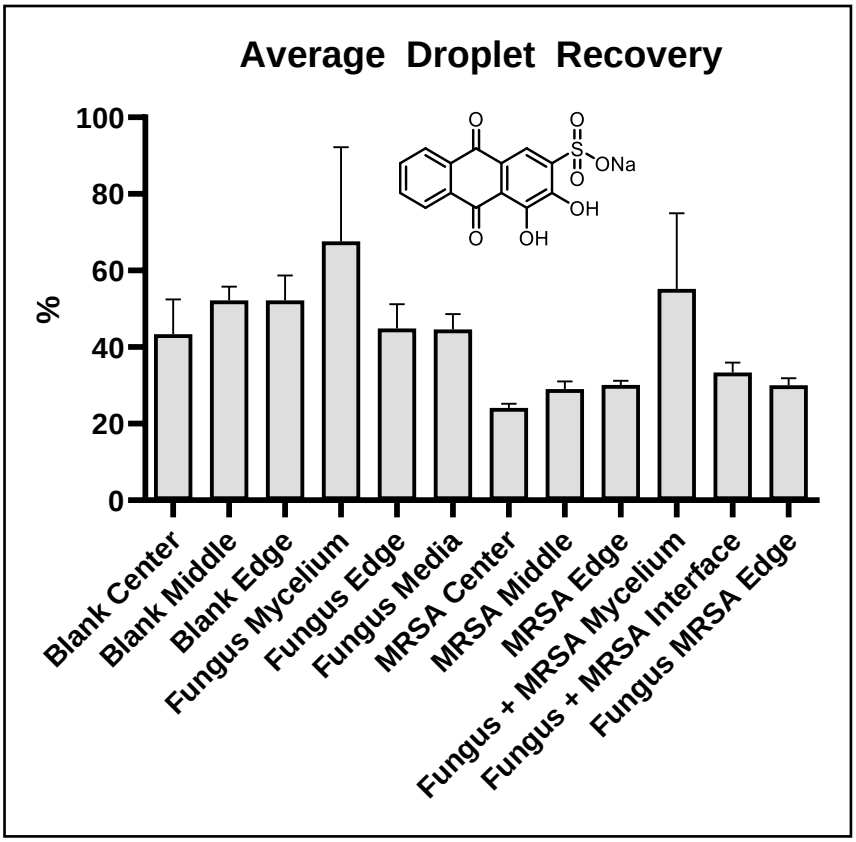

Figure 17. The Internal Standard Compound: Alizarin Red S and its Droplet Recovery on Various Tested Surfaces. This technique involves the addition of a droplet to the surface of a sample, which leaves residual solvent on the surface. Agar absorbs some water, but the mycelium of a fungus is shown to have the greatest variability in droplet recovery. Six microextractions were performed for each spot. Each area was measured in triplicate biological replicates. In each 4 μL droplet, 0.001 mg/mL Alizarin Red S was present. The percent recovery shown above was utilized to normalize the amount of each of the metabolite in further studies.

In this preliminary study, the cultures (**Figure 18**) were examined to determine if the autoinducing peptide (AIP) could be measured from the surface of mono and coculture. Four different conditions were examined, a blank with no growth of any bacteria or fungus on Sabouraud dextrose agar, monoculture *P. restrictum*, monoculture *S. aureus*, and the coculture of both microorganisms. Sabouraud dextrose agar is the agar

favored by fungi and specifically by *P. restrictum* from media studies. This was chosen because of the slow growth of fungi compared to bacteria. *P. restrictum* was inoculated on the plates two weeks prior to the addition of the bacteria. The *S. aureus* was added to the plates around and across the mycelium before overnight incubation.

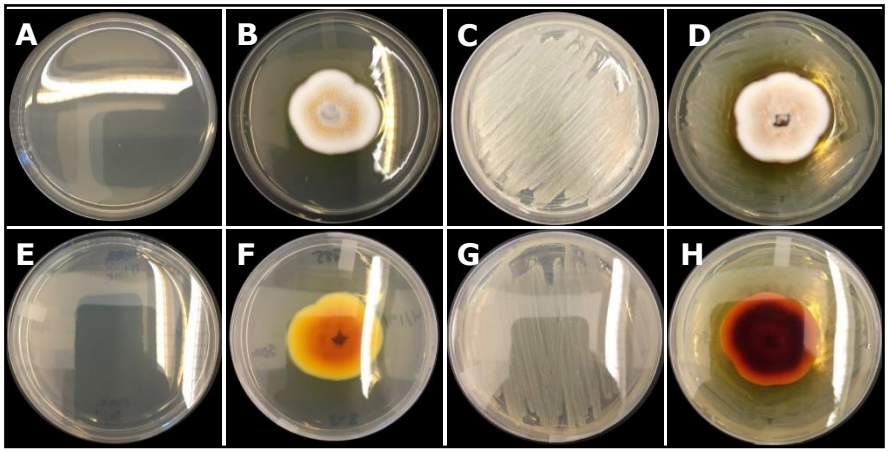

Figure 18. Example Cultures of Mono and Coculture *Penicillium restrictum* and Methicillin-Resistant *Staphylococcus aureus* (AH1263) on Sabouraud Dextrose Agar (SDA). The top row are the plates from a top-down perspective, and the bottom row contains the same plates from underneath to show the difference between the topside and underside of the growths. **A** and **E** show SDA with no growth. **B** and **F** are *P. restrictum* cultured for two weeks in light and dark cycles. **C** and **D** are the plates of AH1263 incubated for 16 hours. **D** and **H** contain *P. restrictum* grown for two weeks and MRSA incubated for 16 hours.

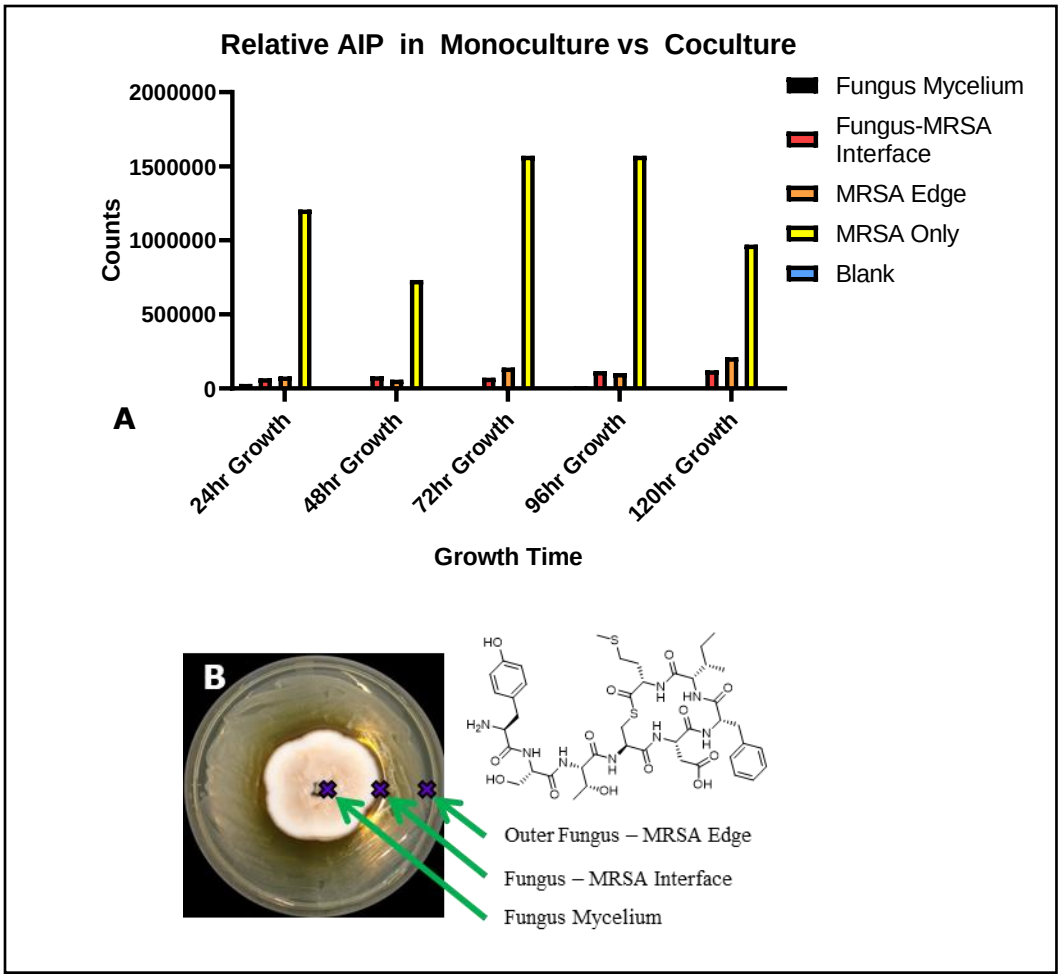

Figure 19. The Autoinducing Peptide (AIP) and the Relative Amount of Virulence via Indirectly Measuring the Amount of AIP ([M+H] = 961.3744 m/z) via Droplet Probe Coupled to UPLC-HRESIMS (A). The effects of ω-hydroxyemodin is known to bind to AgrA, which triggers the agr pathway that cause bacterial virulence. Measurements of the sample were taken over the course of 5 days to determine if virulence would be affected by long term growth. The graph shows different spots for the fungus due to asymmetrical growth of the fungus. The co-culture and example sampling locations on the plate (**B**). Measurements were taken at different intervals because previous measurements of ω-hydroxyemodin from *P. restrictum* on SDA showed higher concentration towards the edges of the mycelium.

By utilizing the known accurate mass of AIP as well as knowing its retention time in LC-HRESIMS, AIP was detected on the surface all the plates that were incubated with *S. aureus*. On the plates that included the fungus whether sampled at the mycelium, interface, or edge of the plate, the amount of AIP was lower compared to the plate containing the monoculture of *S. aureus* (**Figure 19**). This study was promising in the ability to observe antivirulence through studying AIP and utilizing droplet probe.

In order to show that the lower production of AIP was due to the compound as is known from literature, we also sought to analyze a compound known as aureusimine B, which is a metabolite produced by *S. aureus* but is not connected to the quorum sensing pathway. By reprocessing previous data from these studies, we were able to identify and relatively measure that metabolite as well as compare the average amount of ω-hydroxyemodin isolated from the mono and coculture plates. There was a lower amount of aureusmine B present in the coculture spots compared to the amount of aureusimine B in the monoculture of *S. aureus* (**Figure 20**). This suggested an antimicrobial effect, which could be from the lack of nutrients since fungus was growing on the plate for two weeks longer than the bacteria. The primary metabolites or even some secondary metabolites produced by *P. restrictum* could also have achieved an overall antimicrobial effect.

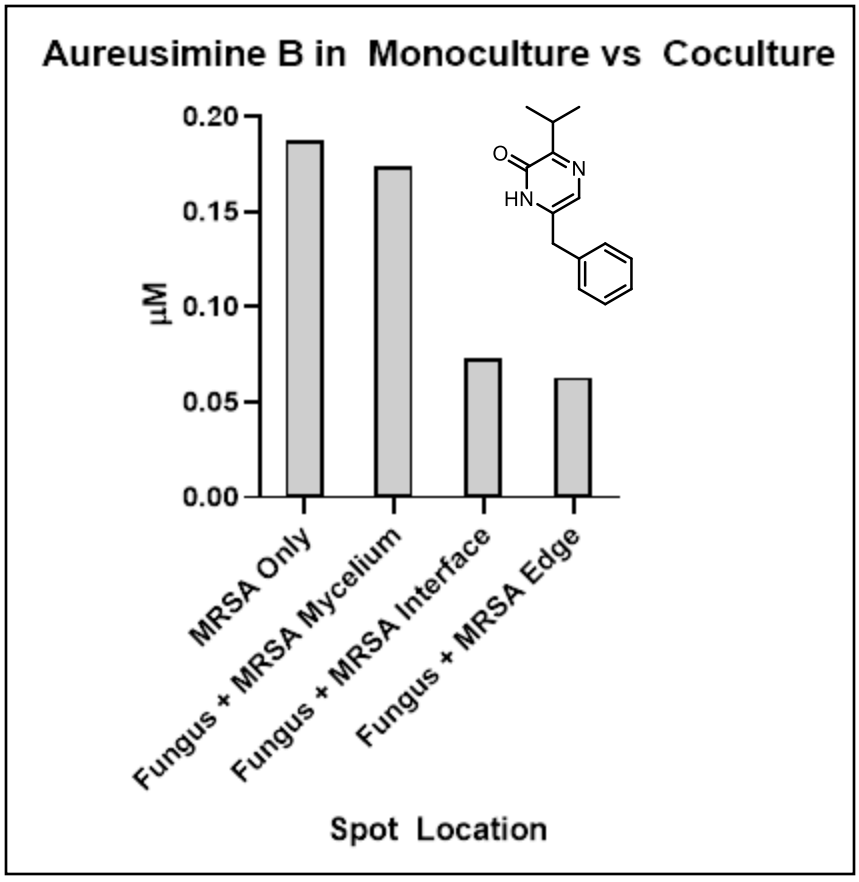

Figure 20. Aureusmine B, which is Produced by *S. aureus* and is a Measure of Growth on the Mono and Coculture Plates at 24 Hours (N=3).

In order to combat the potential antimicrobial effects from a coculture, the method was refined for the exclusion of the fungus and the inclusion of 64 µM of ω-hydroxyemodin, the antivirulence compound from *P. restrictum*. This was the concentration from a previous study known to show antivirulence. The results of this study showed a consistent amount of aureusimine B and ω-hydroxyemodin, but the amount of AIP vacillated greatly (**Figure 21**). Because the fungus was no longer present in the experiment, the media was altered to tryptic soy broth (TSB) and tryptic soy agar (TSA), a medium more conducive to the growth of *S. aureus*. Alizarin Red S continued

to be the internal standard used to normalize the droplet in later analysis. There was a distinct trend where the amount of AIP was lower in the plates with ω-hydroxyemodin, but the error bars showed unreliability in this observation. Because the concentration of aureusimine B isolated from the bacteria was so consistent, we do not believe there was any growth problems with *S. aureus*.

In order to determine if the inconsistency of the AIP was related to the interaction with ω-hydroxyemodin, the experiment was performed a second time with 100μM ambuic acid,[91] another fungal metabolite that causes antivirulence in *S. aureus*. After the analysis of aureusimine B and AIP, there was still considerable inconsistency in the production of AIP (**Figure 22**). The AIP was lower as a trend as seen in **Figure 21**, but the wide error bars show a lack of reliability to determine antivirulence *in situ*. The trends are shown to be present for compounds known to have antivirulence effects against *S. aureus*. However, the variability maybe related to the study that was performed on solid media rather than liquid per the *in vitro* studies that allow for the direct injection of the remnants of the bacteria to determine AIP inhibition.

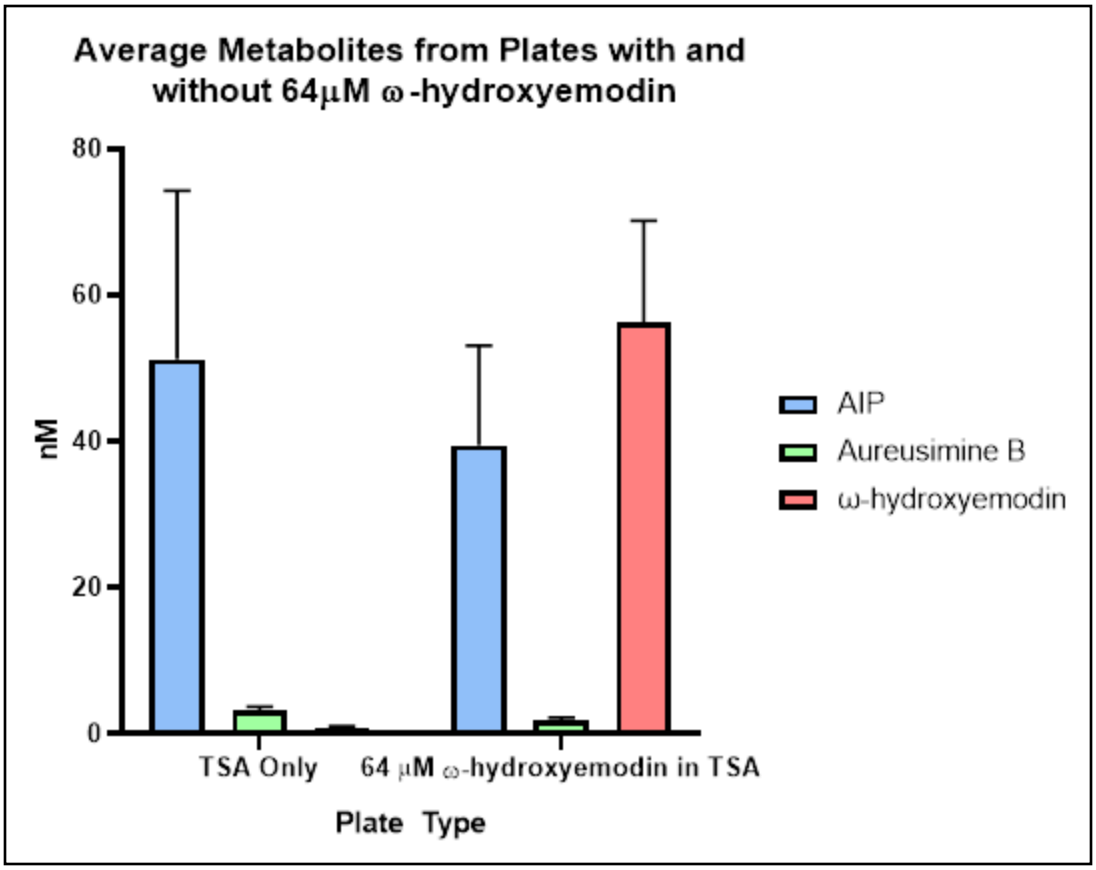

Figure 21. TSA without Additives Compared to TSA with 64 µM ω-Hydroxyemodin. The absorbance of the colonies as 0.770 (6.09E.08 CFU/mL) and 200 µL of AH1263 in TSB was added to each plate for approximately 1.22E8 CFU/plate. Duplicate plates were tested and measured for aureusimine B and AIP. The average is shown based on n=5 spots per plate.

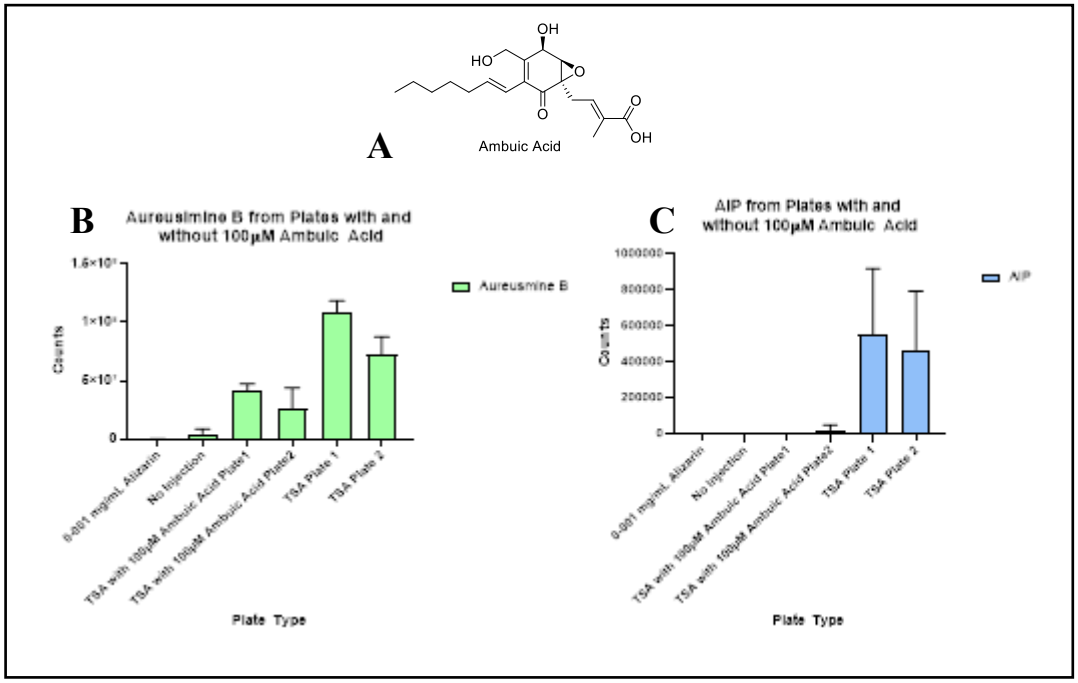

Figure 22. The Repeated Experiment of Standard TSA and TSA with 100 µM Ambuic Acid (A). The absorbance of the colonies as 0.285 ($4.84x10^7$ CFU/mL) and 200 µL of AH1263 in TSB was added to each plate for $9.61x10^6$ CFU. Duplicate plates were tested and measured for aureusimine B (**B**) and AIP (**C**). The average is shown based on n=5 spots per plate.

Experimental

Preliminary co-culture

Two plates of Sabouraud dextrose agar (SDA) (Difco) were inoculated with *Pencillium restrictum*. Due to the difference in the growth of fungi, which can take between 2-4 weeks of growth, *P. restrictum*, the fungus that produces the polyhydroxyanthraquinones, was grown for two weeks. After those two weeks, a single colony from the strain AH1263 (USA300 CA-MRSA strain) was added to one of the two plates containing two-week-old *P. restrictum* around and inside the fungal growth and one plate of SDA without fungal growth. The plates were incubated for 16 hours at 37 ºC.

Droplet probe analysis was conducted on the plates after 24 hours and at 24-hour intervals up to 120 hours. Studies were performed comparing four different conditions: 1 plate of SDA without *P. restrictum* or AH1263, 1 plate with just the *P. restrictum,* 1 plate with just the AH1263, and 1 plate that contained both *P. restrictum* and *S. aureus*.

Plate preparation and incubation of surface 64 μM ω-Hydroxyemodin

Tryptic soy agar (TSA) was utilized as the media for the experiment without any fungus. Each plate of 100mmx25mm contained 20 mL of TSA. To half the plates of TSA, 100 μL of 64 μM ω-hydroxyemodin was added to the surface and spread using a plate spreader.

A single isolated colony of AH1263 was incubated in 5 mL of Tryptic Soy Broth (TSB) overnight at 37 °C with shaking at 250 rpm so that the colonies would reach the stationary phase. An aliquot of this mixture was diluted 1/100 (50 μL in 50 mL of TSB). The dilution was incubated for until the broth reached between 0.4 to 0.9 turbidity (OD_{600}). Checking the absorbance to determine the growth phase of the colonies began at 2 hours but may have also taken up to 4 hours. Once the growth phase was reached, 100 μL of TSB the seed culture was added to 3 plates of TSA and 3 plates of TSA with 64 μM ω-hydroxyemodin added on the surface. A total of six plates were incubated at 37 °C for 16 hours. Droplet probe studies were conducted comparing these two conditions as well as two blank conditions without any bacterium for a total of 8 plates tested. These methods were repeated with 128 μM and 16 mM ω-hydroxyemodin.

Plate preparation and incubation of media 64 μM ω-Hydroxyemodin

Two conditions of media were analyzed as in *Experimental B*. One condition was TSA alone. The second condition was also TSA but also contained 64 μM ω-hydroxyemodin in the media rather than on the surface. To achieve this, the compound was dissolved in DMSO and added post autoclave when the agar was lukewarm. The media was stirred vigorously for a homogenous mixture. Each plate contained 20 mL of 64 μM ω-hydroxyemodin in TSA or 20 mL of TSA with no additives. The plates utilized were 100mmx25mm. These plates were stored at 4 ºC when not in use. This method was repeated with ambuic acid but the concentration of the plates with an additive was 100 μM ambuic acid.

When preparing the plates for analysis, a single isolated colony of AH1263 was incubated in 5 mL of Tryptic Soy Broth (TSB) overnight so that the colonies would reach the stationary phase. An aliquot of this mixture was diluted 1/100 (50 μL in 50 mL of TSB). The dilution was incubated until the turbidity of the broth and microorganism reached between (0.4 to 0.9). Determination of the growth phase of the colonies began at 2 hours but may also have taken up to 4 hours. Once the growth phase was reached, 200 μL of TSB with the diluted *S. aureus* was added to 3 plates of TSA and 3 plates of TSA with 64 μM ω-hydroxyemodin (**Figure 23**). The total of six plates were incubated at 37 °C for 16 hours. Droplet probe studies were conducted comparing these two conditions as well as two blank conditions without USA300 AH1263 added for a total of 8 plates tested. For ambuic acid, the experiment was conducted in duplicate rather than triplicate biological replicates.

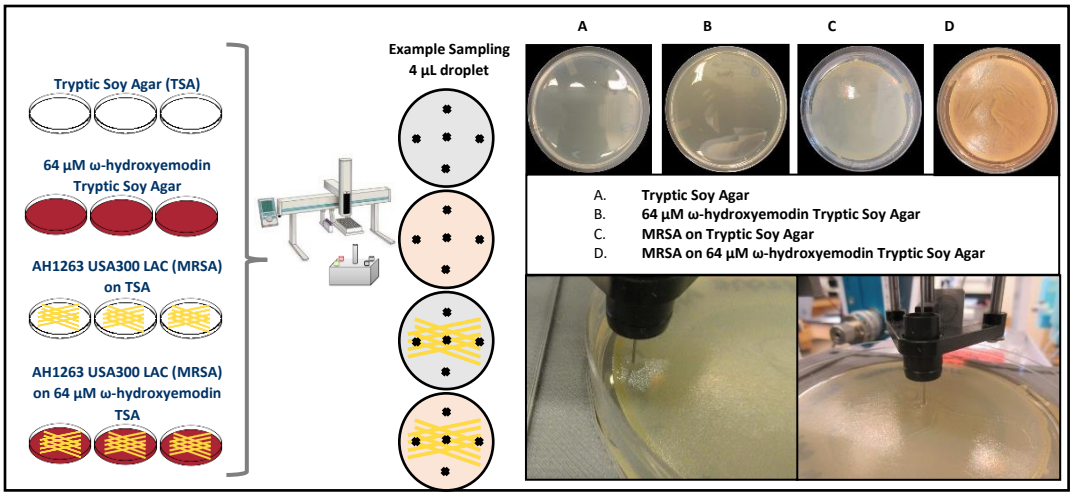

Figure 23. The Methodology Shown for the Droplet Probe Analysis of the Plates Made with and without 64 µM ω-Hydroxyemodin. The cross marks show an example of sampling location for each type of condition: TSA (**A**), TSA with 64µM ω-hydroxyemodin (**B**), TSA with *S. aureus* (**C**), *S. aureus* on TSA with 64µM ω-hydroxyemodin (**D**). There are also example images of the sampling process of the plates. The left real time imagine is another example of **C** and the right real time image is another example of **D**.

Droplet probe analysis

The droplet−liquid microjunction-surface sampling probe was optimized for natural products studies via an earlier collaboration with Oak Ridge National Laboratory.[40] Briefly, a CTC/LEAP HTC PAL autosampler (LEAP Technologies Inc., Pflugerville, TX) was converted into an automated droplet system via dropletProbe Premium, which was developed by Oak Ridge National Laboratory.[92-96] Extractions were performed using Fisher Optima LC/MS grade solvents consisting of 1:3 MeOH:H_2O to enhance the solubility of the water soluble MRSA metabolites. For the purpose of investigating the polyhydroxyanthranquinones present, each droplet contained 0.001 mg/mL of Alizarin Red S (Sigma-Aldrich) as an internal standard. Five spots were

selected per plate for analysis. Approximately 4 μL of solvent was drawn into the syringe for each microextraction and dispensed onto the surface of the media at a rate of 2 μl/s. The syringe with the dispensed droplet paused over the surface for two seconds before being drawn back into the syringe. This process was repeated a total of 6 times for a single spot prior to injection into the UPLC−HRMS system. In between plates, 4 μL of 0.001 mg/mL Alizarin Red S without surface sampling as well as a completely blank injection was run to ensure a lack of carryover. The droplet probe was coupled with a Waters Acquity ultraperformance liquid chromatography (UPLC) system (Waters Corp.) to a Thermo QExactive Plus MS (ThermoFisher).

The QExactive Plus collected data from 200 to 2000 *m/z* at a mass resolution of 70,000. The voltage for the positive ionization mode was set to 4.0 kV with a nitrogen sheath gas set to 50 arb and an auxiliary gas set to 15 arb. The S-Lens RF level was set to 50.0 and capillary temperature at 300°C. The flow rate of the UPLC was set to 0.3 mL/min using a BEH C_{18} (2.1 × 50 mm, 1.7 μm particle size) column. The column was equilibrated at 40 °C, and the sample manager was not used. The mobile phase consisted of Fisher Optima UPLC−HRMS grade CH_3CN:H_2O with 0.1% HCOOH. The initial gradient began at 15% CH_3CN and held for 2 minutes before increasing linearly to 100% CH_3CN over 2 min. For 1 minute, the column was held at 100% CH_3CN to clean the column before being re-equilibrated to the initial starting conditions over 1 minute. The PDA was set to acquire from 200 to 500 nm with a resolution of 4 nm.

Plate data analysis

A calibration curve run in triplicate containing δ-toxin, AIP-1, ω-hydroxyemodin, alizarin red S, and aureusimine B containing at least 11 points were also run in triplicate (**Figure C1-C4**). Calculations of concentrations were based on peak area ratios, and calibration curves were generated by weighted (1/X) linear regression. All data were processed using the Quan Browser module of Xcalibur version 2.2 (Thermo Fisher Scientific). The chromatographic peak areas were integrated using the Xcalibur Processing Setup version 2.2 (Thermo Fisher Scientific). ICIS peak detection was applied for a list of putatively annotated ions. The Grubbs' test was performed for an n=4 number of observations after the average and standard deviation of each compound was determined at each site. The measurements that were considered outliers at a 5% significance level were excluded from our assessments.

Conclusion

The ability to determine droplet recovery coupled to the inclusion of an internal standard was a success when determining a relatively accurate amount of metabolite per spot with greater reliability. The droplet recovery showed what had been observed previously when analyzing the mycelium of a fungus with droplet probe in that the surface can be especially inconsistent because of its sponge-like surface. AIP can be measured from surface sampling with the droplet probe, which has never been previously shown before. A decrease in the AIP production was shown when the MRSA strain was cocultured with the fungal strain that biosynthesized polyhydroxyanthraquinones,

although this was later shown to likely be due to an antimicrobial effect based on the lowered production of aureusimine B. The secondary metabolite, aureusimine B, was shown as a reliable metabolite to indirectly measure growth for the purpose of determining an antimicrobial effect for *in situ* measurements. Attempts to demonstrate the antivirulence effects of ω-hydroxyemodin are inconclusive due to the wide margin of error in the measurement of AIP. Because AIP can be extracted from the mixture of 1:3 MeOH:H_2O on the agar plates with droplet probe and due to the consistency of aureusmine B measurements, the inconsistency when measuring AIP may be a biological effect. This was the first instance in which a microextraction of the MRSA strain from a solid agar media has never been performed so there could be a difference in what triggers the production of AIP such as solid media versus liquid as in previously published *in vitro* studies that showed the antivirulence effect of ω-hydroxyemodin and ambuic acid.

Acknowledgements

Diana Kao was supported by the National Center for Complementary and Integrated Health, NIH via grant F31 AT009264. We thank, Drs. Vilmos Kertesz and Gary J. Van Berkel (Mass Spectrometry and Laser Spectroscopy Group, Chemical Sciences Division, Oak Ridge National Laboratory) for inspiration and guidance with the droplet probe. We also thank Tyler Graf of UNCG for helpful discussions pertaining to evaluation of metabolites. The mass spectrometry data were acquired in the Triad Mass Spectrometry Facility.

CHAPTER V

A NON-DESTRUCTIVE CHEMICAL ANALYSIS OF *GARCINIA MANGOSTANA* L. (MANGOSTEEN) HERBARIUM VOUCHER SPECIMEN

This has been published in *Phytochemistry Letters* and is presented in that style. Kao, D., Henkin, J. M., Soejarto, D. D., Kinghorn, A. D., Oberlies, N. H. *Phytochem. Lett.* **2018**, 28, 124-129.

Introduction

Herbarium voucher specimens have been integral to science as far back as 1556, when the Italian botanist, Luca Ghini, first produced them from dried plants, employing sheets of heavy paper bound together and stored vertically, as formal and permanent documentation.[97] Subsequently, Carl Linnaeus in 1735 laid the foundation for taxonomic identification of plants via herbarium vouchers.[98] In addition to being a permanent record of a plant, these specimens present a unique opportunity to study plants and other preserved species over time. They are a snapshot that researchers can examine, providing opportunities to look at the phenotype, genotype, and chemotype during a specific window of time,[99, 100] albeit with the recognition that some degradation or other changes may occur to the voucher during storage. Herbarium specimens provide a glimpse into the past that researchers of the present (and perhaps future) are capable of studying with modern and next-generation techniques, documenting and investigating changes over time.[101, 102] However, to do this, some techniques require the destruction

of a portion of the sample for DNA and/or metabolite analysis.[100] While valuable, the sampling process is permanent, visible, and invasive, forever altering the integrity and scientific value of the voucher.

Over the past three years, our team has been utilizing the droplet-liquid microjunction-surface sampling probe (droplet probe) as a tool to examine the chemistry of fungal cultures *in situ*. Essentially, this sampling system dispenses a droplet of approximately 4 µl on the surface of a sample, enabling a microextraction, which can then be analyzed by UPLC-HRMS.[40, 103-105] In addition to a suite of applications on fungal cultures, we have also shown its potential in studying various plant parts *in situ*, including fruits, seeds, stems, and even rarely studied flower petals.[55] In the current study, we turned our attention to the use of droplet probe for the examination of herbarium vouchers. In principle, they should behave in a manner similar to plant tissues, which have been sampled with this technique previously.[55] However, due to the delicate, and at times precious, nature of these specimens, we wanted to ensure that the specimen's appearance would not be altered by the analysis, as the physical characteristics of these specimens are critical for taxonomic studies.

Garcinia mangostana L. (Clusiaceae commonly known as mangosteen, was chosen because this plant is known for its numerous biological applications, including as an antimicrobial, anti-inflammatory, and antioxidant, among many other purposes.[106-110] Mangosteen has been used traditionally to treat disorders ranging from skin infection to dysentery to abdominal pains.[111] Xanthones are the major metabolites that have been isolated and investigated from this plant. Modern studies have shown antibacterial,

antifungal, antihistamine, anti-HIV, antineoplastic, aromatase inhibitory, cancer chemopreventive, and cytotoxic activities from this class of compounds.[111-124]

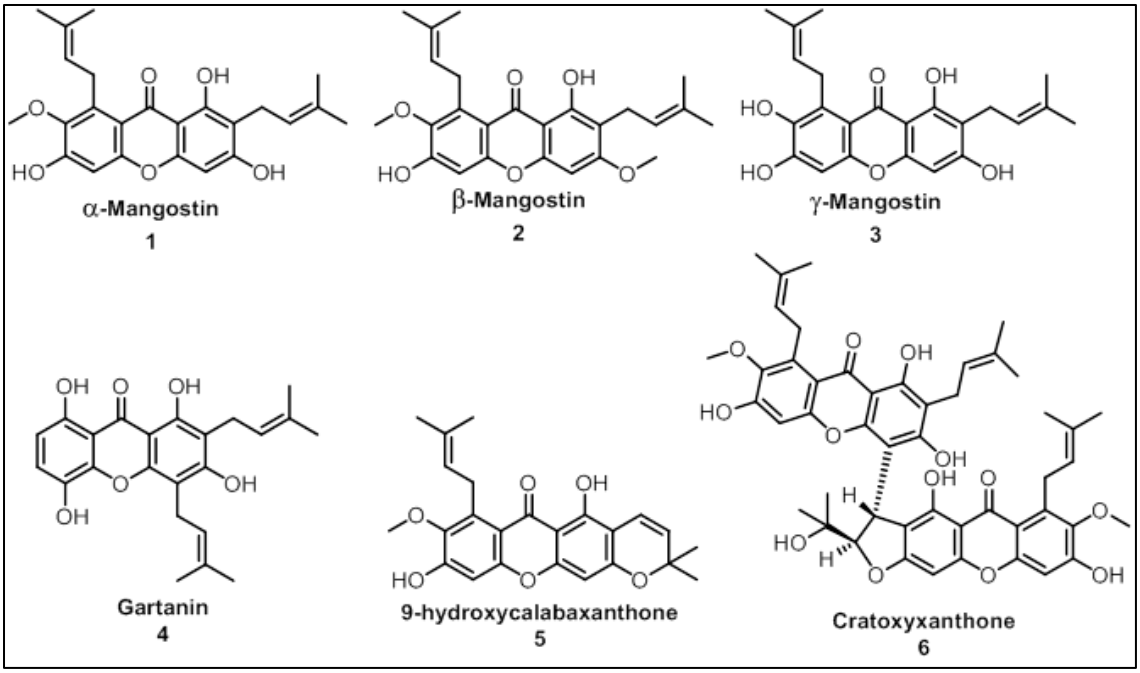

Figure 24. Six Prenylated Xanthones Previously Isolated from *Garcinia mangostana* *F*ruit or Stem Bark.[117, 121] These were used as reference standards when analyzing the droplet probe data from the herbarium voucher.

In this study, we investigated six xanthones of mangosteen: α-mangostin (**1**), β-mangostin (**2**), γ-mangostin (**3**), gartanin (**4**), 9-hydroxycalabaxanthone (**5**), and cratoxyxanthone (**6**) (**Figure 24**).[125, 126] Many of these compounds are found in one or more of the pericarp, stem, and whole fruit of *G. mangostana*.[127] Using a herbarium voucher specimen of *G. mangostana*, our goal was to extract chemical knowledge via the droplet probe technique without marring the physical appearance of the voucher.

Results and Discussion

The main objective of this project was to identify prenylated xanthones from the herbarium voucher specimen of *Garcinia mangostana*, as compared to isolated reference standards, without damaging the voucher. The sampling of the herbarium voucher specimen was performed using the droplet probe technique, in which a droplet of approximately 4 µl of 50:50 DMSO:H_2O was dispersed onto the surface of the sample. Metabolites from the herbarium voucher specimen were dissolved and analyzed using the droplet probe system (**Figure 25**).

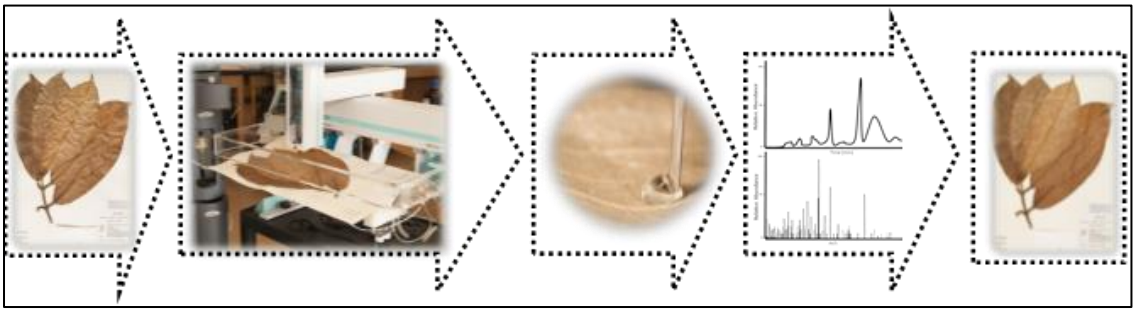

Figure 25. General Procedure for Detecting and Analyzing Prenylated Xanthones from the *Garcinia mangostana* Herbarium Specimen.

The herbarium voucher was sampled at four sites of both the leaf and the stem (**Figure 26**). Essentially, the droplet probe performs a microextraction from the surface of the voucher, and the concentrated droplet is then analyzed via UPLC-HRMS. This permitted a comparison of chromatographic and spectrometric data to that of the reference standards (**Figure 24** and **D1**), while keeping the whole sample intact and undamaged in appearance for taxonomic posterity.

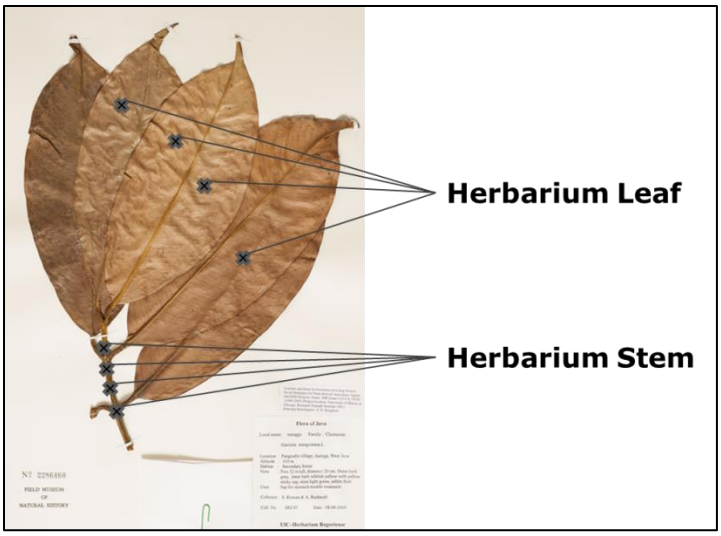

Figure 26. *Garcinia mangostana* Leaf Herbarium Specimen (No. 2286460) from The Field Museum of Natural History in Chicago, IL. Sites that were sampled by the droplet probe are marked with crosses on the leaf and stem of the voucher. A droplet containing approximately 4 µl of 50:50 DMSO:H_2O with an internal standard was dispensed onto the surface at each of these sights before UPLC-HRMS analysis.

A herbarium specimen is important for future taxonomic studies. To demonstrate this innocuous property of this technique, photographic close ups of the voucher, both before and after droplet probe analysis are included (**Figure 27**). Chemical sampling of the *G. mangostana* voucher via droplet probe was non-destructive, and at least at the optical level, deterioration of the specimen was not observed. This was important since a non-destructive chemical analysis of a voucher has not yet been reported, although recently there has been a non-destructive analysis of DNA from herbarium specimens.[128]

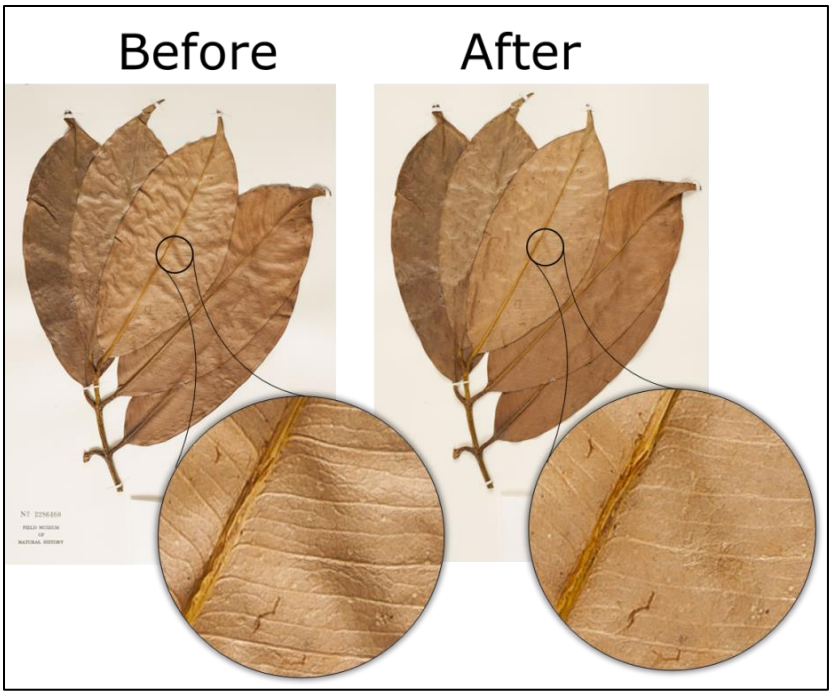

Figure 27. *Garcinia mangostana* Herbarium Voucher Specimen Before and After Sampling by Droplet Probe. The photos were taken within three hours of each other and show the same area with a zoom in before and after sampling.

Previous methods from our laboratory have utilized water and methanol as the solvent combination for droplet microextractions,[40, 55, 103, 104] but the xanthones were found to be semi-soluble in methanol and not at all soluble in water. The droplet probe technique relies on droplets that contain water, which maintains surface tension when making contact with the sample. Thus, DMSO was included in the microextraction solvent because of its improved solubility with the xanthones.

In preliminary studies, a total of five microextractions per droplet were used to sample the herbarium voucher specimen; however, the xanthones were not well detected. In order to concentrate the microextraction further, the number of microextractions was increased by five until α-mangostin (**1**), β-mangostin (**2**), and γ-mangostin (**3**) could be

detected consistently on the herbarium voucher specimen. In total, 15 microextractions per droplet were performed, which was three times more than required previously with fungal cultures.[40]

The ability to retain a droplet on the tip of the syringe and concentrate the microextractions via repeated sampling is a benefit of the droplet probe system. However, in doing so, some amount of the solvent may be retained on the sample, and this could result in inconsistencies and variability in sampling. Therefore, we sought an internal standard that could be used to normalize the data, and to solve this challenge Alizarin Red S (0.0001 mg/mL) was included in the sampling solvent.

The six xanthones were analyzed from each site on the herbarium voucher specimen (**Figure 27**), and the average of the leaf and stem sites respectively were averaged together (**Figure 28**). Of the prenylated xanthones, α-mangostin (**1**) and β-mangostin (**2**) were detected in the highest concentrations of all the compounds across all sites, whereas 9-hydroxycalabaxanthone (**5**) and cratoxyxanthone (**6**) were not detectable at all. The herbarium voucher leaves were observed to have less of each of the compounds, if present at all, compared to the sites on the herbarium voucher stem. It is unknown whether these observations were due to the amount of those compounds in the leaves at the time of collection, or if they degraded upon processing and storage as a voucher; there is literature precedent for the latter with benzofuran ketones.[129, 130] Irrespective, it is a fact that at the time of analysis, the herbarium voucher leaves had a smaller amount of those compounds.

Furthermore, there was interest in comparing the xanthones of the herbarium voucher specimen to a dried fruit sample (**Figure 29**) of the same species. Overall, the sampling of the stem was observed to contain higher concentrations of xanthones on both the dried fruit as well as the herbarium voucher specimen. However, gartanin (**4**) was not detected on the herbarium voucher specimen, but the metabolite was detected in the dried fruit sample, notably on the endocarp (Inside Fruit) and the pedicel (Fruit Stem) (**Figure 28**). As with the herbarium voucher specimen, there was no detection of 9-hydroxycalabaxanthone (**5**) and cratoxyxanthone (**6**) on any of the dried fruit sites, despite the fact that the dried fruit sites showed an overall higher concentration of the xanthones compared to the herbarium voucher specimen. In a previous study from the stem bark of *G mangostana*, compounds **1** and **2** had been isolated in significantly greater quantities compared to compounds **4-6.**[121] This may explain the lower concentration or lack of detection in some cases for compounds **4**-**6**.

The data in **Figure 28** show that there was some variability in the measurements, especially for compounds of lower concentration, and there could be several reasons for this. The xanthones detected on the endocarp may have varied because that surface was more absorbent, leading to fluctuating droplet recovery of as low as 1% to as high as ~50% over the course of 15 microextractions per site. In contrast, the pericarp, leaf, and stems all provided hard and/or relatively flat surfaces that permitted facile and reproducible microextraction sampling. In addition, there may be inconsistency between the sites sampled with the droplet probe, simply due to inherent variability of secondary metabolite distribution in the plant.[131] Since it was observed that the stems have a higher

concentration of xanthones, it is possible that examining a spot closer to the stem of a leaf or fruit may be more concentrated in secondary metabolites. Moreover, the effects of collection, preparation, and storage time of herbarium voucher specimens are not known, which can be limiting when performing *in situ* analyses.

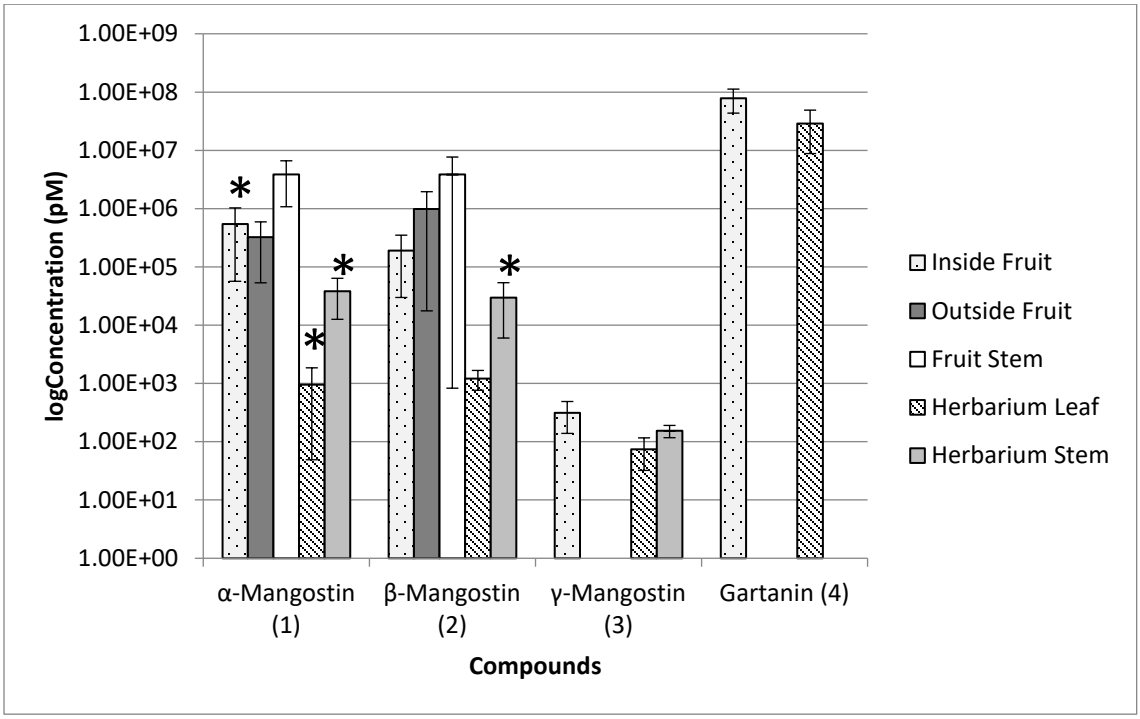

Figure 28. Concentration of Compounds 1-4 from *Garcinia mangostana* Detected from a Dried Fruit Hull Compared to the Herbarium Specimen. The UPLC-HRMS data collected from four sites were sampled, normalized, and then averaged at each location (n=4). However, due to some variability in the measurements, the Grubbs Test was used to eliminate outliers, and in those cases, n=3. The bars with an asterisk are where n=4. Two of the compounds, 9-hydroxycalabaxanthone (**5**) and cratoxyxanthone (**6**), were tested but not detected at all sites.

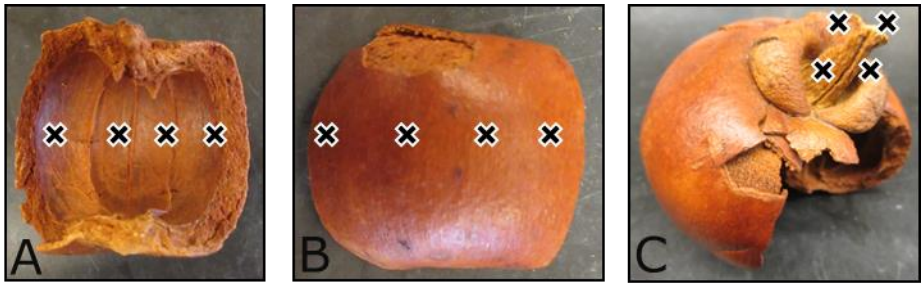

Figure 29. *Garcinia mangostana* Dried Fruit Specimen. The sampling locations are denoted with an X, and 15 microextractions per droplet were performed on the A) Inside Fruit, B) Outside Fruit, and C) Fruit Stem.

With the droplet probe, metabolites can be detected from herbarium vouchers via surface sampling. In addition, with this method we can discern metabolite concentrations that may vary across the sample, which yields physiological information without requiring multiple parts of the plant for extraction purposes. By maintaining the integrity of a herbarium voucher specimen with this technique, there is now the opportunity to safely apply chemotype analysis to such samples and yet preserve their appearance. This type of chemical analysis, where the integrity of the source material is preserved, may become increasingly valuable. Whether these samples are on species that are derived from threatened, endangered, and even extinct plants, or perhaps materials that illustrate pieces of history, chemical analyses need to be both effective and conserve these materials for future generations.

Experimental Section

General experimental procedures

The droplet−liquid microjunction-surface sampling probe was optimized for natural products studies via an earlier collaboration with Oak Ridge National Laboratory.[40] Briefly, a CTC/LEAP HTC PAL autosampler (LEAP Technologies Inc., Pflugerville, TX) was converted into an automated droplet system via dropletProbe Premium, which was developed by Oak Ridge National Laboratory.[92-96] Extractions were performed using Fisher Optima LC/MS grade solvents consisting of 50:50 DMSO:H_2O to enhance the solubility of the prenylated xanthones of interest. For the purpose of investigating the xanthones present, each droplet contained 0.0001 mg/mL of Alizarin Red S (Sigma-Aldrich) as an internal standard. Approximately 4 µl of solvent was drawn into the syringe for each microextraction and dispensed onto the surface of the herbarium specimen at a rate of 2 µl/s. The syringe with the dispensed droplet paused over the surface for two seconds before being drawn back into the syringe. This process was repeated a total of 15 times for a single spot prior to injection into the UPLC−HRMS system. We suggest that users of this methodology notate where samples were acquired on the herbarium specimen, so as to inform future scientists. The droplet probe was coupled with a Waters Acquity ultraperformance liquid chromatography (UPLC) system (Waters Corp.) to a Thermo QExactive Plus MS (ThermoFisher).

The QExactive Plus collected data from 200 to 2000 *m/z* at a mass resolution of 70,000. The voltage for the positive ionization mode was set to 4.0 kV with a nitrogen sheath gas set to 50 arb and an auxiliary gas set to 15 arb. The S-Lens RF level was set to

50.0 and capillary temperature at 300°C. The flow rate of the UPLC was set to 0.3 mL/min using a BEH C_{18} (2.1 × 50 mm, 1.7 μm particle size) column. The column was equilibrated at 40 °C, and the sample manager was not used. The mobile phase consisted of Fisher Optima UPLC−HRMS grade CH_3CN:H_2O with 0.1% HCOOH. The initial gradient began at 75% CH_3CN and increased linearly to 100% CH_3CN over 2 min. For 1.5 minutes, the column was held at 100% CH_3CN to clean the column before being re-equilibrated to the initial starting conditions. The PDA was set to acquire from 200 to 500 nm with a resolution of 4 nm.

Plant material

The herbarium voucher (No. 2286460) of *Garcina mangostana L. (*Clusiaceae) was provided by The Field Museum (Chicago, IL). The *G. mangostana* dried fruit, which included the pericarp, calyx, and pedicel, was provided by one of the authors (ADK).

Droplet probe analysis

The xanthone standards were isolated and characterized as detailed previously.[117, 121] Calibration curves were recorded using a minimum of 12 different concentrations for compounds **1-6** (**Figures D2-D7**). The UPLC-HRMS data for each compound, ranging from 0.00125-512 μM, were measured in triplicate. Calculations of concentrations were based on peak area ratios, and calibration curves were generated by weighted (1/X) linear regression. All data were processed using the Quan Browser module of Xcalibur version 2.2 (Thermo Fisher Scientific). The chromatographic peak areas were integrated using

the Xcalibur Processing Setup version 2.2 (Thermo Fisher Scientific). ICIS peak detection was applied for a list of putatively annotated ions. The Grubbs' test was performed for an n=4 number of observations after the average and standard deviation of each compound was determined at each site. The measurements that were considered outliers at a 5% significance level were excluded from our assessments.[132]

Conclusion

With this method, secondary metabolites from a herbarium voucher specimen of *Garcinia mangostana* were compared and identified with droplet probe coupled to UPLC-HRMS. Importantly, chemical information was gleaned from this technique without the physical alteration of even a portion of the delicate sample. While this study focused on herbarium vouchers, we postulate that it may be applicable to other materials, such as macrofungi, rare/endangered species, or even historical samples and artifacts. This approach may pave the way for the *in situ* chemical analysis of delicate and/or priceless pieces from across time.

Acknowledgements

Diana Kao was supported by the National Center for Complementary and Integrated Health, NIH via grant F31 AT009264. Support also came from the National Cancer Institute, NIH via grant P01 CA125066. To the Botany Collections Manager, John G. Searle Herbarium of the Field Museum, we express our thanks for the loan of the *Garcinia mangostana* specimen and for the permission to submit the specimen for the

present study. The images of the plant specimen were graciously photographed by Daniel Smith of UNCG. We thank, Drs. Vilmos Kertesz and Gary J. Van Berkel (Mass Spectrometry and Laser Spectroscopy Group, Chemical Sciences Division, Oak Ridge National Laboratory) for inspiration and guidance with the droplet probe. We also thank Tyler Graf and Dr. Daniel Todd of UNCG for helpful discussions pertaining to evaluation of metabolites. The mass spectrometry data were acquired in the Triad Mass Spectrometry Facility.

CHAPTER VI

CONCLUSION

The paradigm of natural products research began with the medicinal properties of plants, but contemporary research expands into the less explored microbiome. Techniques applied to analyzing plant material can be refitted to examine microorganisms, and likewise-the techniques developed for examining microorganisms can be implemented for use in analyzing macroorganisms. The research conducted here combines traditional, modern, and innovative techniques for natural products research that can be employed to analyze the medicinal properties from a variety organisms.

By pursuing new leads for drug discovery in the biosynthetic pathways of microorganisms, we are not only investigating an unknown source but also investigating the underlying purpose by which complex and specific molecules are designed, specifically in response which of nature's environmental factors such as viruses, pathogens, and the like. As we advance this research so should we also advance and revise the tools we are applying to detect, to isolate, and to analyze potential drugs and their targets. This is an unending journey because the nature of diseases is to evolve, and in response so should our efforts.

REFERENCES

[1] B. B. Jarvis, Y. W. Lee, S. N. Cömezoglu, C. S. Yatawara, *Appl. Environ. Microbiol.* **1986**, *51*, 915-918.

[2] R. A. Shank, N. A. Foroud, P. Hazendonk, F. Eudes, B. A. Blackwell, *Toxins* **2011**, *3*, 1518-1553.

[3] M. P. de Carvalho, H. Weich, W. R. Abraham, *Curr. Med. Chem.* **2016**, *23*, 23-35.

[4] B. B. Jarvis, G. P. Stahly, G. Pavanasasivam, E. P. Mazzola, *J. Med. Chem.* **1980**, *23*, 1054-1058.

[5] P. W. Brian, J. C. McGowan, *Nature* **1946**, *157*, 334-334.

[6] B. B. Jarvis, E. P. Mazzola, *Acc. Chem. Res.* **1982**, *15*, 388-395.

[7] B. B. Jarvis, J. O. Midiwo, E. P. Mazzola, *J. Med. Chem.* **1984**, *27*, 239-244.

[8] A. A. Sy-Cordero, T. N. Graf, M. C. Wani, D. J. Kroll, C. J. Pearce, N. H. Oberlies, *J. Antibiot.* **2010**, *63*, 539-544.

[9] T. Amagata, C. Rath, J. F. Rigot, N. Tarlov, K. Tenney, F. A. Valeriote, P. Crews, *J. Med. Chem.* **2003**, *46*, 4342-4350.

[10] A. E. Desjardins, *J. Agric. Food Chem.* **2009**, *57*, 4478-4484.

[11] S. R. Lee, S. Seok, R. Ryoo, S. U. Choi, K. H. Kim, *J. Nat. Prod.* **2019**, *82*, 122-128.

[12] L. T. T. Nguyen, J. Y. Jang, T. Y. Kim, N. H. Yu, A. R. Park, S. Lee, C. H. Bae, J. H. Yeo, J. S. Hur, H. W. Park, J. C. Kim, *Pestic. Biochem. Physiol.* **2018**, *148*, 133-143.

[13] Q. Wu, X. Wang, E. Nepovimova, A. Miron, Q. Liu, Y. Wang, D. Su, H. Yang, L. Li, K. Kuca, *Arch. Toxicol.* **2017**, *91*, 3737-3785.

[14] M. H. Raza, K. Gul, A. Arshad, N. Riaz, U. Waheed, A. Rauf, F. Aldakheel, S. Alduraywish, M. U. Rehman, M. Abdullah, M. Arshad, *J. Cancer Res. Clin. Oncol.* **2019**, *145*, 49-63.

[15] M. S. Syrkina, M. A. Rubtsov, *Biochemistry Mosc.* **2019**, *84*, 773-781.

[16] A. D. Kinghorn, D. E. B. EJ, D. M. Lucas, H. L. Rakotondraibe, J. Orjala, D. D. Soejarto, N. H. Oberlies, C. J. Pearce, M. C. Wani, B. R. Stockwell, J. E. Burdette, S. M. Swanson, J. R. Fuchs, M. A. Phelps, L. Xu, X. Zhang, Y. Y. Shen, *Anticancer Res.* **2016**, *36*, 5623-5637.

[17] G. Pavanasasivam, B. B. Jarvis, *Appl. Environ. Microbiol.* **1983**, *46*, 480-483.

[18] M. A. M. Mondol, M. Z. Surovy, M. T. Islam, A. Schüffler, H. Laatsch, *J. Agric. Food Chem.* **2015**, *63*, 8777-8786.

[19] H.-X. Liu, W.-Z. Liu, Y.-C. Chen, Z.-H. Sun, Y.-Z. Tan, H.-H. Li, W.-M. Zhang, *J. Asian. Nat. Prod. Res.* **2016**, *18*, 684-689.

[20] B. B. Jarvis, S. N. Comezoglu, M. M. Rao, N. B. Pena, *J. Org. Chem.* **1987**, *52*, 45-56.
[21] S. Schoettler, M. Bascope, O. Sterner, T. Anke, *Z. Naturforsch. C* **2006**, *61*, 309-314.
[22] T. R. Hoye, C. S. Jeffrey, F. Shao, *Nat. Protoc.* **2007**, *2*, 2451-2458.
[23] M. Gardes, T. J. White, J. A. Fortin, T. D. Bruns, J. W. Taylor, *Can. J. Bot.* **1991**, *69*, 180-190.
[24] T. J. White, T. Bruns, S. H. Lee, J. W. Taylor, *PCR protocols: a guide to methods and application. San Diego*, San Diego, **1990**.
[25] H. A. Raja, A. N. Miller, C. J. Pearce, N. H. Oberlies, *J. Nat. Prod.* **2017**, *80*, 756-770.
[26] L. Lombard, J. Houbraken, C. Decock, R. A. Samson, M. Meijer, M. Reblova, J. Z. Groenewald, P. W. Crous, *Persoonia* **2016**, *36*, 156-246.
[27] C. S. M. Amrine, H. A. Raja, B. A. Darveaux, C. J. Pearce, N. H. Oberlies, *J. Ind. Microbiol. Biotechnol.* **2018**, *45*, 1053-1065.
[28] H. A. Raja, A. Kaur, T. El-Elimat, M. Figueroa, R. Kumar, G. Deep, R. Agarwal, S. H. Faeth, N. B. Cech, N. H. Oberlies, *Mycology* **2015**, *6*, 8-27.
[29] M. Figueroa, A. K. Jarmusch, H. A. Raja, T. El-Elimat, J. S. Kavanaugh, A. R. Horswill, R. G. Cooks, N. B. Cech, N. H. Oberlies, *Journal of Natural Products* **2014**, *77*, 1351-1358.
[30] S. M. Daly, B. O. Elmore, J. S. Kavanaugh, K. D. Triplett, M. Figueroa, H. A. Raja, T. El-Elimat, H. A. Crosby, J. K. Femling, N. B. Cech, A. R. Horswill, N. H. Oberlies, P. R. Hall, *Antimicrob. Agents Chemother.* **2015**, *59*, 2223-2235.
[31] B. Spellberg, J. G. Bartlett, D. N. Gilbert, *New England Journal of Medicine* **2013**, *368*, 299-302.
[32] N. B. Cech, A. R. Horswill, *Future microbiology* **2013**, *8*, 1511-1514.
[33] B. A. Lanman, *Science* **2017**, *358*, 166-167.
[34] J. L. Liang, H. C. Cha, S. H. Lee, J.-K. Son, H. W. Chang, J.-E. Eom, Y. Kwon, Y. Jahng, *Arch. Pharm. Res.* **2012**, *35*, 447-454.
[35] R. Jacobson, R. Adams, *Journal of the American Chemical Society* **1924**, *46*, 1312-1316.
[36] L. Teich, K. S. Daub, V. Krügel, L. Nissler, R. Gebhardt, K. Eger, *Bioorg. Med. Chem.* **2004**, *12*, 5961-5971.
[37] W. K. Anslow, J. Breen, H. Raistrick, *Biochemical Journal* **1940**, *34*, 159.
[38] J. C. Frisvad, J. Smedsgaard, T. O. Larsen, R. A. Samson, *Stud. Mycol* **2004**, *49*, 201-241.
[39] J. C. Frisvad, R. A. Samson, *Studies in mycology* **2004**, *49*, 1-174.
[40] V. P. Sica, H. A. Raja, T. El-Elimat, V. Kertesz, G. J. Van Berkel, C. J. Pearce, N. H. Oberlies, *Journal of Natural Products* **2015**, *78*, 1926-1936.
[41] C. S. M. Amrine, H. A. Raja, B. A. Darveus, C. J. Pearce, N. H. Oberlies, *J. Ind. Microbiol. Biotechnol.* **2018**.
[42] V. P. Sica, E. R. Rees, H. A. Raja, J. Rivera-Chávez, J. E. Burdette, C. J. Pearce, N. H. Oberlies, *Phytochemistry* **2017**, *143*, 45-53.

[43] H. A. Raja, N. D. Paguigan, J. Fournier, N. H. Oberlies, *Mycological Progress* **2017**, *16*, 535-552.
[44] V. P. Sica, E. R. Rees, E. Tchegnon, R. H. Bardsley, H. A. Raja, N. H. Oberlies, *Frontiers in Microbiology* **2016**, *7*, 1126-1114.
[45] T. El-Elimat, H. A. Raja, M. Figueroa, J. O. Falkinham III, N. H. Oberlies, *Phytochemistry* **2014**, *104*, 114-120.
[46] T. El-Elimat, H. A. Raja, T. N. Graf, S. H. Faeth, N. B. Cech, N. H. Oberlies, *Journal of Natural Products* **2014**, *77*, 193-199.
[47] T. Sudhakar, S. Dash, R. Rao, R. Srinivasan, S. Zacharia, M. Atmanand, B. Subramaniam, S. Nayak, *Current Science* **2013**, *104*, 178.
[48] V. Kertesz, G. J. Van Berkel, *Analytical chemistry* **2010**, *82*, 5917-5921.
[49] K. M. Vandermolen, H. A. Raja, T. El-Elimat, N. H. Oberlies, *AMB Express* **2013**, *3*, 71.
[50] G. F. Bills, A. W. Dombrowski, M. A. Goetz, in *Fungal Secondary Metabolism: Methods and Protocols* (Eds.: N. P. Keller, G. Turner), Springer, **2012**, pp. 79-96.
[51] Y. Kumarasamy, in *Natural Products Isolation*, Springer, **2012**, pp. 465-472.
[52] D. A. Dias, S. Urban, U. Roessner, *Metabolites* **2012**, *2*, 303-336.
[53] B. Schmidt, D. M. Ribnicky, A. Poulev, S. Logendra, W. T. Cefalu, I. Raskin, *Metabolism* **2008**, *57*, S3-S9.
[54] W. P. Jones, A. D. Kinghorn, in *Natural products isolation*, Springer, **2006**, pp. 323-351.
[55] V. P. Sica, T. El-Elimat, N. H. Oberlies, *Anal. Methods* **2016**, *8*, 6143-6149.
[56] V. P. Sica, E. R. Rees, E. Tchegnon, R. H. Bardsley, H. A. Raja, N. H. Oberlies, *Frontiers in Microbiology* **2016**, *7*, DOI: 10.3389/fmicb.2016.00544.
[57] R. T. Hewage, T. Aree, C. Mahidol, S. Ruchirawat, P. Kittakoop, *Phytochemistry* **2014**, *108*, 87-94.
[58] C. F. P. Hemphill, P. Sureechatchaiyan, M. U. Kassack, R. S. Orfali, W. Lin, G. Daletos, P. Proksch, *J. Antibiot.* **2017**, *70*, 726.
[59] M. Figueroa, A. K. Jarmusch, H. A. Raja, T. El-Elimat, J. S. Kavanaugh, A. R. Horswill, R. G. Cooks, N. B. Cech, N. H. Oberlies, *J. Nat. Prod.* **2014**, *77*, 1351-1358.
[60] H. A. Raja, A. Kaur, T. El-Elimat, M. Figueroa, R. Kumar, G. Deep, R. Agarwal, S. H. Faeth, N. B. Cech, N. H. Oberlies, *Mycology* **2015**, *6*, 8-27.
[61] P. Spiteller, *Nat. Prod. Rep.* **2015**, *32*, 971-993.
[62] S. Kusari, M. Spiteller, *Nat. Prod. Rep.* **2011**, *28*, 1203-1207.
[63] G. L. Challis, *J. Med. Chem.* **2008**, *51*, 2618-2628.
[64] N. P. Keller, *Nat. Rev. Microbiol.* **2018**, 1.
[65] N. P. Keller, G. Turner, J. W. Bennett, *Nat. Rev. Microbiol.* **2005**, *3*, 937.
[66] J. Orjala, N. H. Oberlies, C. Pearce, S. Swanson, A. D. Kinghorn, in *Discovery of Potential Anticancer Agents from Aquatic Cyanobacteria, Filamentous Fungi, and Tropical Plants* (Ed.: C. Tringali), CRC PRess, **2011**, pp. 37-64.
[67] C. M. Crnkovic, A. Krunic, D. S. May, T. A. Wilson, D. Kao, J. E. Burdette, J. R. Fuchs, N. H. Oberlies, J. Orjala, *J. Nat. Prod.* **2018**, *81*, 2083-2090.
[68] F. Q. Alali, X.-X. Liu, J. L. McLaughlin, *J. Nat. Prod.* **1999**, *62*, 504-540.

[69] J. L. McLaughlin, *J. Nat. Prod.* **2008**, *71*, 1311-1321.
[70] M.-H. Woo, D.-H. Kim, J. L. McLaughlin, *Phytochemistry* **1999**, *50*, 1033-1040.
[71] M. H. Woo, K. Y. Cho, Y. Zhang, L. Zeng, Z.-M. Gu, J. L. McLaughlin, *J. Nat. Prod.* **1995**, *58*, 1533-1542.
[72] K. He, G.-X. Zhao, G. Shi, L. Zeng, J.-F. Chao, J. L. McLaughlin, *Bioorg. Med. Chem.* **1997**, *5*, 501-506.
[73] G.-X. Zhao, M. Rieser, Y.-H. Hui, L. Miesbauer, D. Smith, J. McLaughlin, *Phytochemistry* **1993**, *33*, 1065-1073.
[74] S. Ratnayake, K. J. Rupprecht, W. M. Potter, J. L. McLaughlin, *J. Econ. Entomol.* **1992**, *85*, 2353-2356.
[75] V. Sica, T. El-Elimat, N. Oberlies, *Anal. Methods.* **2016**, *8*, 6143-6149.
[76] M.-H. Woo, S.-O. Chung, D.-H. Kim, *Bioorg. Med. Chem.* **2000**, *8*, 285-290.
[77] J. Le Ven, I. Schmitz-Afonso, G. Lewin, O. Laprévote, A. Brunelle, D. Touboul, P. Champy, *J. Mass Spectrom.* **2012**, *47*, 1500-1509.
[78] D. Kao, J. M. Henkin, D. D. Soejarto, A. D. Kinghorn, N. H. Oberlies, *Phytochem. Lett.* **2018**, *28*, 124-129.
[79] R. G. Cooks, Z. Ouyang, Z. Takats, J. M. Wiseman, *Science* **2006**, *311*, 1566-1570.
[80] K. M. VanderMolen, B. A. Darveaux, W.-L. Chen, S. M. Swanson, C. J. Pearce, N. H. Oberlies, *RSC advances* **2014**, *4*, 18329-18335.
[81] G. F. Bills, G. Platas, A. Fillola, M. R. Jiménez, J. Collado, F. Vicente, J. Martín, A. González, J. Bur-Zimmermann, J. R. Tormo, F. Peláez, *Journal of Applied Microbiology* **2008**, *104*, 1644-1658.
[82] H. Wei, Z. Lin, D. Li, Q. Gu, T. Zhu, *Acta microbiologica Sinica* **2010**, *50*, 701-709.
[83] E. Kuhnert, S. Heitkämper, J. Fournier, F. Surup, M. Stadler, *Fungal Biol* **2014**, *118*, 242-252.
[84] M. Stadler, *Cur Res Env App Microbiol* **2011**, *1*, 75-133.
[85] S. Hutwimmer, H. Wang, H. Strasser, W. Burgstaller, *Mycologia* **2010**, *102*, 1-10.
[86] X. Wang, J. G. Sena Filho, A. R. Hoover, J. B. King, T. K. Ellis, D. R. Powell, R. H. Cichewicz, *J. Nat. Prod.* **2010**, *73*, 942-948.
[87] A. Koulman, G. A. Lane, M. J. Christensen, K. Fraser, B. A. Tapper, *Phytochemistry* **2007**, *68*, 355-360.
[88] M. Figueroa, A. K. Jarmusch, H. A. Raja, T. El-Elimat, J. S. Kavanaugh, A. R. Horswill, R. G. Cooks, N. B. Cech, N. H. Oberlies, *J. Nat. Prod.* **2014**, *77*, 1351-1358.
[89] S. M. Daly, B. O. Elmore, J. S. Kavanaugh, K. D. Triplett, M. Figueroa, H. A. Raja, T. El-Elimat, H. A. Crosby, J. K. Femling, N. B. Cech, A. R. Horswill, N. H. Oberlies, P. R. Hall, *Antimicrob Agents Chemother* **2015**, *59*, 2223-2235.
[90] M. Thoendel, J. S. Kavanaugh, C. E. Flack, A. R. Horswill, *Chem Rev* **2011**, *111*, 117-151.
[91] D. A. Todd, C. P. Parlet, H. A. Crosby, C. L. Malone, K. P. Heilmann, A. R. Horswill, N. B. Cech, *Antimicrob. Agents Chemother.* **2017**, *61*, e00263-00217.
[92] V. Kertesz, G. J. Van Berkel, *Bioanalysis* **2013**, *5*, 819-826.

[93] V. Kertesz, G. J. Van Berkel, *Rapid Commun. Mass Spectrom.* **2014**, *28*, 1553-1560.
[94] V. Kertesz, N. Paranthaman, P. Moench, A. Catoire, J. Flarakos, G. J. Van Berkel, *Bioanalysis* **2014**, *6*, 2599-2606.
[95] V. Kertesz, T. M. Weiskittel, G. J. Van Berkel, *Anal. Bioanal. Chem.* **2015**, *407*, 2117-2125.
[96] O. S. Ovchinnikova, V. Kertesz, G. J. Van Berkel, *Anal. Chem.* **2011**, *83*, 598-603.
[97] W. T. Stearn, *Biol. J. Linn. Soc. Lond.* **1971**, *3*, 225-233.
[98] S. Müller-Wille, *Endeavour* **2006**, *30*, 60-64.
[99] T. M. Culley, *Appl. Plant Sc.* **2013**, *1*, apps.1300076.
[100] C. G. Willis, E. R. Ellwood, R. B. Primack, C. C. Davis, K. D. Pearson, A. S. Gallinat, J. M. Yost, G. Nelson, S. J. Mazer, N. L. Rossington, T. H. Sparks, P. S. Soltis, *Trends Ecol. Evolut. (Amst.)* **2017**, *32*, 531-546.
[101] L. Z. Drabkova, *Methods Mol. Biol.* **2014**, *1115*, 69-84.
[102] B. Jiang, H. Yang, P. Nuntanakorn, M. J. Balick, F. Kronenberg, E. J. Kennelly, *J. Ethnopharmacol.* **2005**, *96*, 521-528.
[103] N. D. Paguigan, H. A. Raja, C. S. Day, N. H. Oberlies, *Phytochemistry* **2016**, *126*, 59-65.
[104] V. P. Sica, M. Figueroa, H. A. Raja, T. El-Elimat, B. A. Darveaux, C. J. Pearce, N. H. Oberlies, *J. Ind. Microbiol. Biotechnol.* **2016**, *43*, 1149-1157.
[105] V. P. Sica, E. R. Rees, H. A. Raja, J. Rivera-Chavez, J. E. Burdette, C. J. Pearce, N. H. Oberlies, *Phytochemistry* **2017**, *143*, 45-53.
[106] L. G. Chen, L. L. Yang, C. C. Wang, *Food Chem. Toxicol.* **2008**, *46*, 688-693.
[107] Y. W. Chin, H. A. Jung, H. Chai, W. J. Keller, A. D. Kinghorn, *Phytochemistry* **2008**, *69*, 754-758.
[108] P. Williams, M. Ongsakul, J. Proudfoot, K. Croft, L. Beilin, *Free Radic. Res.* **1995**, *23*, 175-184.
[109] Y. W. Chin, A. D. Kinghorn, *Mini Rev. Org. Chem.* **2008**, *5*, 355-364.
[110] P. A. Benatrehina, L. Pan, C. B. Naman, J. Li, A. D. Kinghorn, *J. Tradit. Complement. Med.* **2018**, *8*, 267-277.
[111] M. Y. Ibrahim, N. M. Hashim, A. A. Mariod, S. Mohan, M. A. Abdulla, S. I. Abdelwahab, I. A. Arbab, *Arab. J. Chem.* **2016**, *9*, 317-329.
[112] N. Chairungsrilerd, K. Furukawa, T. Ohta, S. Nozoe, Y. Ohizumi, *Planta Med.* **1996**, *62*, 471-472.
[113] S. X. Chen, M. Wan, B. N. Loh, *Planta Med.* **1996**, *62*, 381-382.
[114] G. Gopalakrishnan, B. Banumathi, G. Suresh, *J. Nat. Prod.* **1997**, *60*, 519-524.
[115] S. Suksamrarn, N. Suwannapoch, W. Phakhodee, J. Thanuhiranlert, P. Ratananukul, N. Chimnoi, A. Suksamrarn, *Chem. Pharm. Bull.* **2003**, *51*, 857-859.
[116] K. Matsumoto, Y. Akao, E. Kobayashi, K. Ohguchi, T. Ito, T. Tanaka, M. Iinuma, Y. Nozawa, *J. Nat. Prod.* **2003**, *66*, 1124-1127.
[117] H. A. Jung, B. N. Su, W. J. Keller, R. G. Mehta, A. D. Kinghorn, *J. Agric. Food Chem.* **2006**, *54*, 2077-2082.

[118] S. Phongpaichit, N. Rungjindamai, V. Rukachaisirikul, J. Sakayaroj, *FEMS Immunol. Med. Microbiol.* **2006**, *48*, 367-372.
[119] M. T. Chomnawang, S. Surassmo, V. S. Nukoolkarn, W. Gritsanapan, *Fitoterapia* **2007**, *78*, 401-408.
[120] M. T. Chomnawang, S. Surassmo, K. Wongsariya, N. Bunyapraphatsara, *Fitoterapia* **2009**, *80*, 102-104.
[121] A. R. Han, J. A. Kim, D. D. Lantvit, L. B. Kardono, S. Riswan, H. Chai, E. J. Carcache de Blanco, N. R. Farnsworth, S. M. Swanson, A. D. Kinghorn, *J. Nat. Prod.* **2009**, *72*, 2028-2031.
[122] H. Tousian Shandiz, B. M. Razavi, H. Hosseinzadeh, *Phytother. Res.* **2017**, *31*, 1173-1182.
[123] M. J. Balunas, B. Su, R. W. Brueggemeier, A. D. Kinghorn, *J. Nat. Prod.* **2008**, *71*, 1161-1166.
[124] C. Chitchumroonchokchai, J. M. Thomas-Ahner, J. Li, K. M. Riedl, J. Nontakham, S. Suksumrarn, S. K. Clinton, A. D. Kinghorn, M. L. Failla, *Mol. Nutr. Food Res.* **2013**, *57*, 203-211.
[125] X. Ji, B. Avula, I. A. Khan, *J. Pharm. Biomed. Anal.* **2007**, *43*, 1270-1276.
[126] E. B. Walker, *J. Sep. Sci.* **2007**, *30*, 1229-1234.
[127] D. Obolskiy, I. Pischel, N. Siriwatanametanon, M. Heinrich, *Phytother. Res.* **2009**, *23*, 1047-1065.
[128] L. D. Shepherd, *PLoS ONE* **2017**, *12*, e0183555.
[129] S. T. Lee, D. Cook, T. Z. Davis, D. R. Gardner, R. L. Johnson, C. A. Stonecipher, *J. Agric. Food Chem.* **2015**, *63*, 872-879.
[130] S. T. Lee, T. Z. Davis, D. Cook, *IJPPR* **2017**, *4*, 36-42.
[131] U. Sukatta, M. Takenaka, H. Ono, H. Okadome, I. Sotome, K. Nanayama, W. Thanapase, S. Isobe, *Biosci. Biotechnol. Biochem.* **2013**, *77*, 984-987.
[132] F. E. Grubbs, *Technometrics* **1969**, *11*, 1-21.

APPENDIX A

SUPPLEMENTARY FIGURES

Table of Contents

described. Based on these parameters, the histogram spans from 1962 to 2019. These are organized in approximately 10-year intervals.

Figure A21. A Histogram Based on a Research Topic Search of "Macrocyclic Trichothecenes" in SciFinder Scholar. This search reported over 300 results but only just over 200 when all duplicates were removed. The search was refined by looking only at those papers published that applied to Biotechnology terms: Substances in Adverse effects (all terms), Toxicology & forensics (all terms), Medicine (all terms), Substances in medicine (all terms), and/or Agriculture (Antibiotics and Antimalarials). The 145 remaining references were denoted according to years with the earliest reported literature of biological tests that fit these parameters in 1980 to the latest in 2019. Each bin width is organized in approximately 10-year intervals.

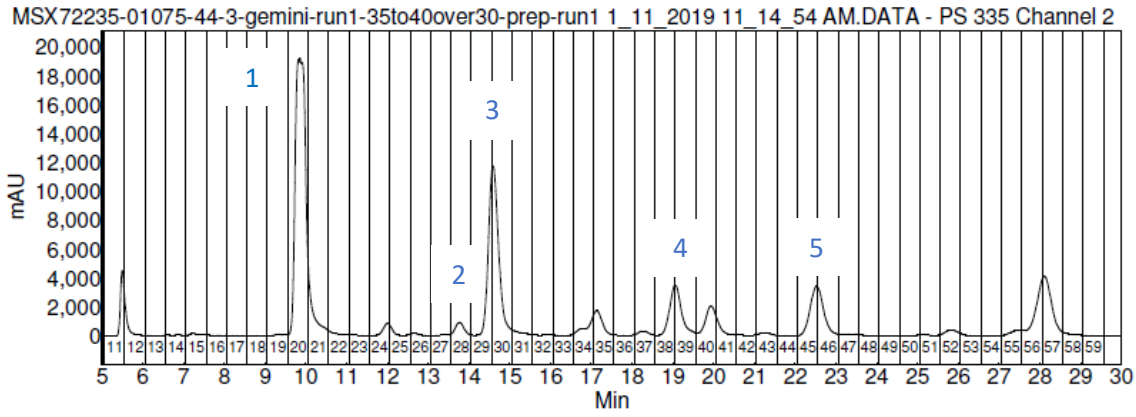

Figure A1. Reversed-phase Preparative HPLC Chromatogram for the Purification of Compounds 1-5 (λ_{max} 254 nm). Data were acquired via a Varian Prostar HPLC system with a Phenomenex Gemini–NX C18 preparative (5 µm; 250 × 21.2 mm) column, and CH_3CN-H_2O (0.1% formic acid) gradient that increased linearly from 35:65 to 40:60 over 30 min at a flow rate of 21.20 mL/min.

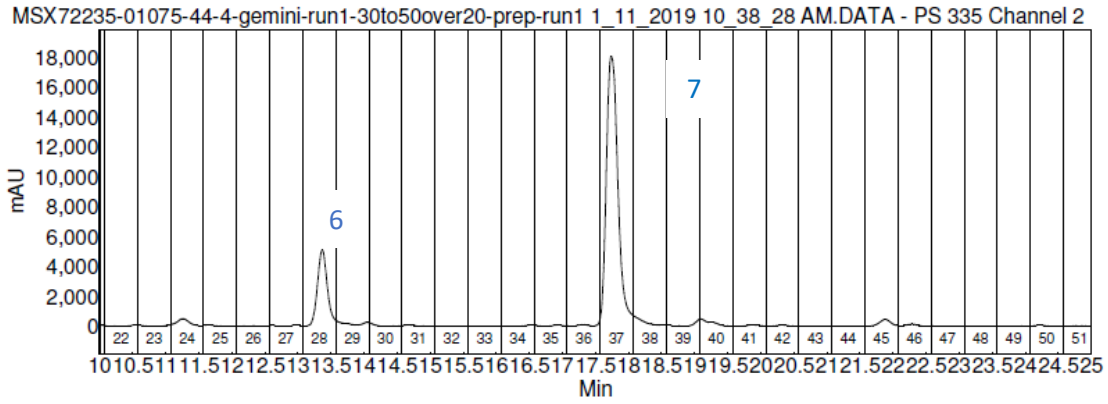

Figure A1.5. Reversed-phase Preparative HPLC Chromatogram for the Purification of Compounds 6 and 7 (λ_{max} 254 nm). Data were acquired via a Varian Prostar HPLC system with a Phenomenex Gemini–NX C18 preparative (5 µm; 250 × 21.2 mm) column, and CH_3CN-H_2O (0.1% formic acid) gradient that increased linearly from 30:50 to 40:60 over 20 min at a flow rate of 21.20 mL/min.

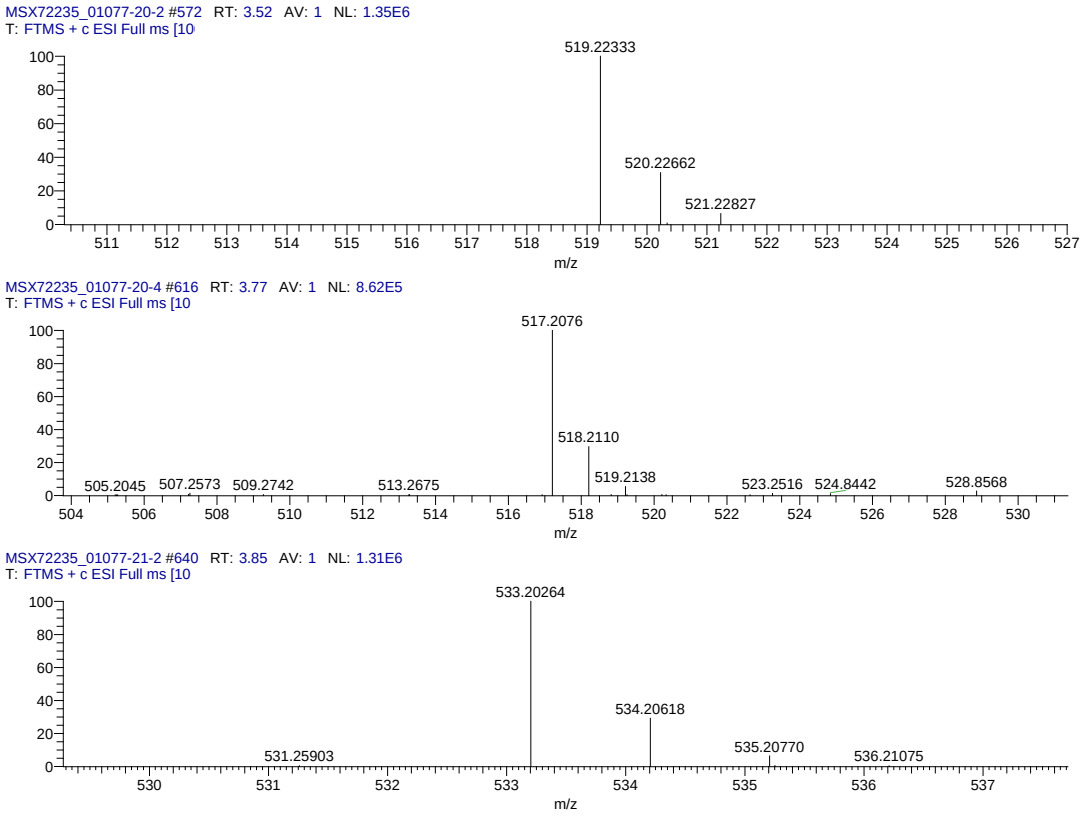

Figure A2. (+)-HRESIMS Spectra of Compounds 1 (top), 2 (middle) and 3 (bottom).

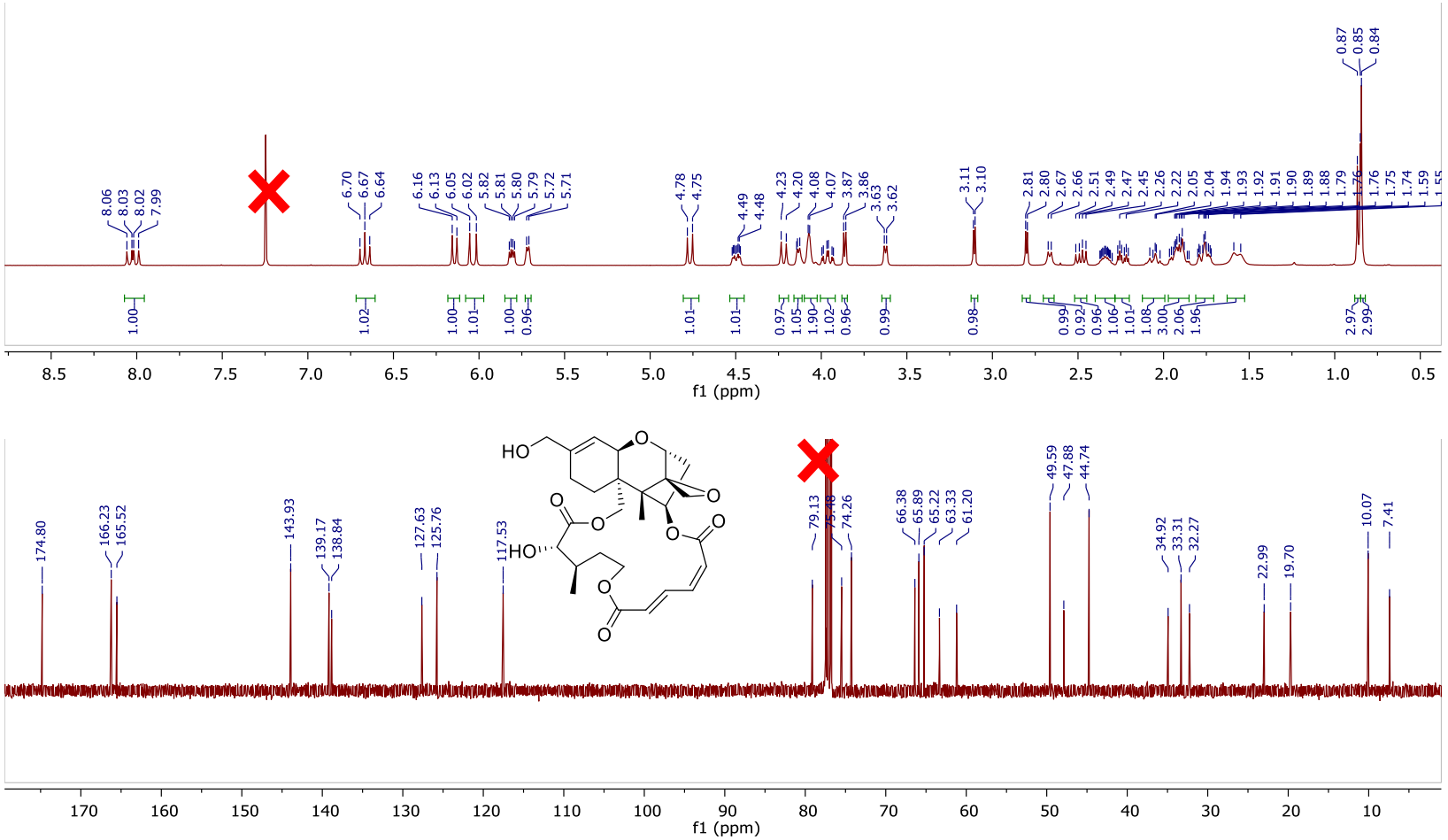

Figure A3. ^{1}H and ^{13}C NMR Spectra of 1 [400 MHz for ^{1}H and 100 MHz for ^{13}C, $CDCl_3$].

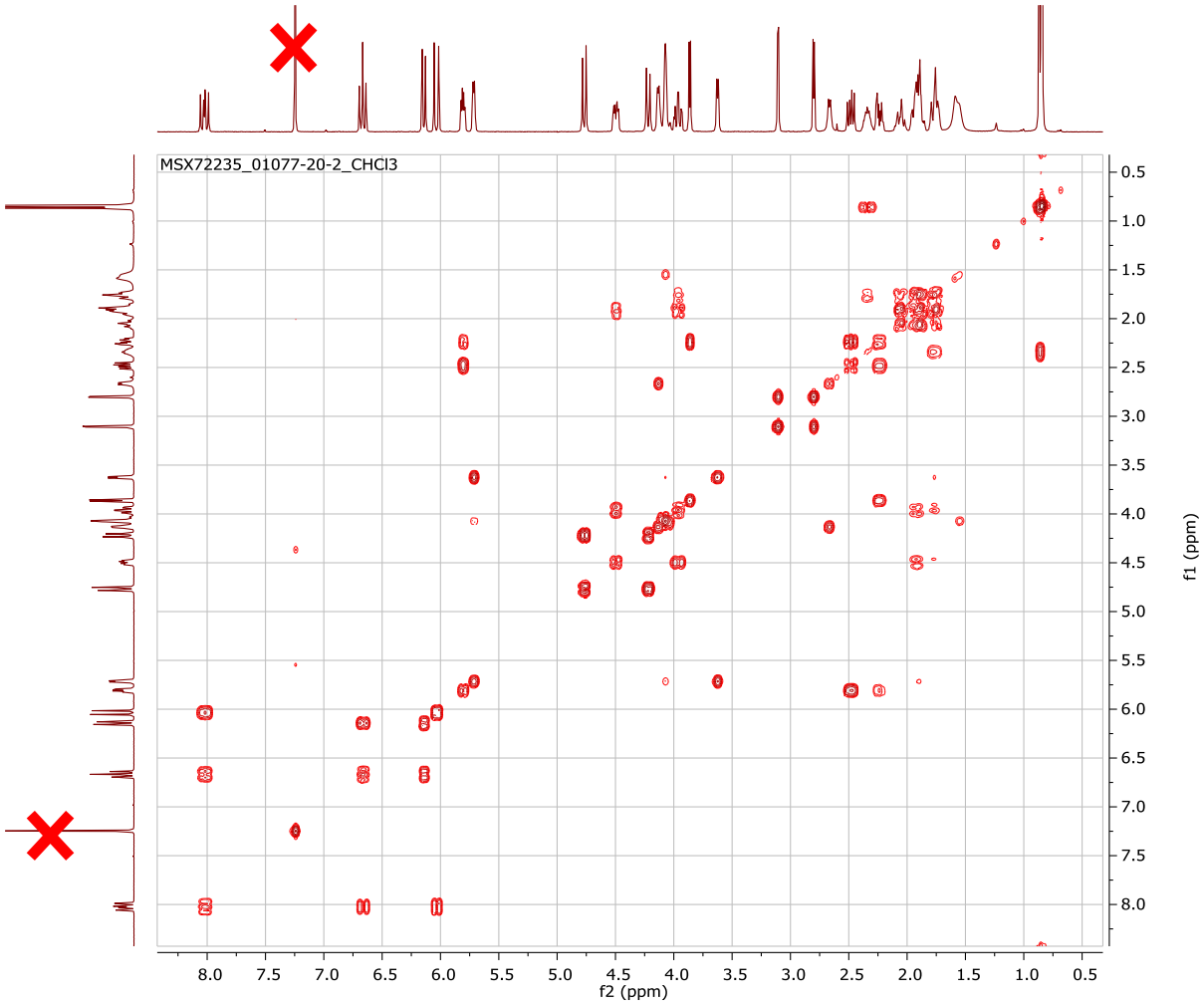

Figure A4. COSY NMR Spectrum of 1 [400 MHz, $CDCl_3$].

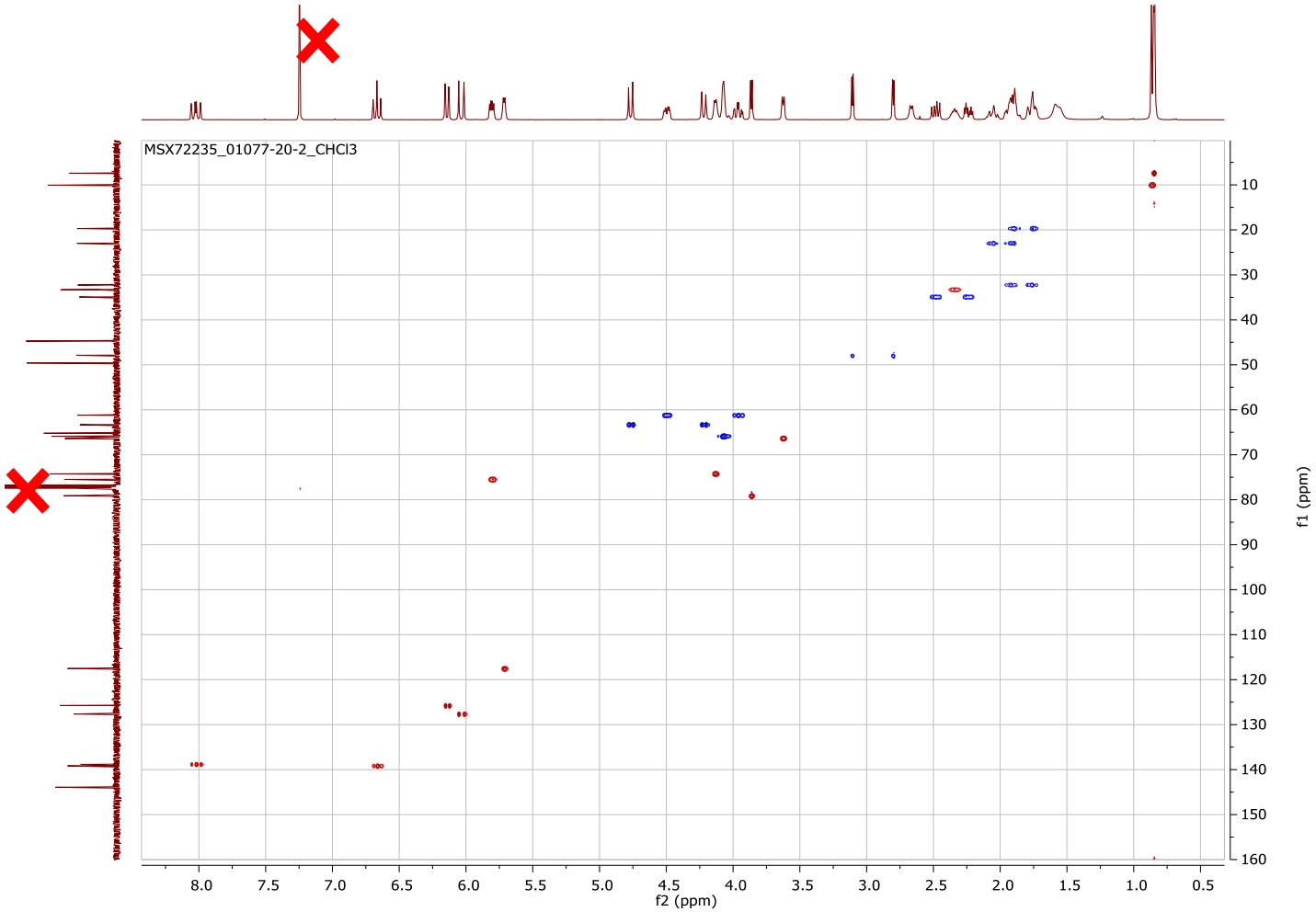

Figure A5. Edited-HSQC NMR Spectrum of 1 [400 MHz for ^{1}H, $CDCl_3$].

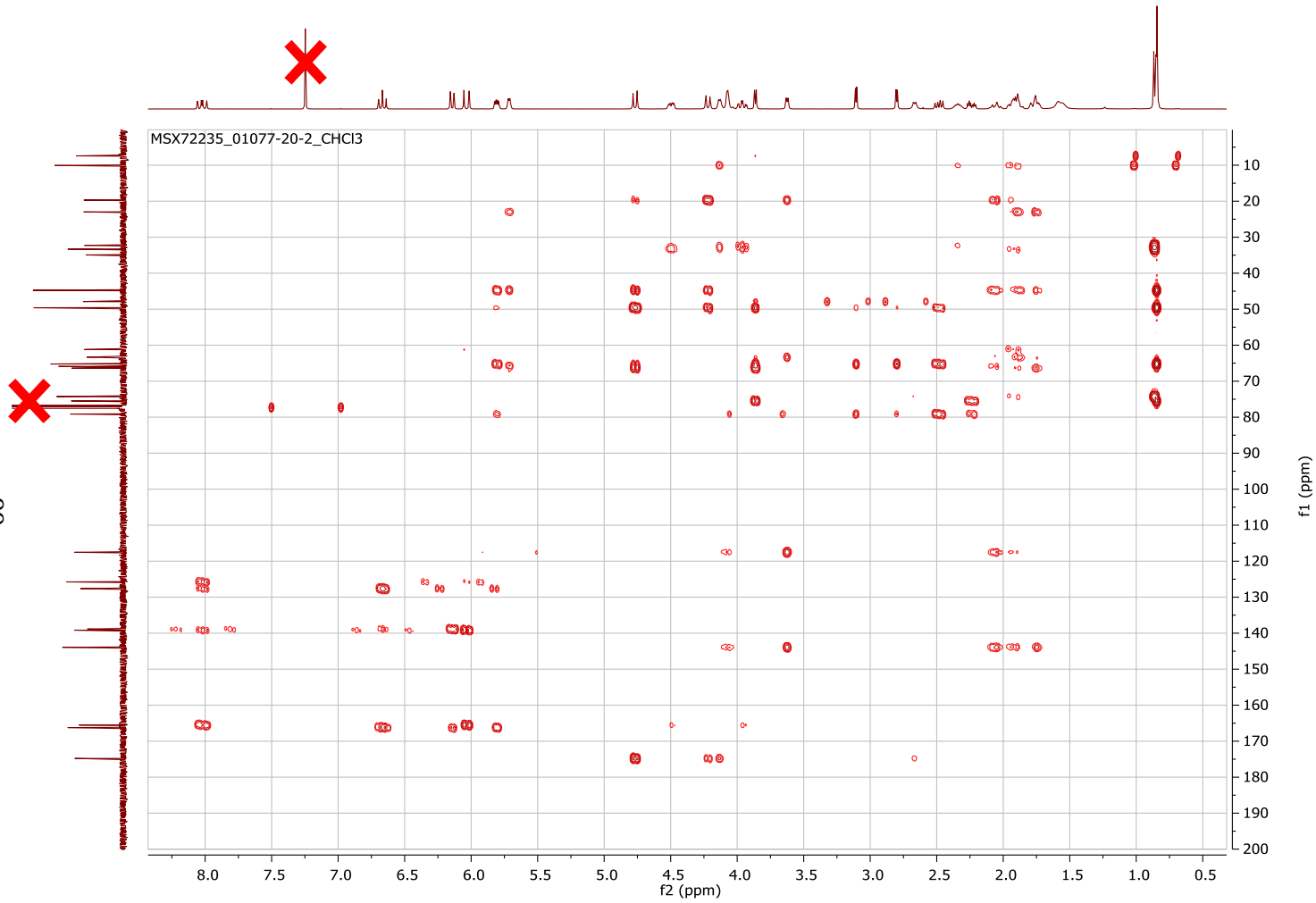

Figure A6. HMBC NMR Spectrum of 1 [400 MHz, $CDCl_3$].

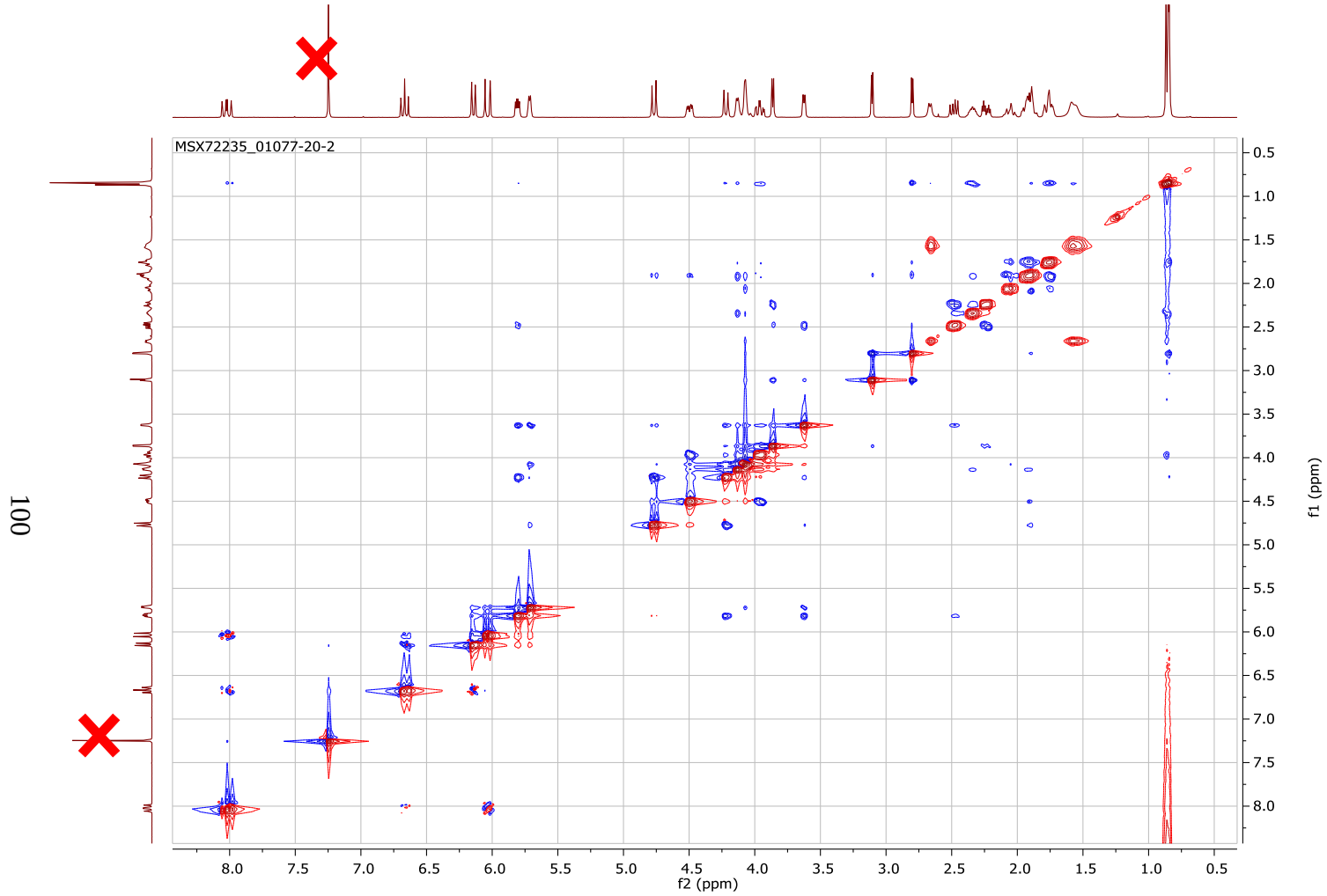

Figure A7. NOESY NMR Spectrum of 1 [400 MHz, $CDCl_3$].

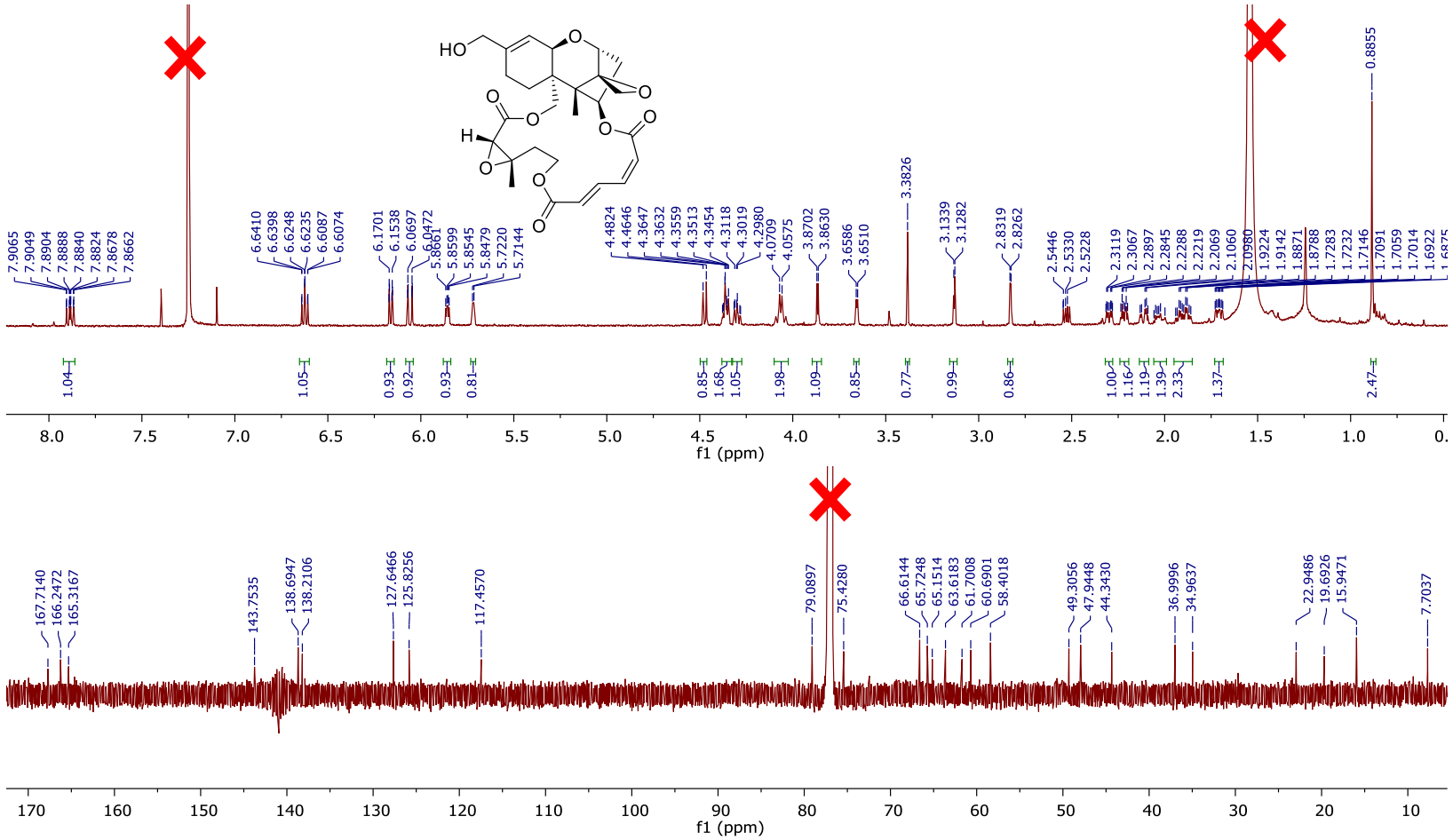

Figure A8. ^{1}H and ^{13}C NMR Spectra of 2 [700 MHz for ^{1}H and 175 MHz for ^{13}C, $CDCl_3$].

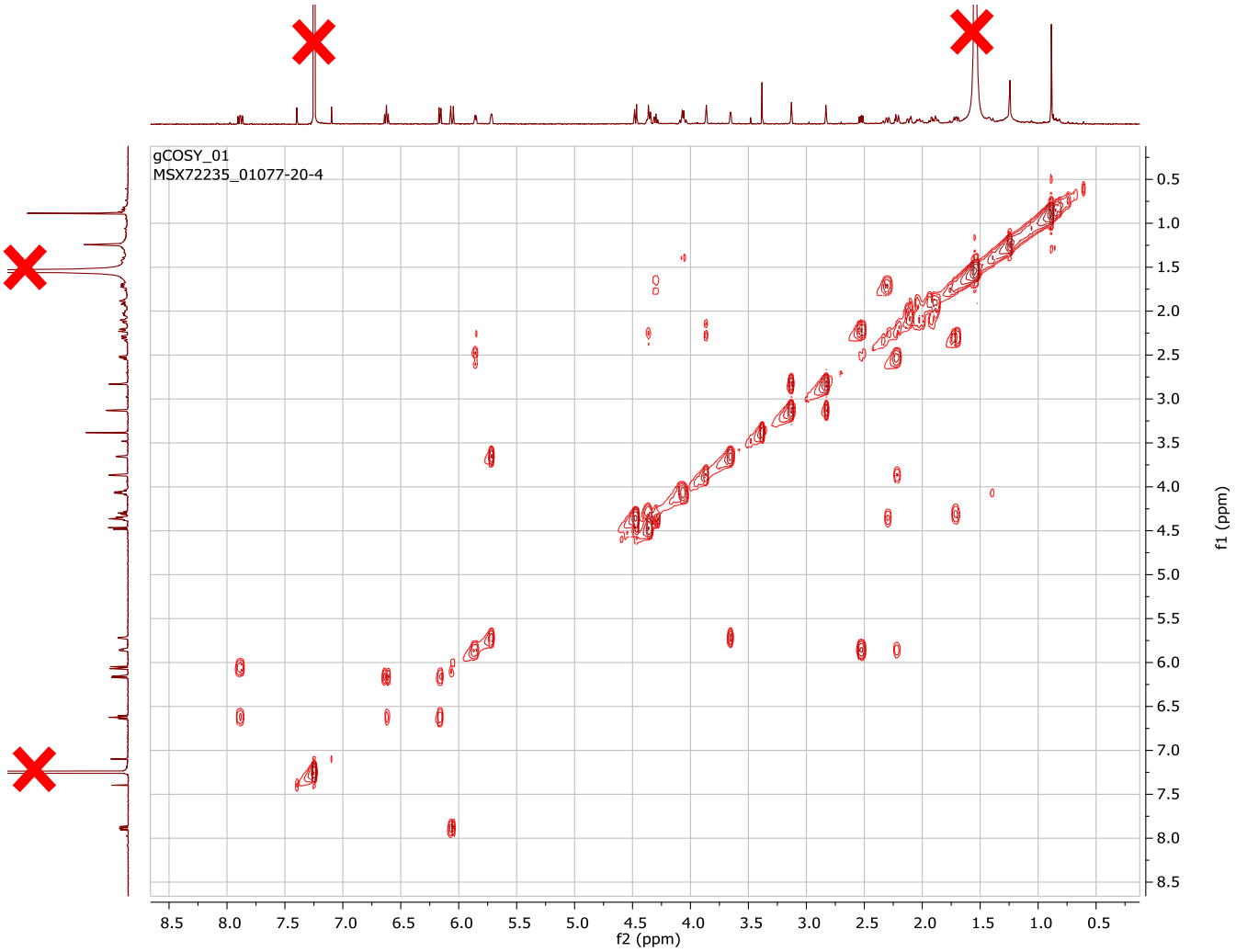

Figure A9. COSY NMR Spectrum of 2 [700 MHz, $CDCl_3$].

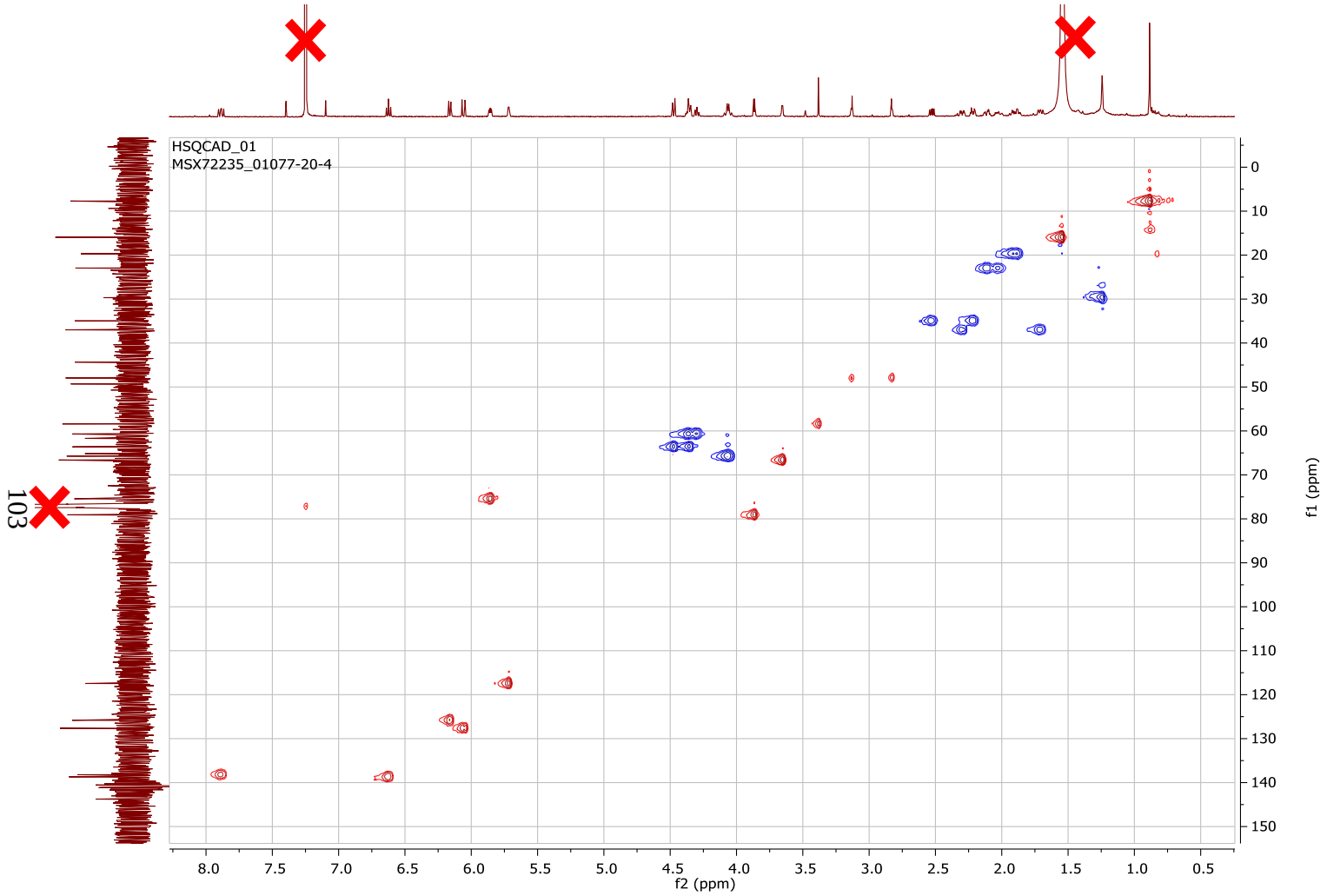

Figure A10. HSQC NMR Spectrum of 2 [700 MHz, $CDCl_3$].

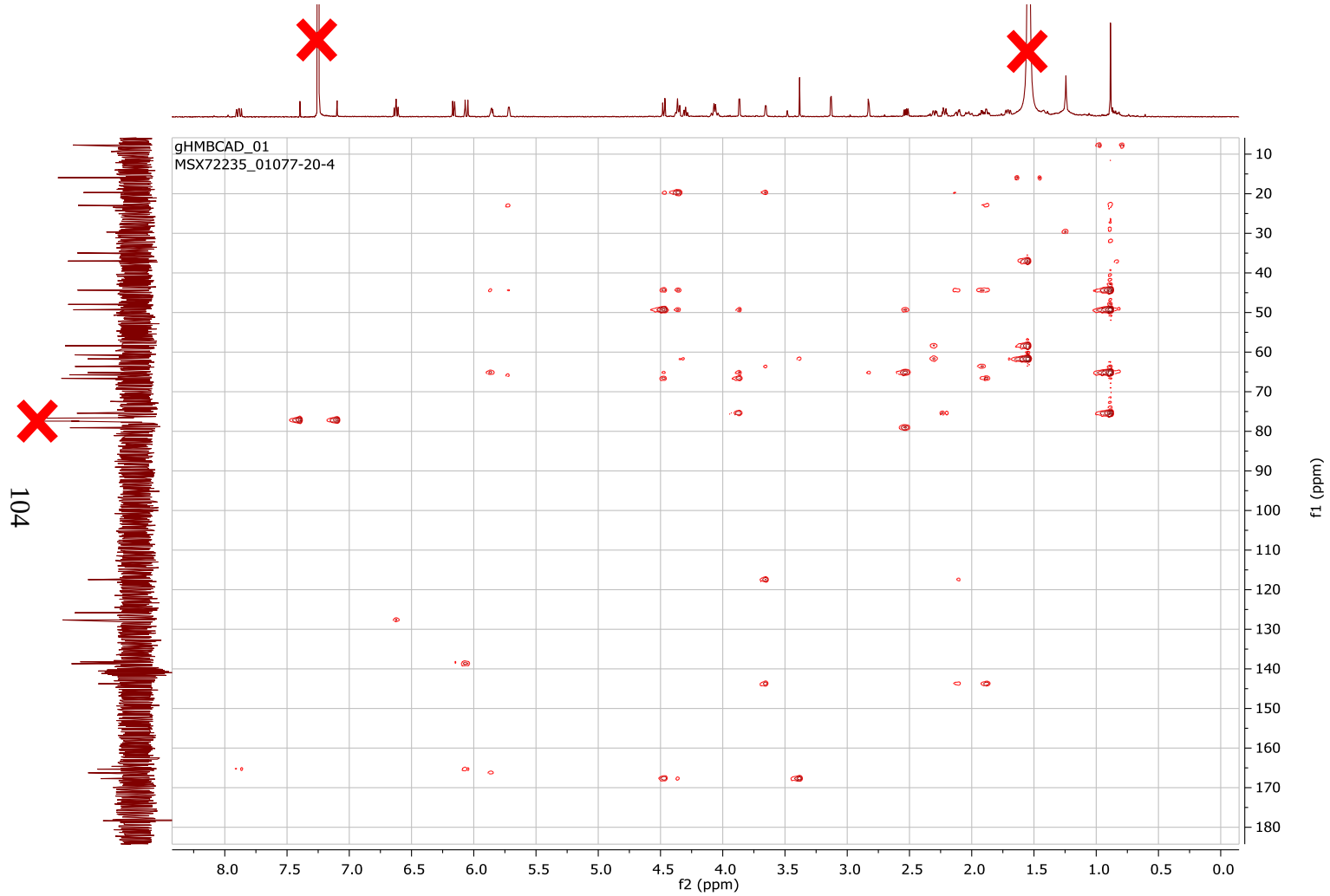

Figure A11. HMBC NMR Spectrum of 2 [700 MHz, $CDCl_3$].

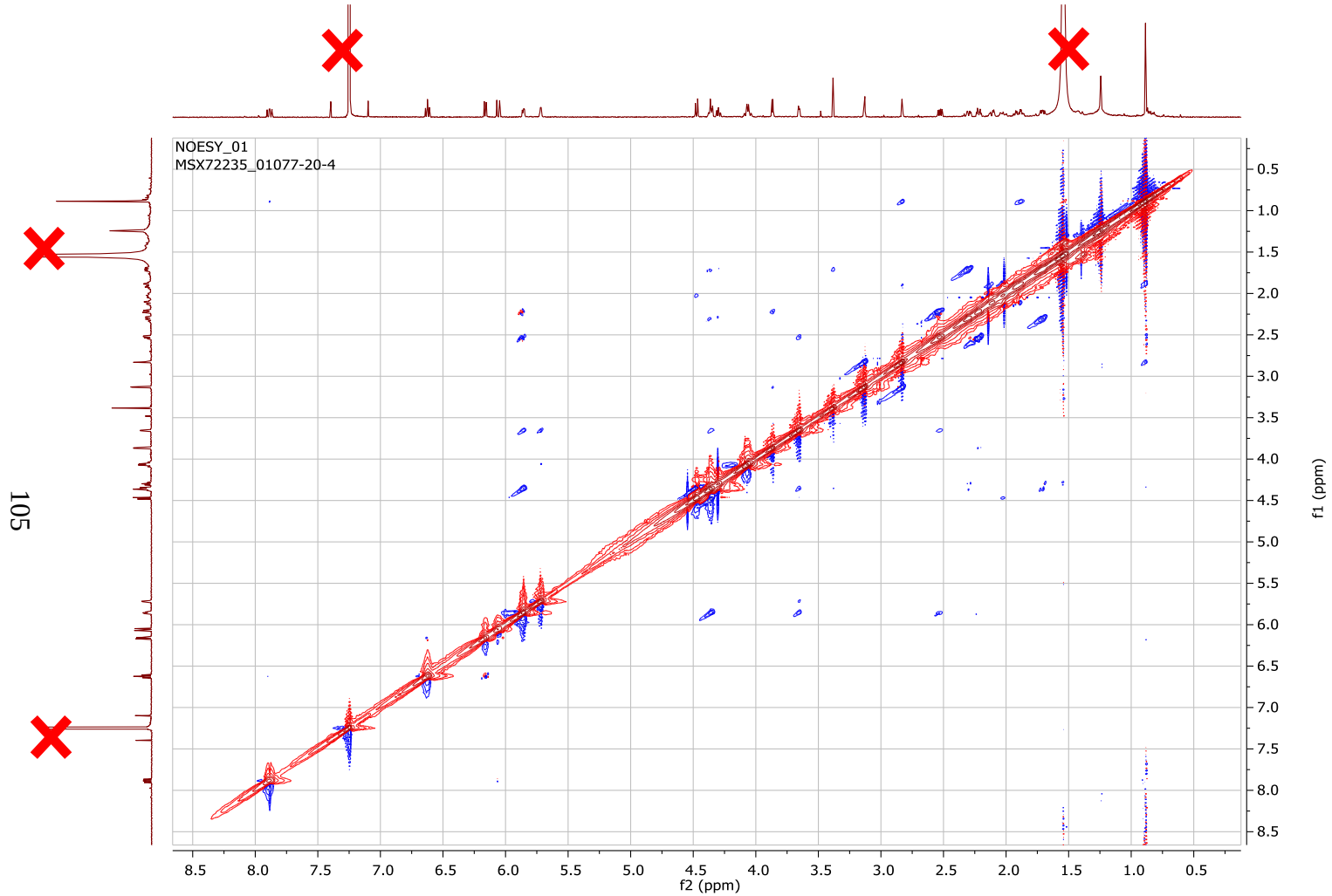

Figure A12. NOESY NMR Spectrum of 2 [700 MHz, $CDCl_3$].

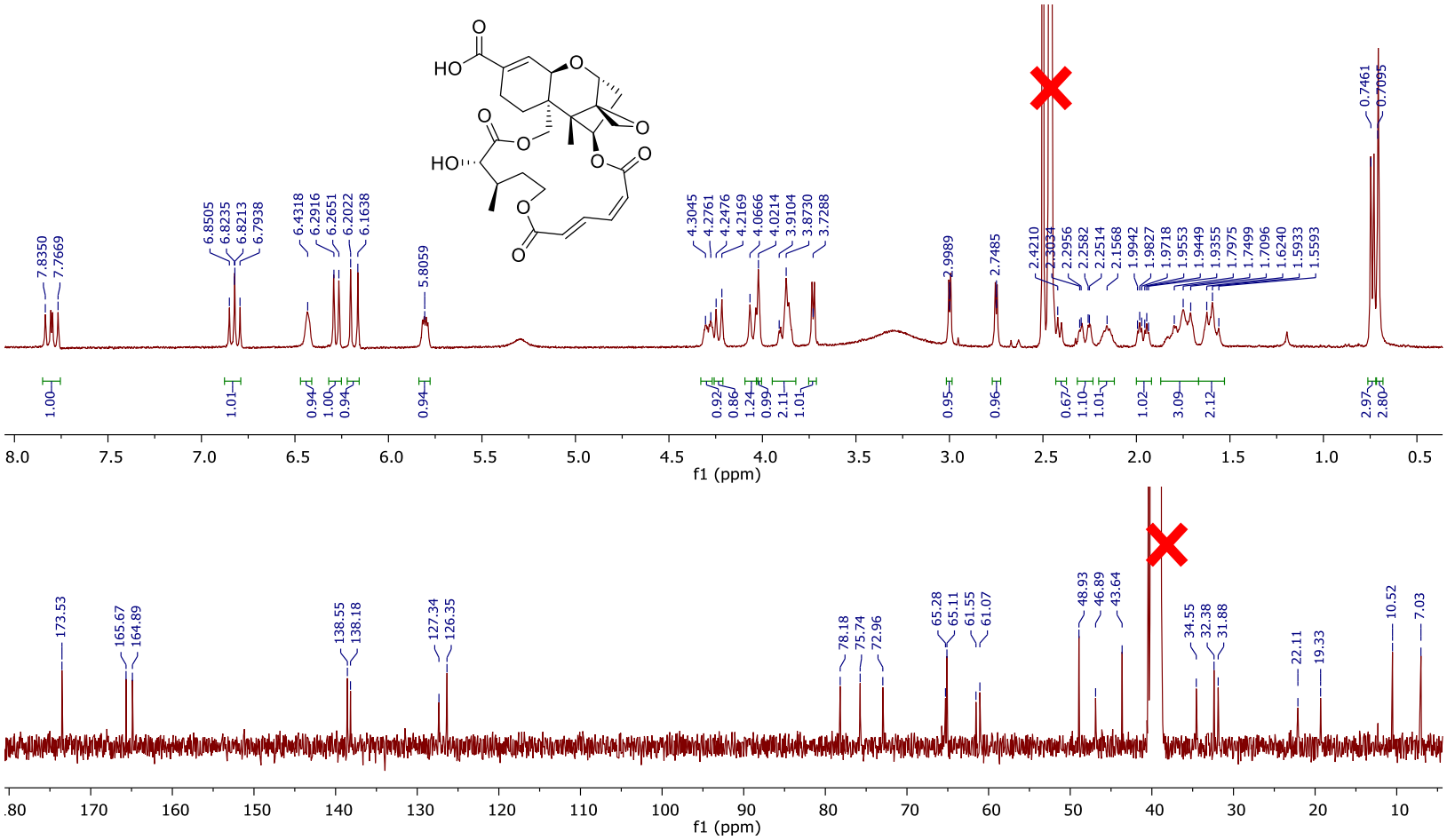

Figure A13. ^{1}H and ^{13}C NMR Spectra of 3 [700 MHz for ^{1}H and 175 MHz for ^{13}C, DMSO-d_6].

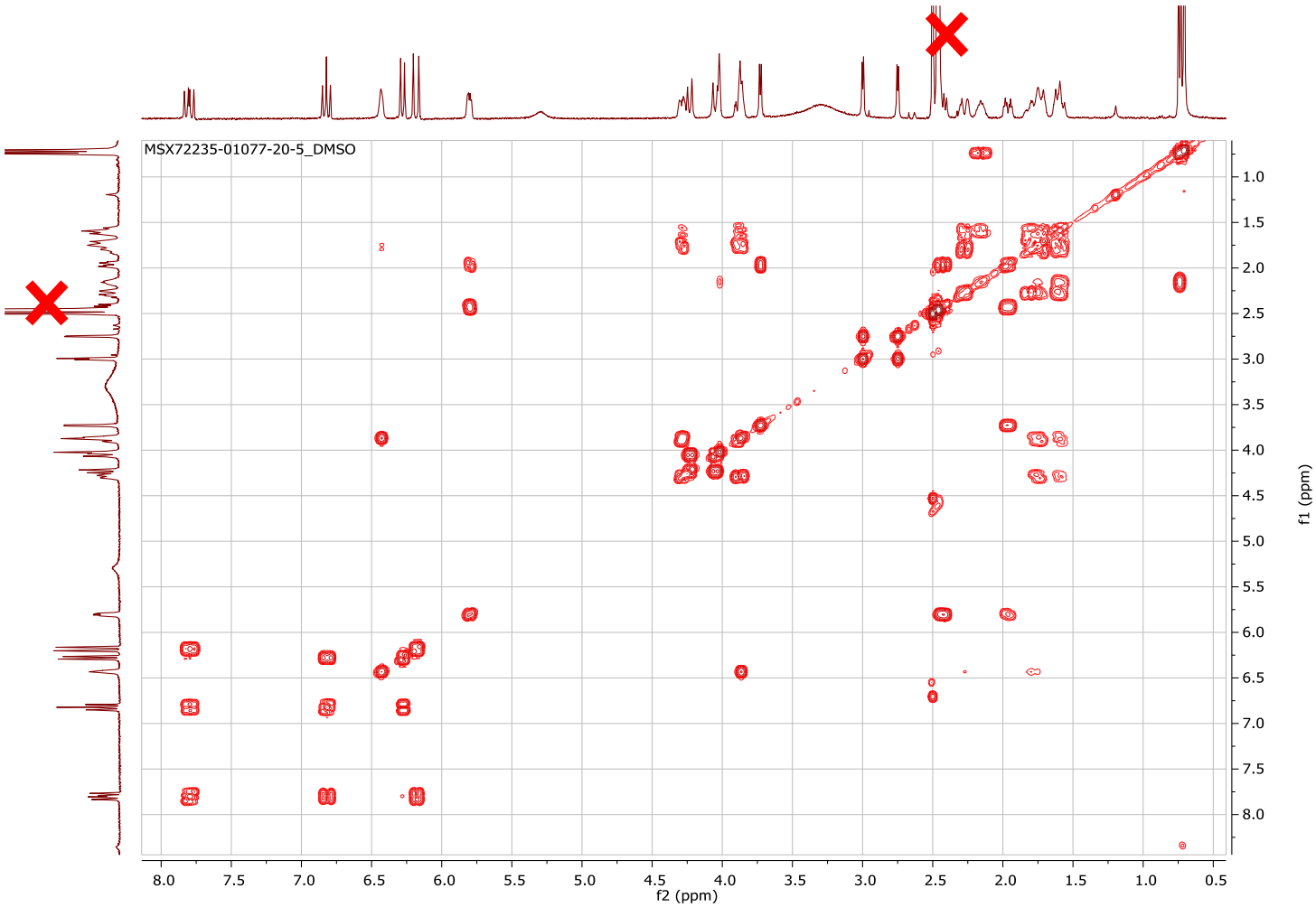

Figure A14. COSY NMR Spectrum of 3 [700 MHz, DMSO-d_6].

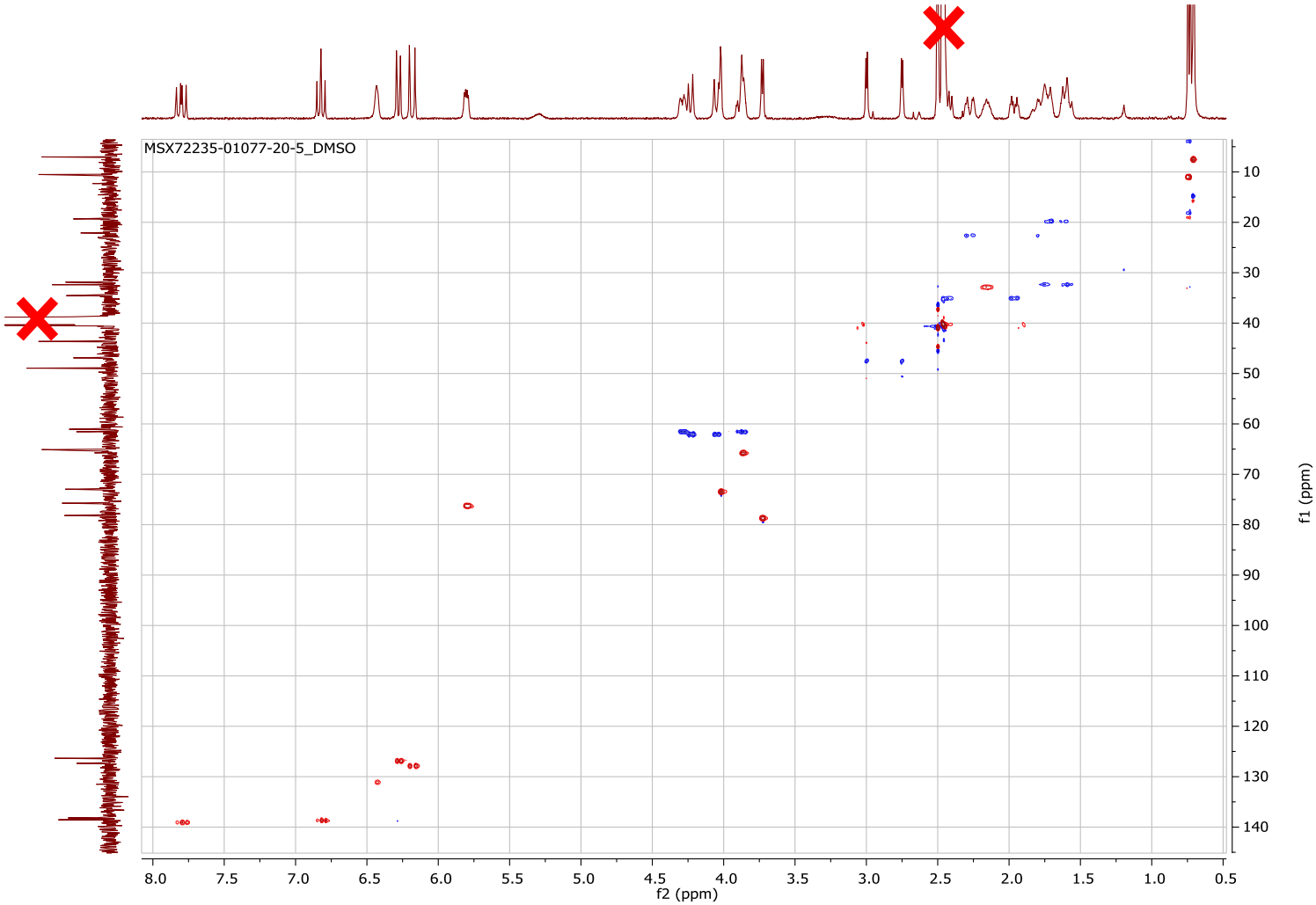

Figure A15. HSQC NMR Spectrum of 3 [700 MHz, DMSO-d_6].

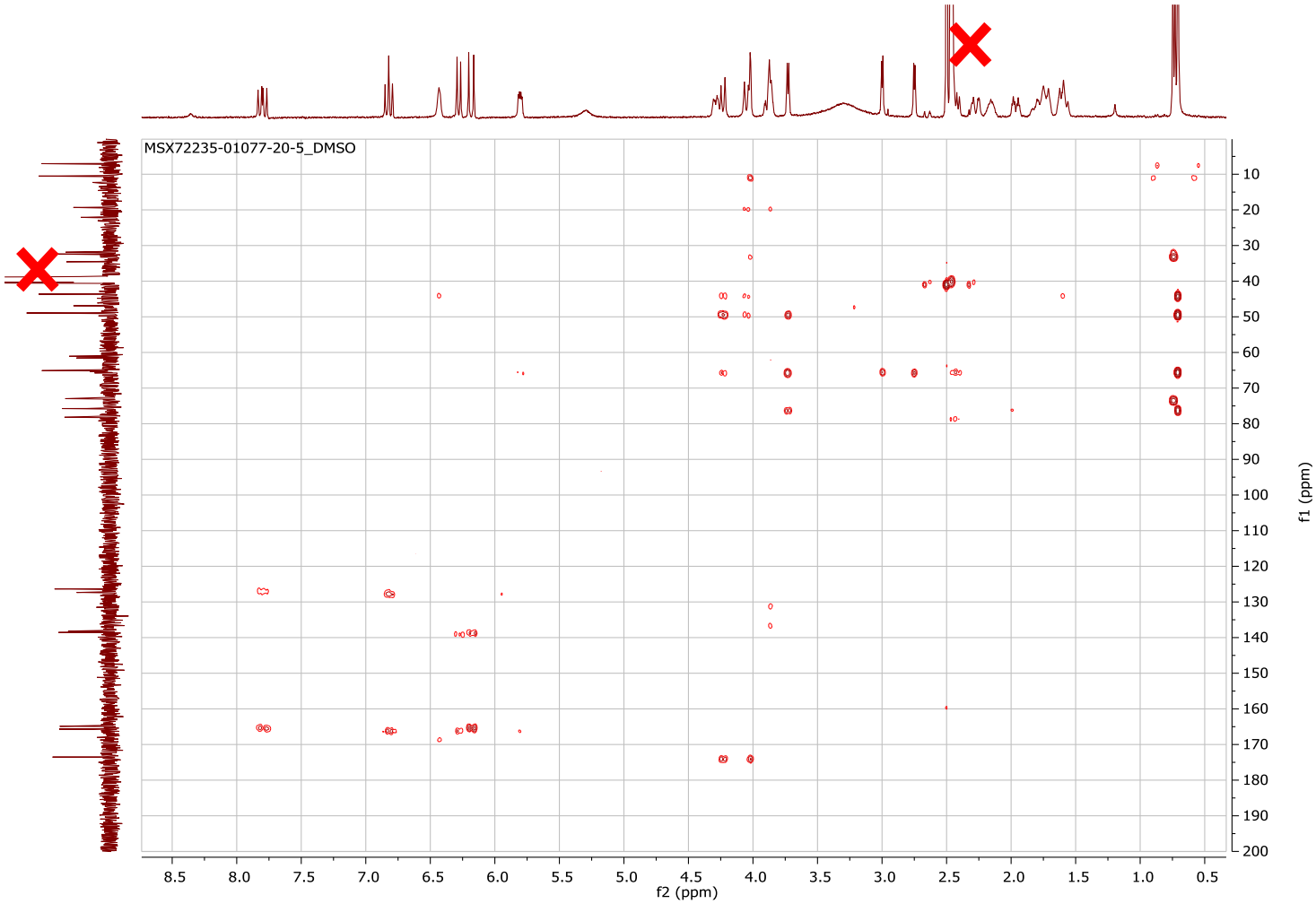

Figure A16. HMBC NMR Spectrum of 3 [700 MHz, DMSO-d_6].

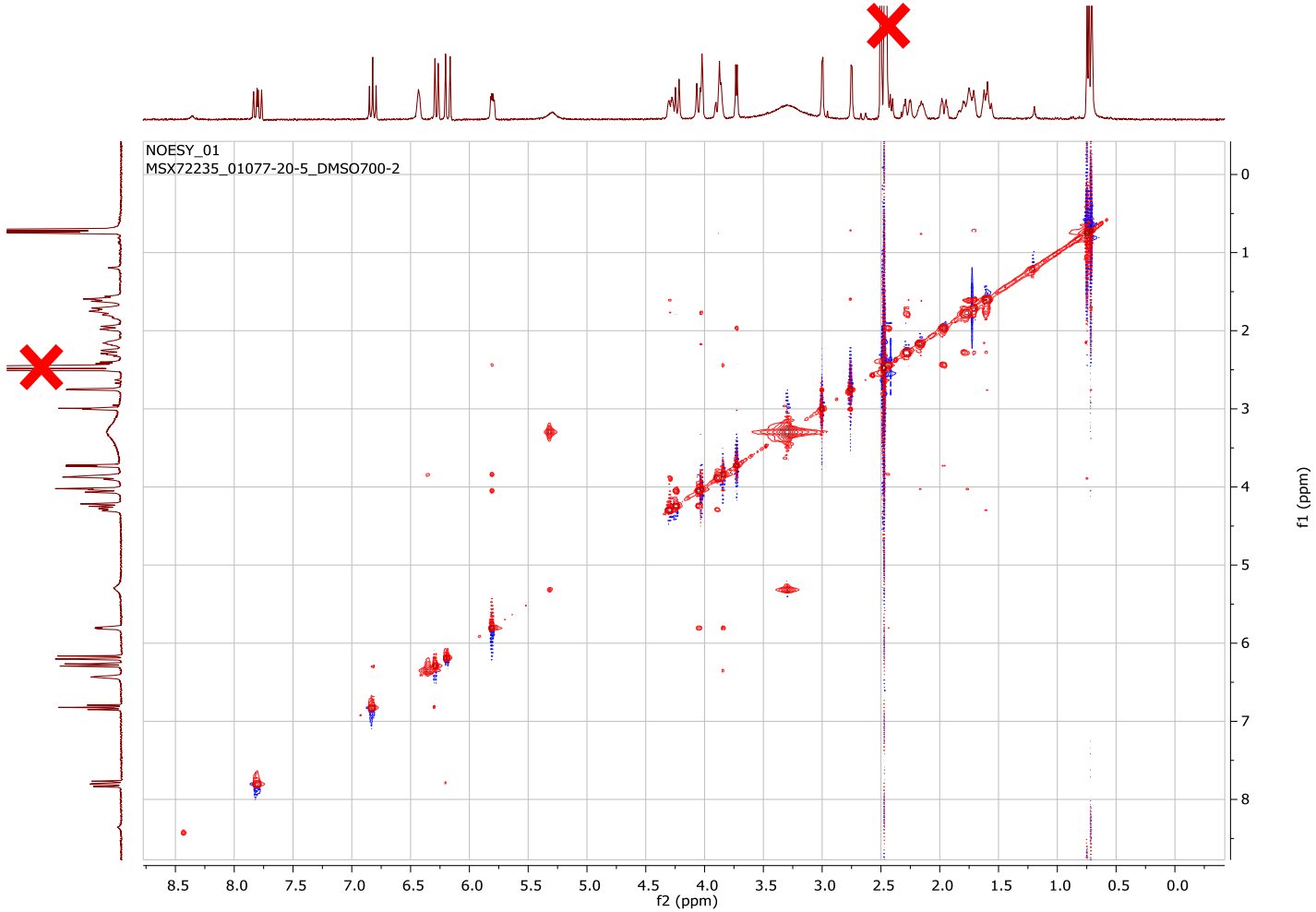

Figure A17. NOESY NMR Spectrum of 3 [700 MHz, DMSO-d_6].

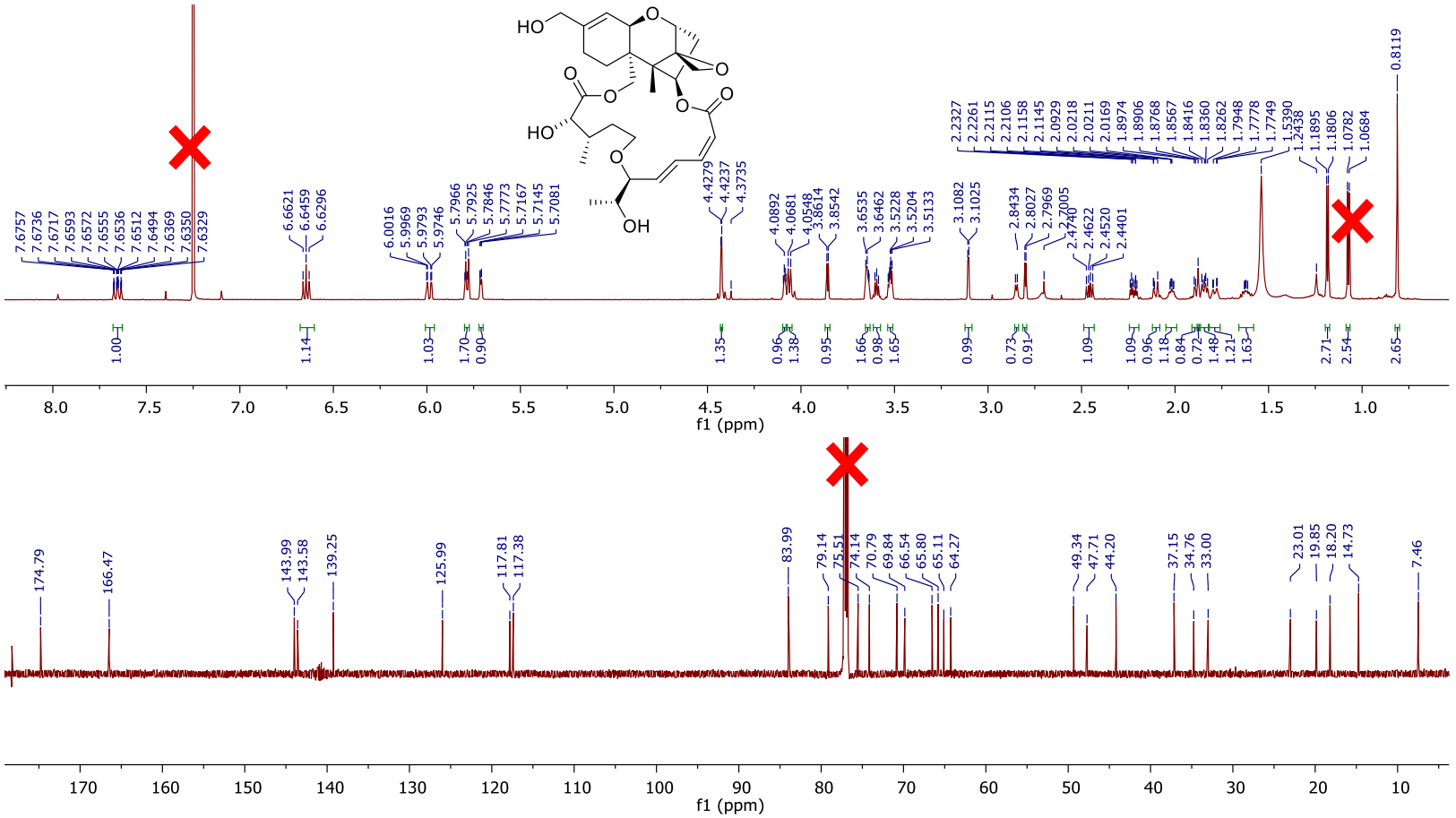

111

Figure A18. ^{1}H and ^{13}C NMR Spectra of 6 [700 MHz for ^{1}H and 175 MHz for ^{13}C, $CDCl_3$].

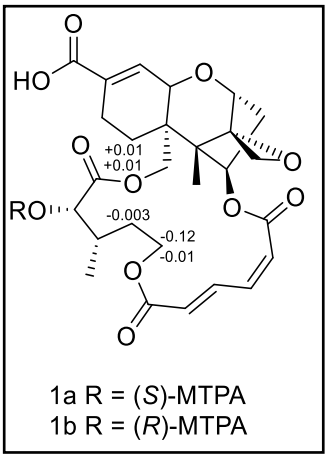

Figure A19. Determination of Configuration of Compound 7 with Mosher's Esters: $\Delta\delta_H$ Values [$\Delta\delta_H$ (in ppm) = δ_S -δ_R].

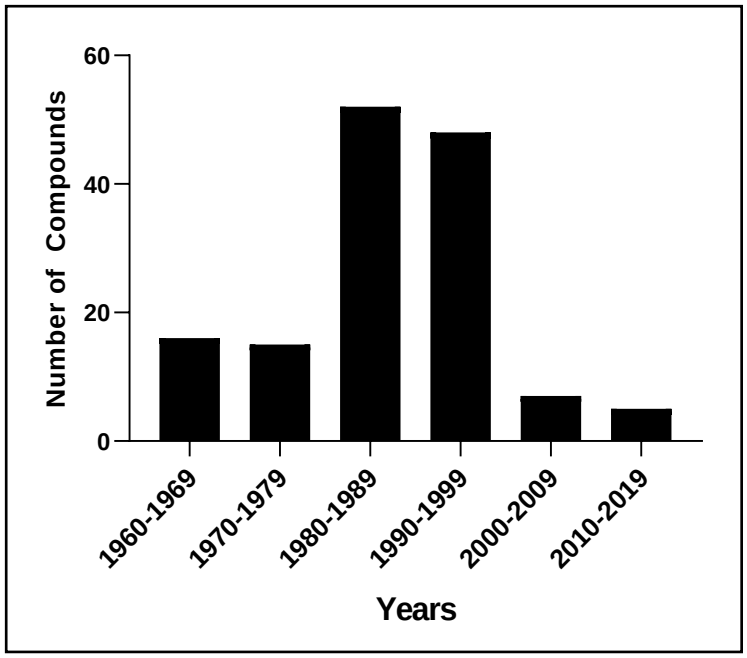

Figure A20. A Histogram Based on Identification Numbers Assigned by SciFinder Scholar to Unique Macrocyclic Trichothecenes. This search was performed using a structure similarity search of macrocyclic trichothecenes with no decorations at C-9, C-2′, C-3′, and C-6′. After over 150 compounds were identified, all reaction reagents and products were eliminated, leaving approximately 130 compounds. Each analogue was then organized according to its earlier reported literature and thus when it was first described. Based on these parameters, the histogram spans from 1962 to 2019. These are organized in approximately 10-year intervals.

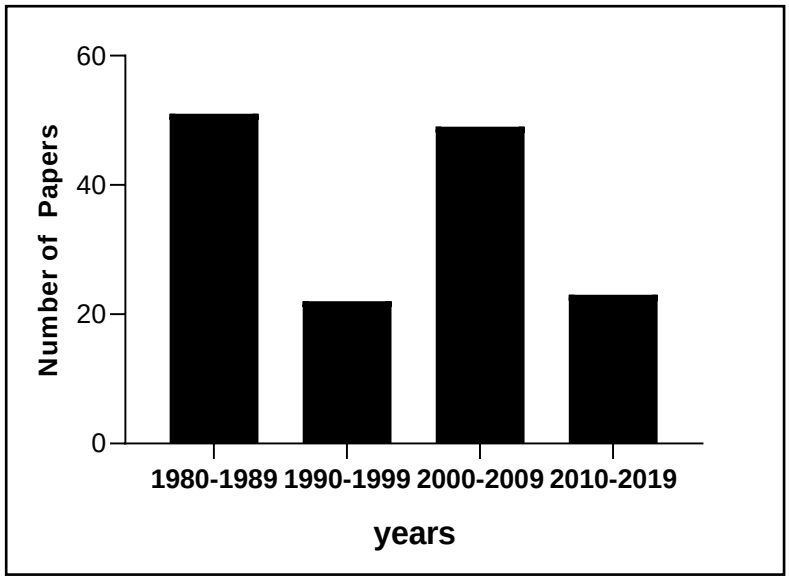

Figure A21. A Histogram Based on a Research Topic Search of "Macrocyclic Trichothecenes" in SciFinder Scholar. This search reported over 300 results but only just over 200 when all duplicates were removed. The search was refined by looking only at those papers published that applied to Biotechnology terms: Substances in Adverse effects (all terms), Toxicology & forensics (all terms), Medicine (all terms), Substances in medicine (all terms), and/or Agriculture (Antibiotics and Antimalarials). The 145 remaining references were denoted according to years with the earliest reported literature of biological tests that fit these parameters in 1980 to the latest in 2019. Each bin width is organized in approximately 10-year intervals.

APPENDIX B

SUPPLEMENTARY FIGURES

Table of Contents

round of acetone extraction. F) third round of acetone extraction. G) fourth round of acetone extraction. H) sugary materials captured upon passing through open silica column.

Figure B5. Chromatographic Purity Evaluation of a Purified Isolate.

Figure B6. NMR Purity and Identity Analysis of a Purified Isolate.

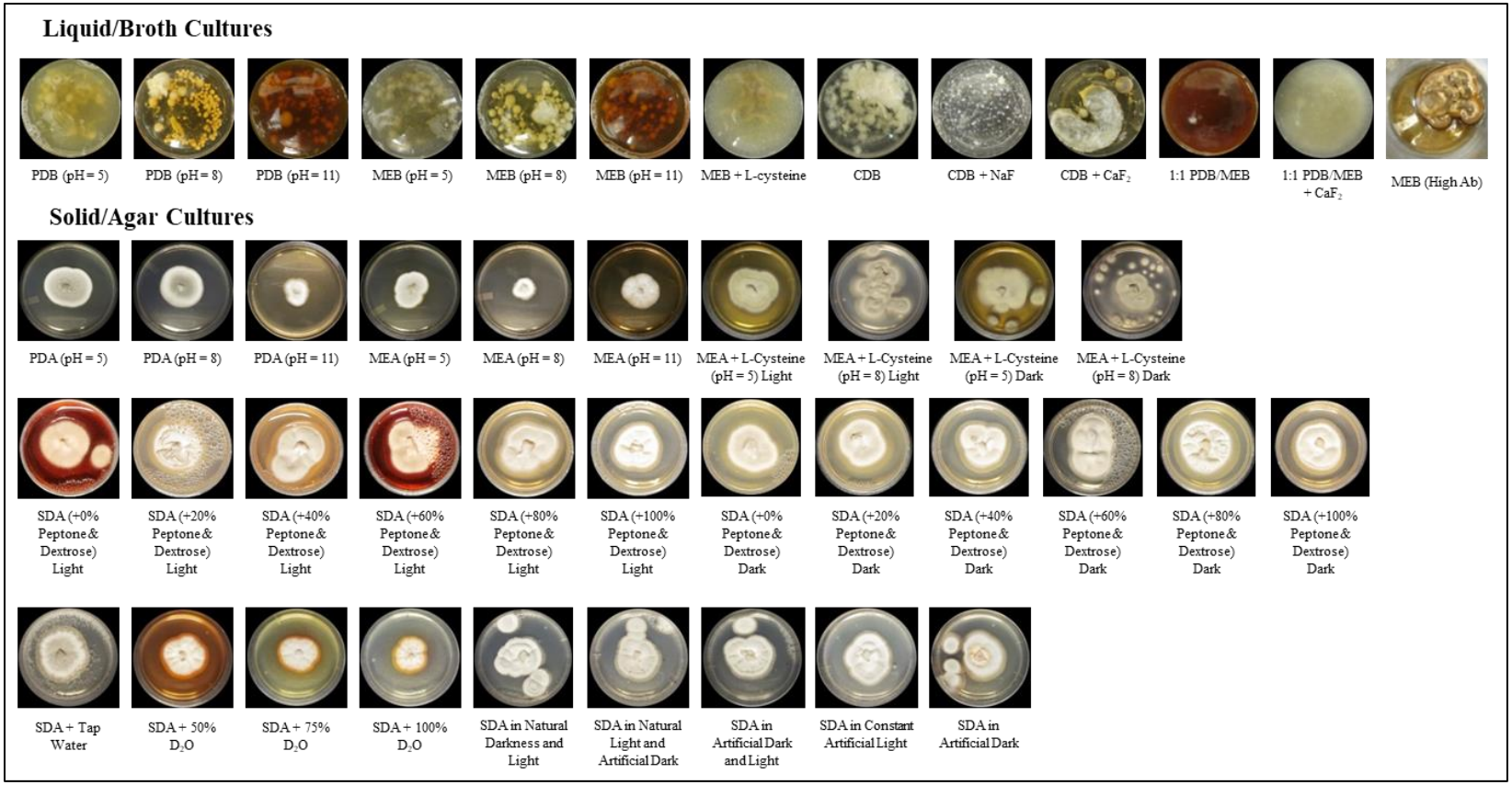

Figure B1. *Penicillium restrictum* (G85) Grown on Different Media and pH Conditions. PDB - Potato Dextrose Broth; PDA - Potato Dextrose Agar; MEB - Malt Extract Broth; MEA - Malt Extract Agar; CDB - Czapek Dox Broth; Ab – Antibiotic; SDA - Sabouraud Dextrose Agar; Light - Light/Dark cycles; Dark - Constant Darkness.

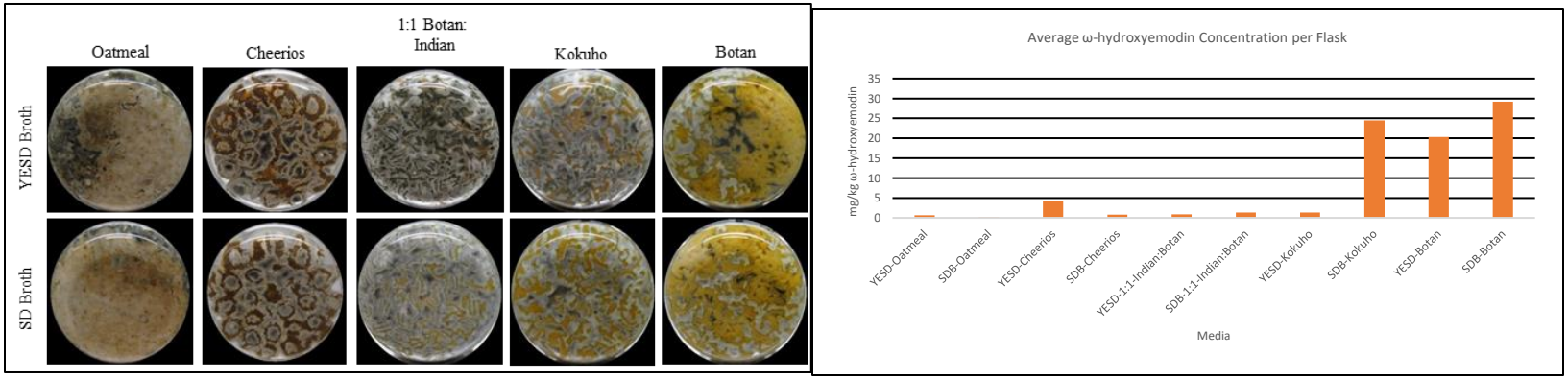

Figure B2. Over Four Weeks, *Penicillium restrictum* (G85) was Grown on Five Different Solid Media: Oatmeal, Cheerios, Botan-Indian Rice Mixture, Kokuho Rice, and Botan Rice. Each of these five solid media used one of two different seed cultures, yeast extract soy dextrose (YESD) broth and Sabouraud dextrose broth (SDB). Each condition was grown in duplicates and their concentrations averaged. The amount of ω-hydroxyemodin concentration per flask was determined by UPLC.

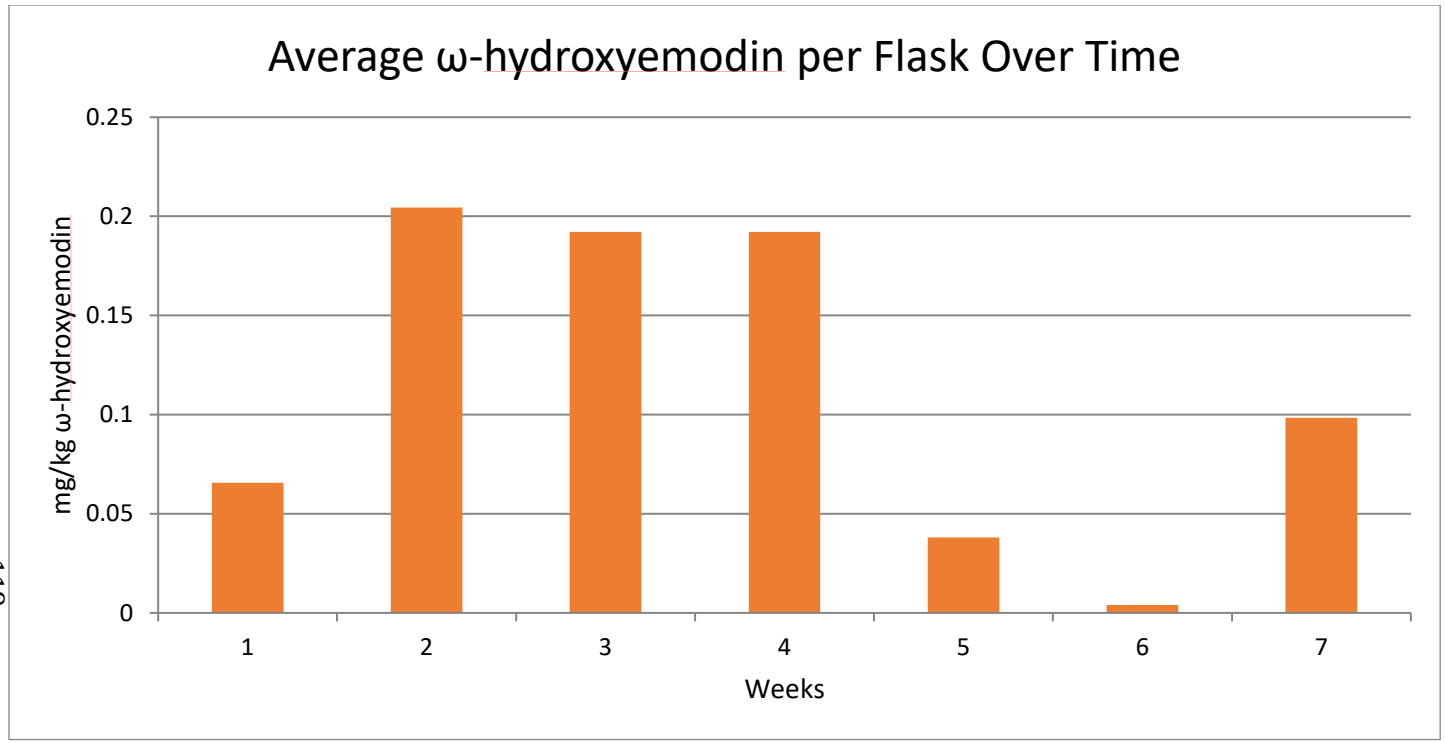

Figure B3. ***Penicillium restrictum*** **(G85) Grown on Botan Rice over the Course of Seven Weeks.** The seed culture used to inoculate these cultures was yeast extract soy dextrose broth. Every week, three flasks were extracted via the traditional extraction methodology. The amount of ω-hydroxyemodin concentration per flask was determined by UPLC. Each of these time points is an average concentration of the three extracted flasks per time point.

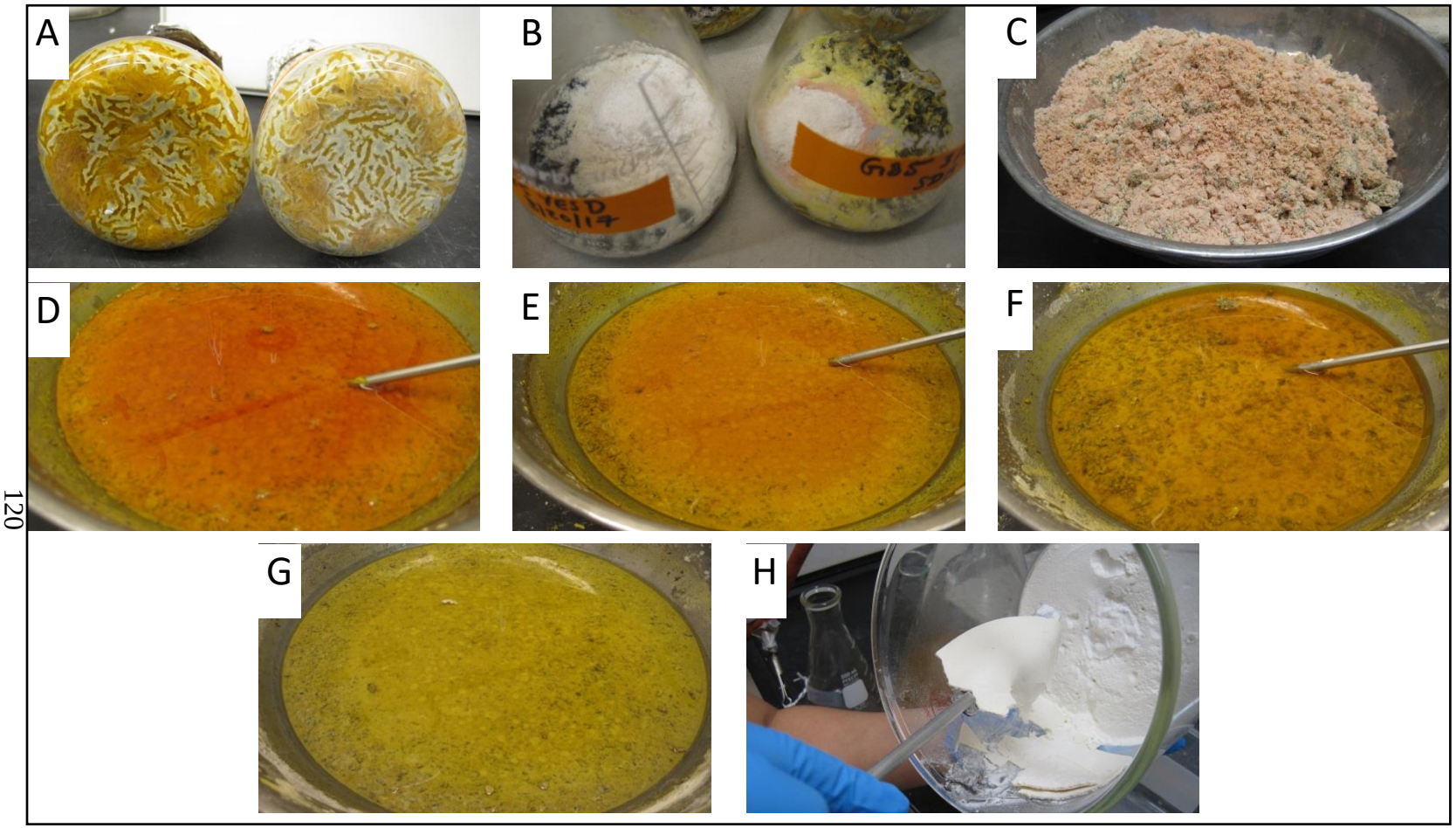

Figure B4. Stages in Generating the Initial Extract. A) SDB and YESD inoculated cultures. B) YESD and SDB inoculated cultures with celite added. C) Numerous SDB cultures mixed with celite in mixing bowl. D) first round of acetone extraction. E) second round of acetone extraction. F) third round of acetone extraction. G) fourth round of acetone extraction. H) sugary materials captured upon passing through open silica column.

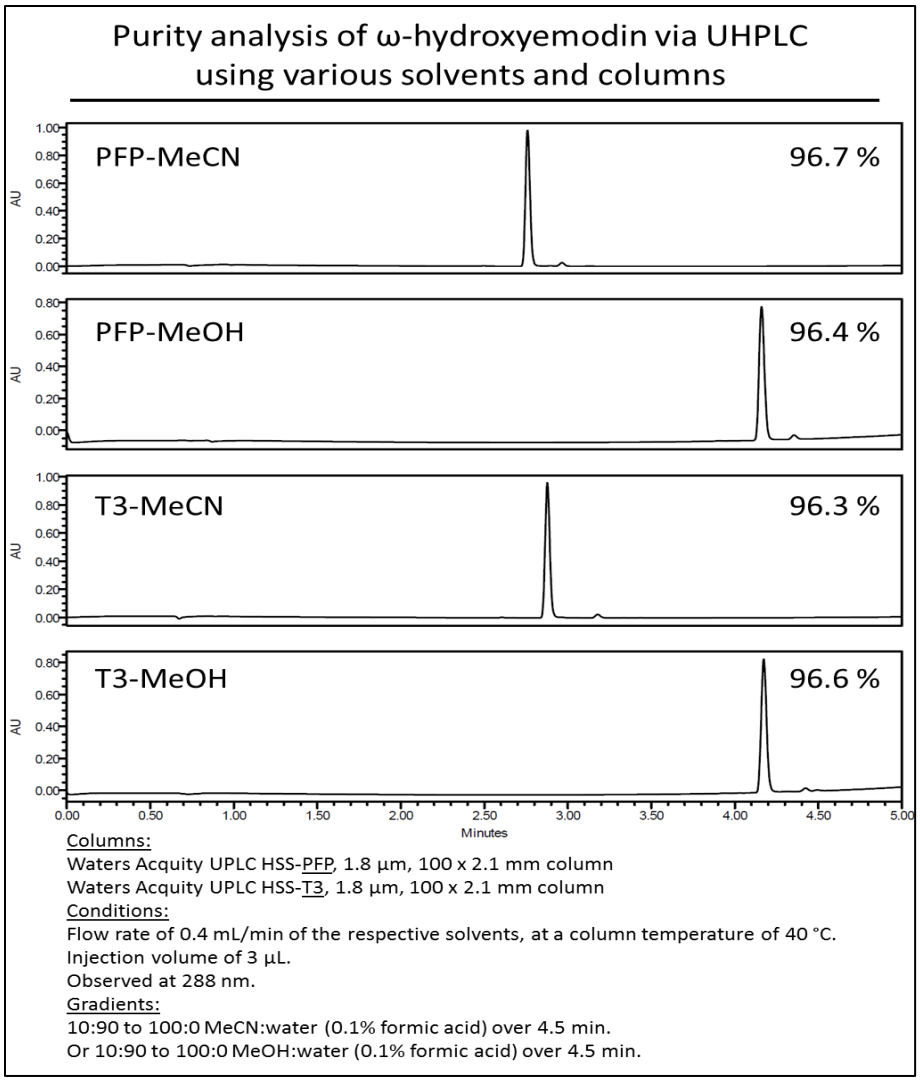

Figure B5. Chromatographic Purity Evaluation of a Purified Isolate.

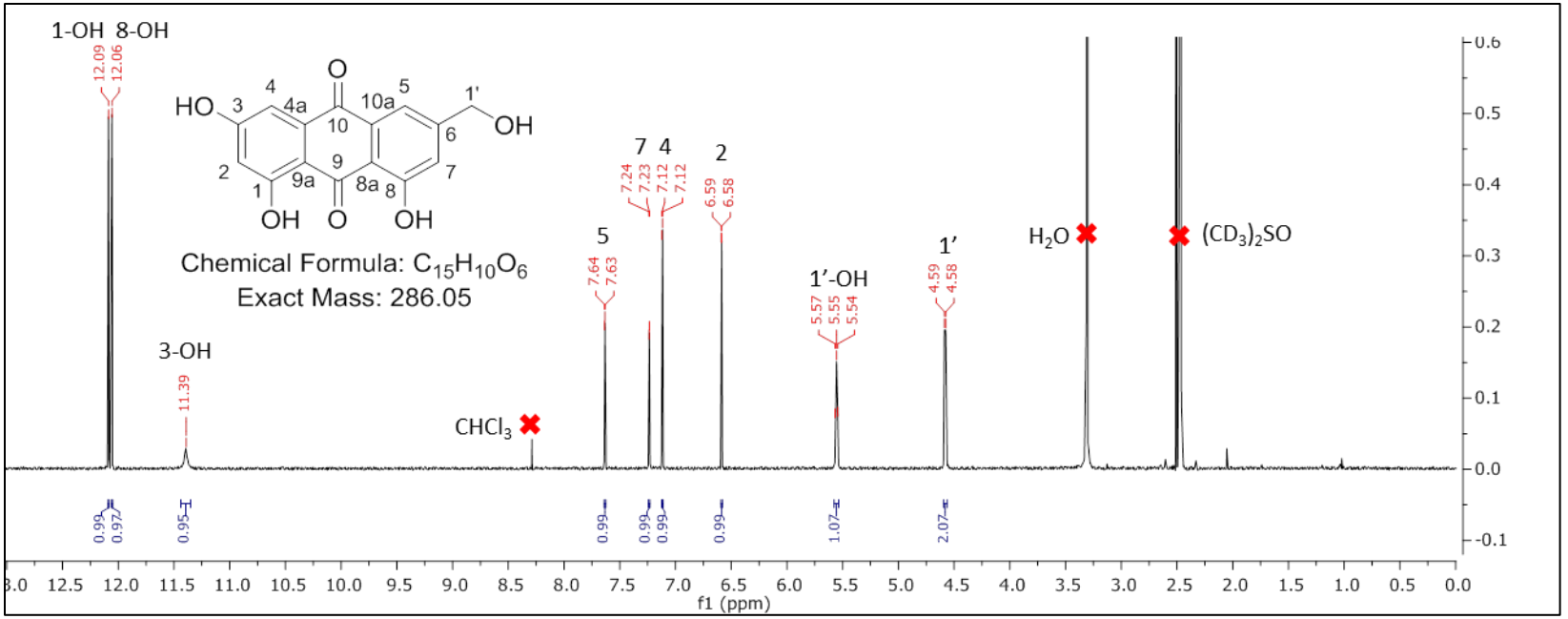

Figure B6. NMR Purity and Identity Analysis of a Purified Isolate.

APPENDIX C

SUPPLEMENTARY FIGURES

Table of Contents

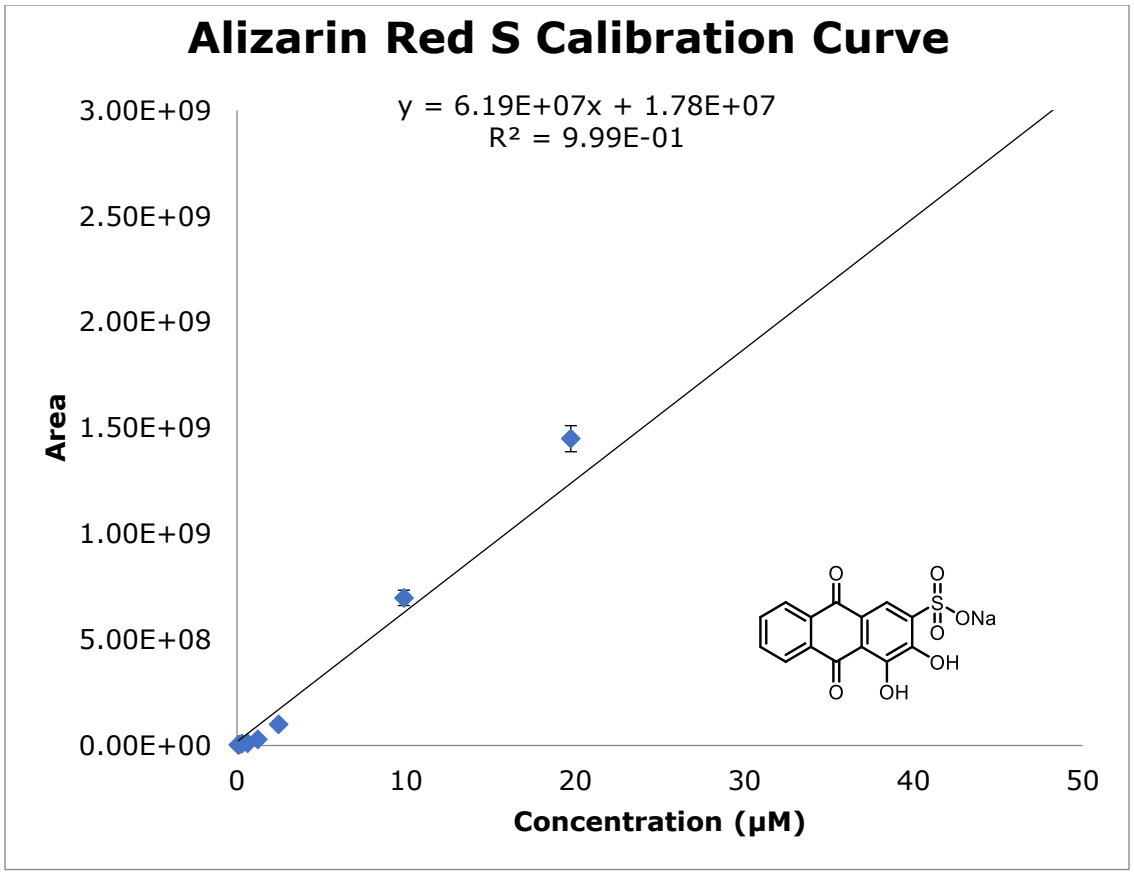

Figure C1. Calibration Curve of Alizarin Red S. Triplicate measurements from 0.125 µM to 64 µM.

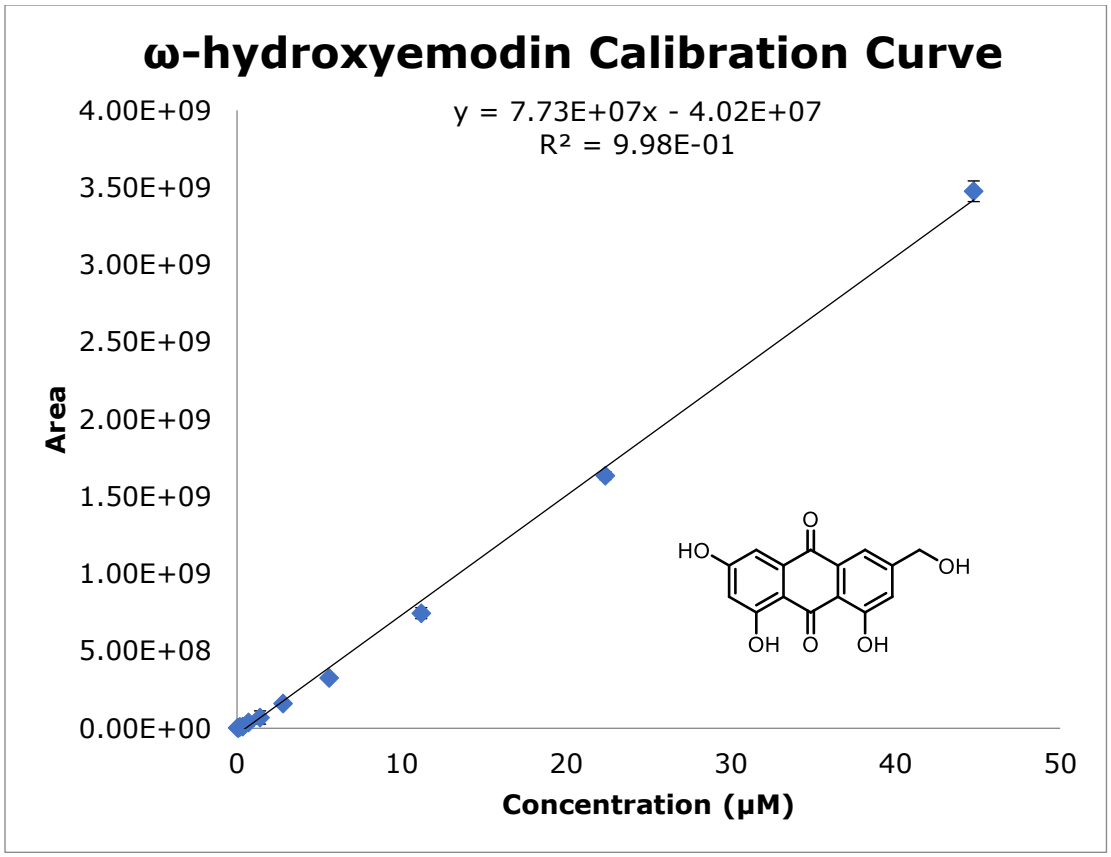

Figure C2. Calibration Curve of ω-Hydroxyemodin. Triplicate measurements from 0.125 μM to 64 μM.

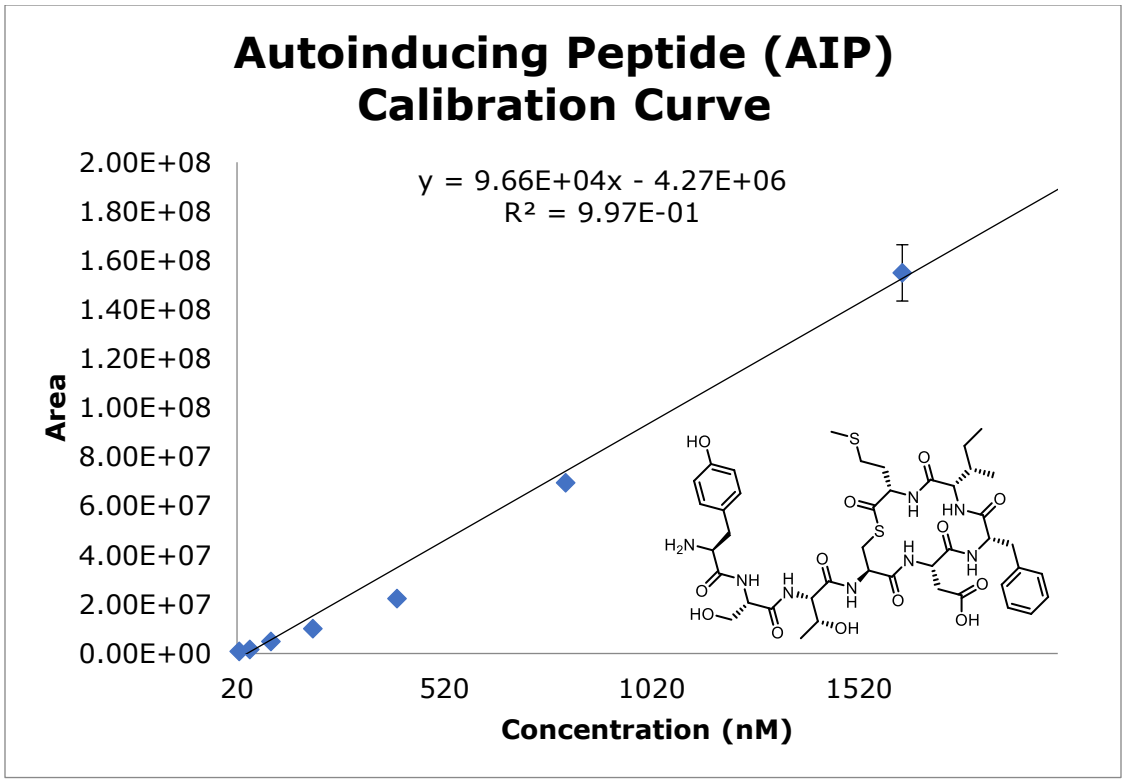

Figure C3. Calibration Curve of AIP. Triplicate measurements from 13 nM to 1600 nM.

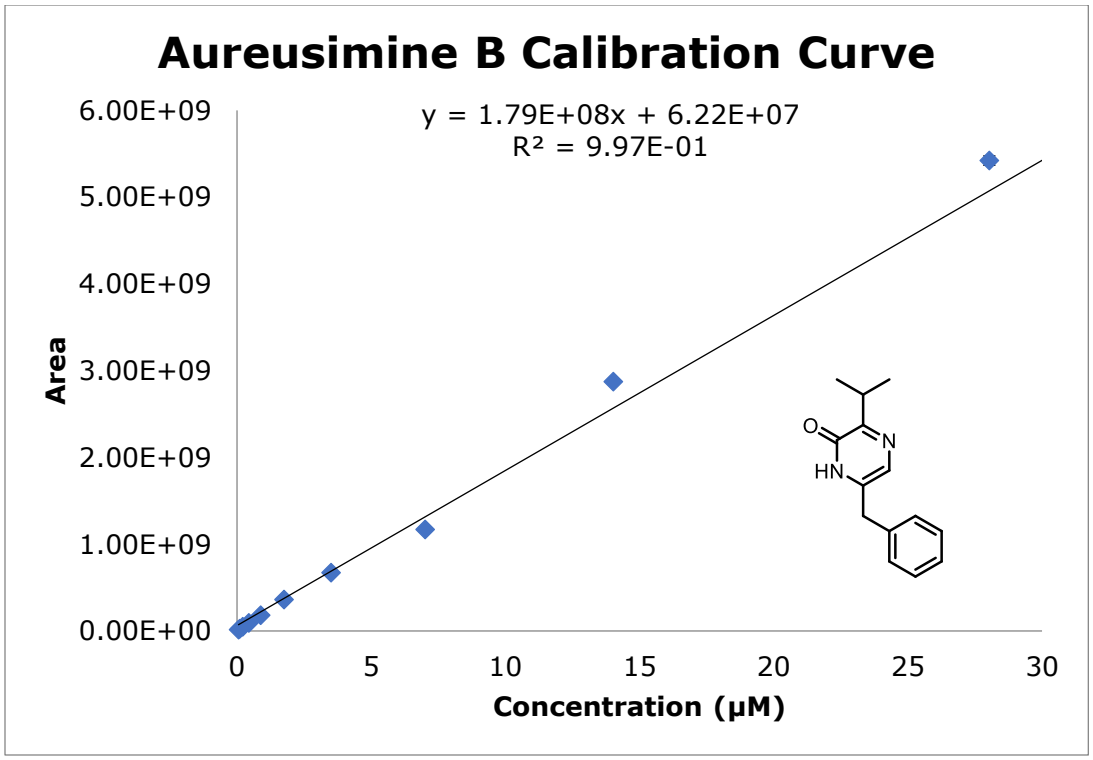

Figure C4. Calibration Curve of Aureusimine B. Triplicate measurements from 0.125 µM to 64 µM.

APPENDIX D

SUPPLEMENTARY FIGURES

Table of Contents

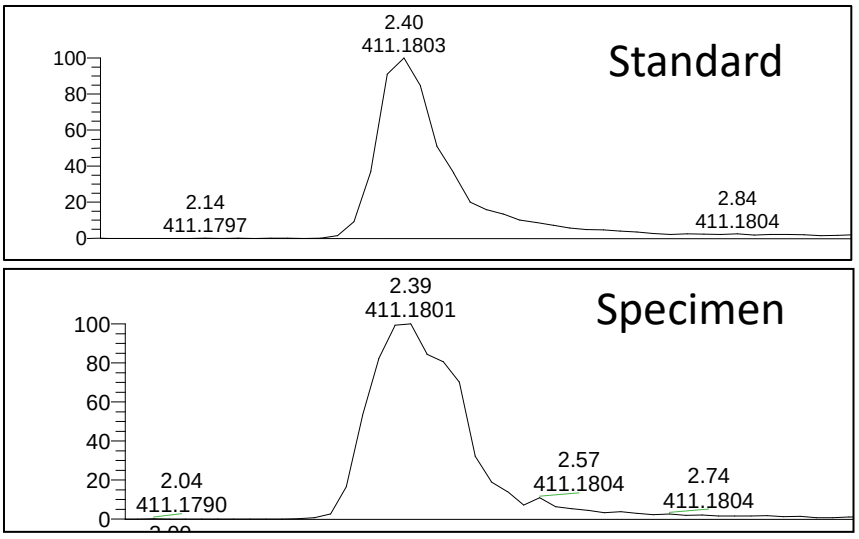

Figure D1. Comparison of Example HRMS and PDA Data for Standard α-Mangostin (1) and Site of the Fruit Stem.

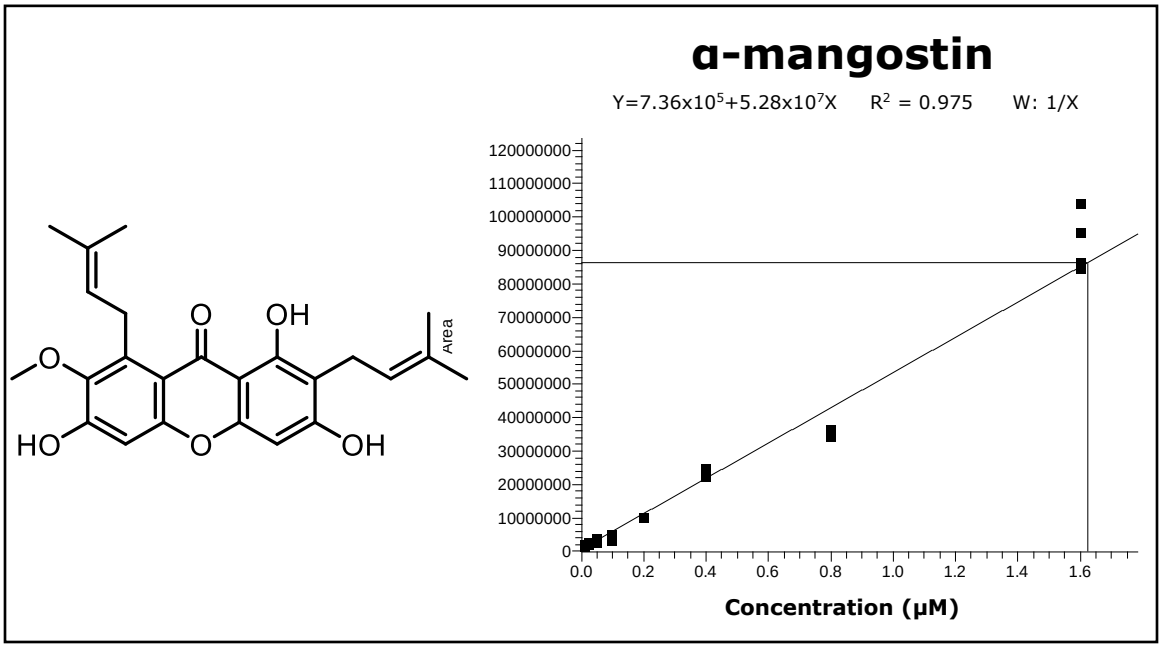

Figure D2. Calibration Curve of α-Mangostin (1). Triplicate measurements from 0.00125 μM to 16 μM.

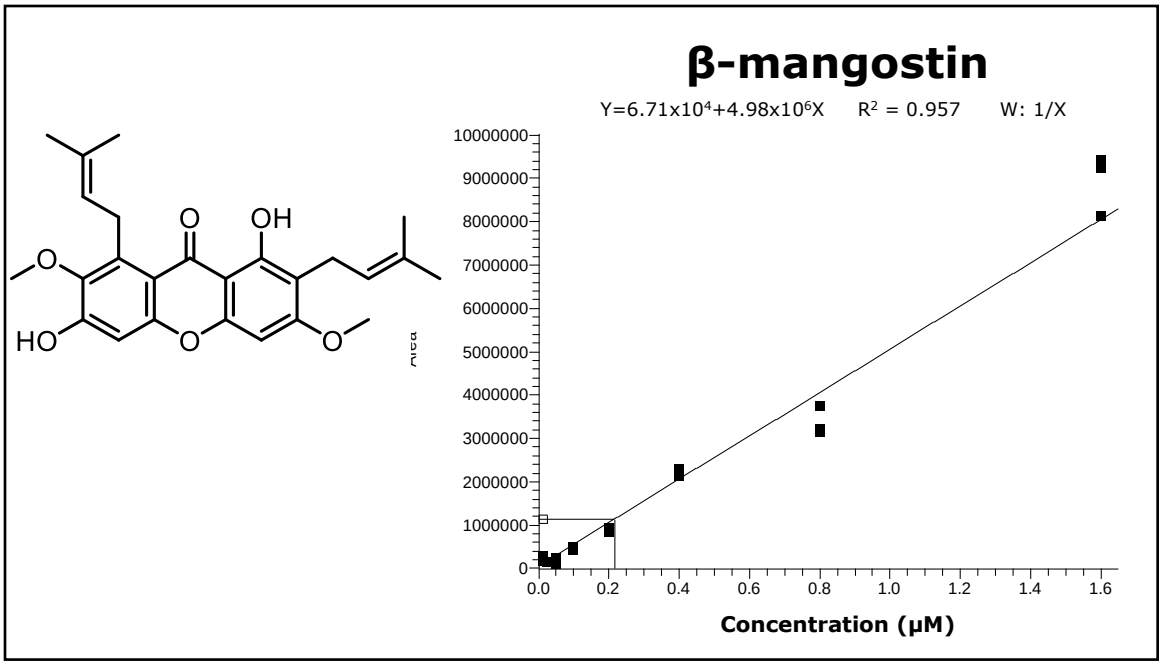

Figure D3. Calibration Curve of β-Mangostin (2). Triplicate measurements from 0.00125 µM to 16 µM.

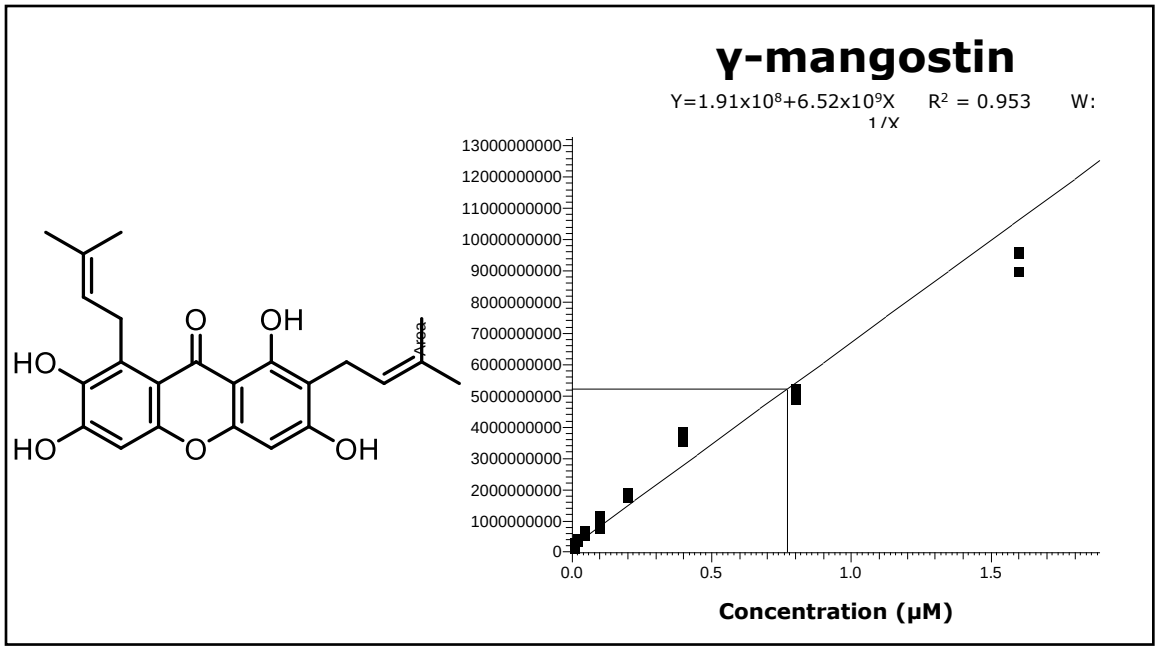

Figure D4. Calibration Curve of γ-Mangostin (3). Triplicate measurements from 0.00125 μM to 16 μM.

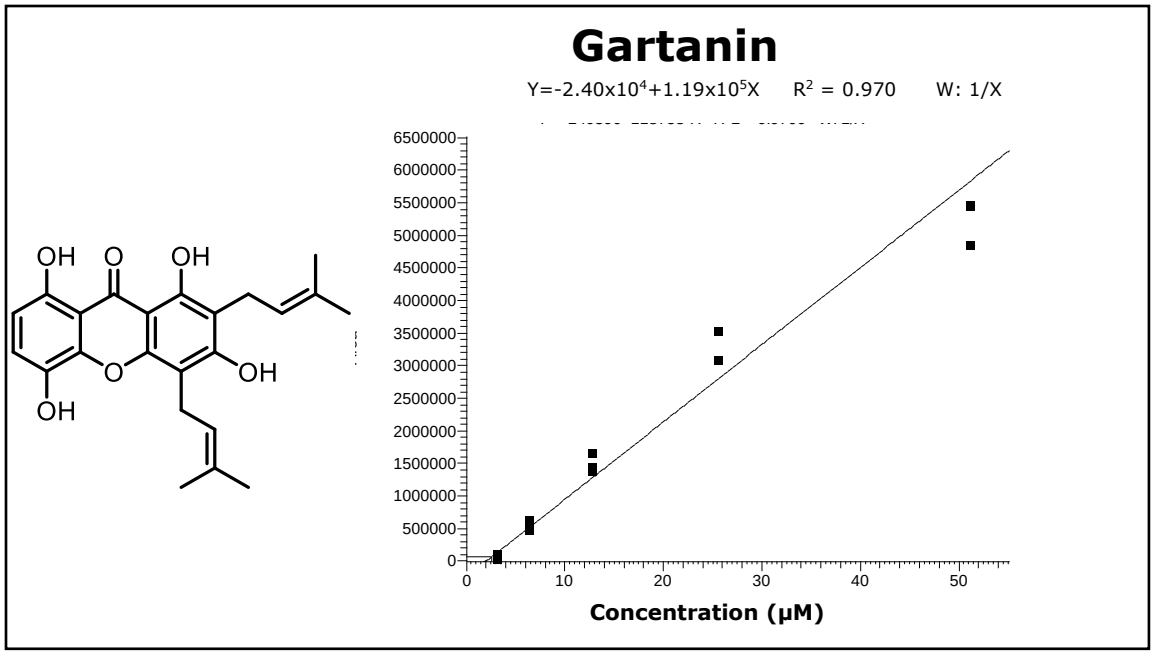

Figure D5. Calibration Curve of Gartanin (4). Triplicate measurements from 0.00125 µM to 48 µM.

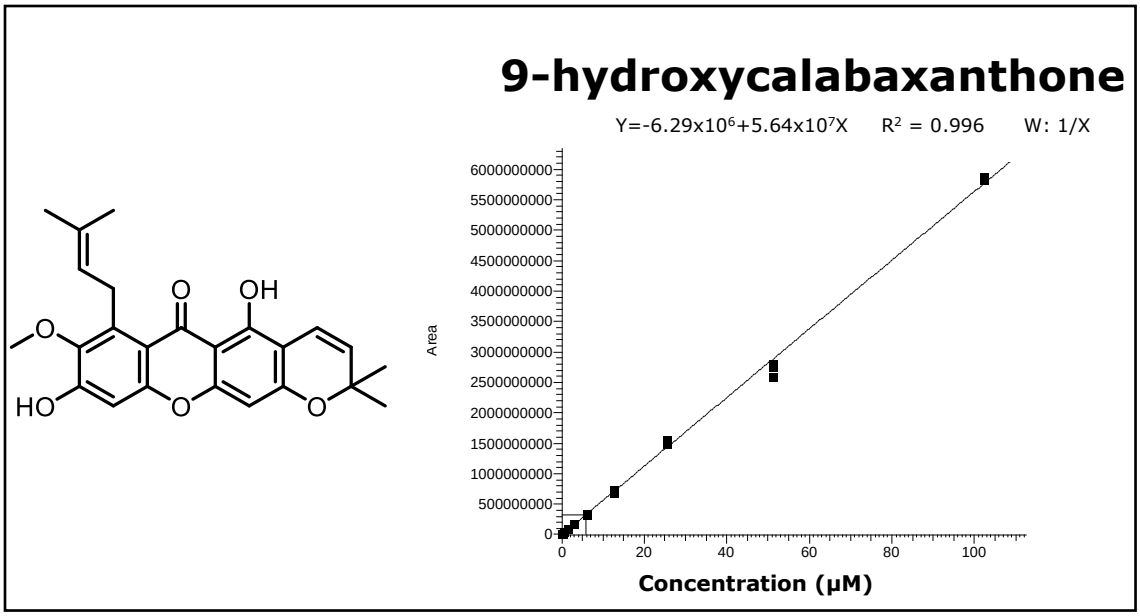

Figure D6. Calibration Curve of 9-Hydroxycalabaxanthone (5). Triplicate measurements from 0.00125 µM to 128 µM.

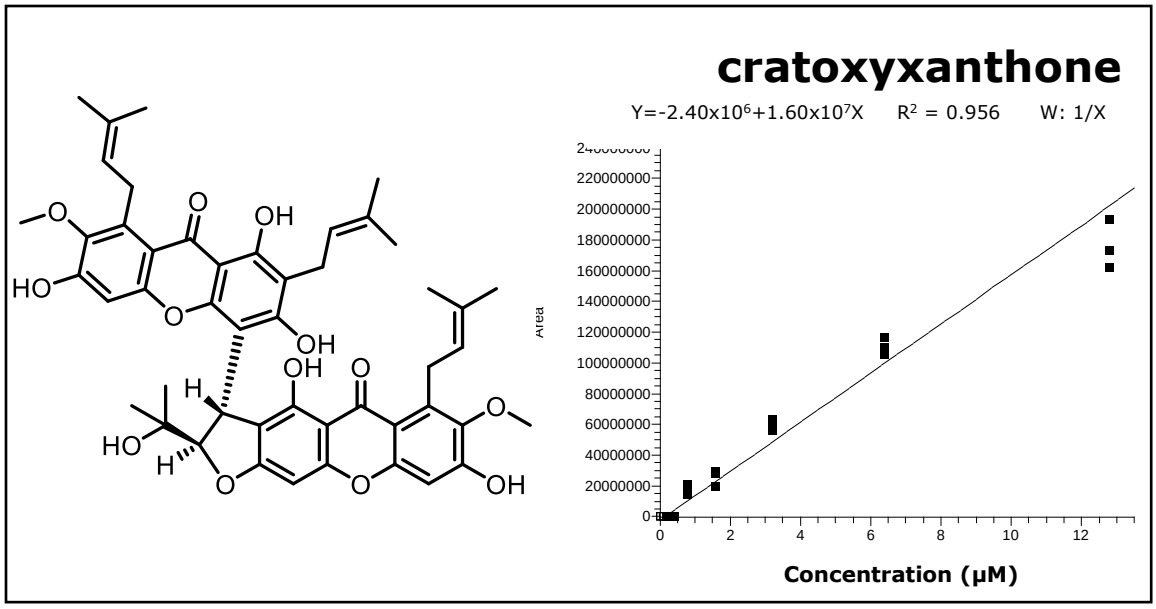

Figure D7. Calibration Curve of Cratoxyxanthone (6). Triplicate measurements from 0.00125 µM to 512 µM.